

Phenomenology of the Lense-Thirring effect in the Solar System

Lorenzo Iorio¹ • Herbert I. M. Lichtenegger² •
Matteo Luca Ruggiero³ • Christian Corda⁴

Abstract Recent years have seen increasing efforts to directly measure some aspects of the general relativistic gravitomagnetic interaction in several astronomical scenarios in the solar system. After briefly overviewing the concept of gravitomagnetism from a theoretical point of view, we review the performed or proposed attempts to detect the Lense-Thirring effect affecting the orbital motions of natural and artificial bodies in the gravitational fields of the Sun, Earth, Mars and Jupiter. In particular, we will focus on the evaluation of the impact of several sources of systematic uncertainties of dynamical origin to realistically elucidate the present and future perspectives in directly measuring such an elusive relativistic effect.

Keywords Experimental tests of gravitational theories Satellite orbits Harmonics of the gravity potential field Ephemerides, almanacs, and calendars Lunar, planetary, and deep-space probes

Lorenzo Iorio

Ministero dell'Istruzione, dell'Università e della Ricerca (M.I.U.R.), Fellow of the Royal Astronomical Society (F.R.A.S.)
Viale Unità di Italia 68, 70125, Bari (BA), Italy.

Herbert I. M. Lichtenegger

Institut für Weltraumforschung, Österreichische Akademie der Wissenschaften. Schmiedlstrasse 12, 8042 Graz, Austria

Matteo Luca Ruggiero

Dipartimento di Fisica, Politecnico di Torino, and INFN-Sezione di Torino. Corso Duca Degli Abruzzi 24, 10129, Torino (TO), Italy.

Christian Corda

Associazione Scientifica Galileo Galilei. Via Pier Cironi 16, I-59100 Prato Italy. Institute for Basic Research, P. O. Box 1577, Palm Harbor, FL 34682, USA

1 Introduction

The analogy between Newton's law of gravitation and Coulomb's law of electricity has been largely investigated since the nineteenth century, focusing on the possibility that the motion of masses could produce a magnetic-like field of gravitational origin. For instance, Holzmüller (1870) and Tisserand (1872, 1890), taking into account the modification of the Coulomb law for the electrical charges by Weber (1846), proposed to modify Newton's law in a similar way, introducing in the radial component of the force law a term depending on the relative velocity of the two attracting particles, as described by North (1989) and Whittaker (1960). Moreover, Heaviside (1894) investigated the analogy between gravitation and electromagnetism; in particular, he explained the propagation of energy in a gravitational field in terms of an electromagnetic-type Poynting vector.

Actually, today the term “gravitomagnetism” (GM) (Thorne 1988; Rindler 2001; Mashhoon 2007) commonly indicates the collection of those gravitational phenomena regarding orbiting test particles, precessing gyroscopes, moving clocks and atoms and propagating electromagnetic waves (Dymnikova 1986; Ruggiero and Tartaglia 2002; Schäfer 2004, 2009) which, in the framework of the Einstein's General Theory of Relativity (GTR), arise from non-static distributions of matter and energy. In the weak-field and slow motion approximation, the Einstein field equations of GTR, which is a highly non-linear Lorentz-covariant tensor theory of gravitation, get linearized, thus looking like the Maxwellian equations of electromagnetism. As a consequence, a “gravitomagnetic” field \vec{B}_g , induced by the off-diagonal components g_{0i} , $i = 1, 2, 3$ of the spacetime metric tensor related to mass-energy currents, does arise. Indeed, bringing together Newtonian gravitation and Lorentz invariance in a consistent

field-theoretic framework necessarily requires the introduction of a “magnetic”-type gravitational field of some form (Khan and O’Connell 1976; Bedford and Krumm 1985; Kolbenstvedt 1988).

In general, GM is used to deal with aspects of GTR by means of an electromagnetic analogy. However, it is important to point out that even though the linearization of the Einstein’s field equations produces the Maxwell-like equations (the so called “linear perturbation approach” to GM, see e.g. Mashhoon (2007)), often written in the literature including time dependent terms, they are, in that case, just formal (i.e., a different notation to write linearized Einstein equations), as the 3-vectors \vec{E}_g and \vec{B}_g (the “gravito-electromagnetic fields”) showing up therein do not have a clear physical meaning. A consistent physical analogy involving these objects is restricted to stationary phenomena only (Clark and Tucker 2000; Costa and Herdeiro 2008, 2010), that is, actually, the case treated here. One may check, for instance, that from the geodesics equation the corresponding Lorentz force is recovered – to first order in v/c – only for stationary fields (Costa and Herdeiro 2008; Bini et al. 2008). Moreover, the Maxwell-like equations obtained by linearizing GTR have limitations¹, since they are self-consistent at linear order only, which is what we are concerned with in this paper; in fact, inconsistencies arise when this fact is neglected².

Far from a localized rotating body with angular momentum \vec{S} the gravitomagnetic field can be written as (Thorne et al. 1986; Thorne 1988; Mashhoon et al. 2001a)

$$\vec{B}_g(\vec{r}) = -\frac{G}{cr^3} \left[\vec{S} - 3 \left(\vec{S} \cdot \hat{r} \right) \hat{r} \right], \quad (1)$$

where G is the Newtonian gravitational constant, c the speed of light in vacuum and \hat{r} a unit vector along \vec{r} . Eq. (1) equals the field of a magnetic dipole with a moment $\vec{\mu}'_g = G\vec{S}/c$ and affects, e.g., a test particle moving with velocity \vec{v} with a non-central acceleration (Mashhoon et al. 2001b; Lichtenegger et al. 2006)

$$\vec{A}_{\text{GM}} = -2 \left(\frac{\vec{v}}{c} \right) \times \vec{B}_g, \quad (2)$$

which is the cause of three of the most famous and empirically investigated GM features with which we will deal here: the Lense and Thirring (1918) effect, the gyroscope precession (Pugh 1959; Schiff 1960a), and the gravitomagnetic clock effect (Mashhoon et al. 2001a).

Corrections of higher order in v/c to orbital motions of pointlike objects have been studied by Capozziello et al. (2009); they may become relevant in stronger gravitational fields like those occurring in astrophysical scenarios (pulsars and black holes). For recent reviews of the Lense-Thirring effect in the astrophysical context see, e.g., Stella and Possenti (2009); Schäfer (2009).

GM manifests itself in the gravitational tidal forces as well. Actually, a gravito-electromagnetic analogy relying on exact and covariant equations stems from the tidal dynamics of both theories (Costa and Herdeiro 2008). In both theories it is possible to define electric and magnetic-type tidal tensors playing analogous physical roles. The electric tidal tensors of electromagnetism are gradients of the electric field, and play in the worldline deviation for two neighboring test particles (with the same ratio charge to mass) the same role as the so called “electric part of the Riemann tensor” in the geodesic deviation equation. The magnetic-type tidal tensors are, in the electromagnetic case, gradients of the magnetic field, and their gravitational counterpart is the so-called magnetic part of the Riemann tensor. Physically, the latter manifests itself, for instance, in the deviation from geodesic motion of a spinning test particle due to a net gravitational force acting on it, in analogy with the electromagnetic force exerted on a magnetic dipole. In the framework of the tidal tensor formalism, the exact gravitational force on a gyroscope (Mathisson 1937; Papapetrou 1951; Pirani 1956) is described by an equation formally identical to the electromagnetic force on a magnetic dipole. Moreover, both Maxwell and part of the Einstein equations (the time-time and time-space projections) may be expressed exactly as equations for tidal tensors and sources, and such equations exhibit a striking analogy. In particular, these equations show explicitly that mass currents generate the gravitomagnetic tidal tensor just like currents of charge involve the magnetic tidal tensor of electromagnetism (Costa and Herdeiro 2008). At this point it is important to make a distinction between the “gravitomagnetic field” causing, e.g., the precession of a gyroscope (see Section 1.2), and the gravitomagnetic tidal field causing e.g. the net force on a the gyroscope. The gravitomagnetic field itself has no physical existence; it is a pure coordinate artifact that can be gauged away by moving to a freely falling (non-rotating) frame. For instance, it is well known that the spin 4-vector of a gyroscope undergoes Fermi-Walker transport, with no real torques applied on it; thus the gyroscope “precession” is a non-covariant notion attached to a specific coordinate system, which is the reference frame of the distant stars, i.e., it does not have a local existence, and can only be measured by locking to the distant stars by means of a

¹See, e.g., Misner et al. (1973) Section 7.1, box 7.1 and Section 18.3, and Ohanian and Ruffini (1994), Chapter 3.

²See, e.g., Tartaglia and Ruggiero (2004).

telescope (Polnarev 1986). The gravitomagnetic tidal tensor, instead, describes physical forces, which can be locally measured (Polnarev 1986).

There have been several proposals to detect the GM tidal forces originating by the proper angular momentum \vec{S} of a central body like the Earth. In principle, they can be detected by an orbiting tidal force sensor, or “gravity gradiometer”, as suggested by Braginsky and Polnarev (1980). In the following years such a concept was further investigated (Mashhoon and Theiss 1982), also from the point of view of a practical implementation in terms of a set of orbiting superconducting gravity gradiometers (SGG) (Mashhoon et al. 1989; Paik 1989). Paik (2008) recently reviewed the feasibility of the gravity gradiometer experiment in view of the latest advancements in the field. According to Paik (2008), the GM field of the Earth could be successfully detected by using an orbiting SGG. Such a mission would benefit from the technologies already developed for GP-B (see Section 1.2). The SGG would be launched in a superfluid helium dewar, and the helium boil-off gas would be used for drag-free control of the satellite. GP-B, like gyros or telescopes, may be used for attitude control of the spacecraft.

Other GM effects which have recently received attention from the phenomenological point of view are those caused by the orbital motion of the Earth-Moon system around the Sun. They have nothing to do with the proper angular momenta \vec{S} of the Earth or the Sun causing the “intrinsic” GM effects like those previously mentioned; in the case of translational mass-energy currents it is customarily to speak about “extrinsic” GM effects. According to Nordtvedt (1988, 2003), the extrinsic GM interaction has already been observed with a relative accuracy of 1 part to 1000 in comprehensive fits of the motions of several astronomical and astrophysical bodies like satellites, binary pulsars and the Moon. In fact, a debate arose about the ability of the Lunar Laser Ranging (LLR) technique (Dickey et al. 1994) of detecting genuine GM effects (Murphy et al. 2007a; Kopeikin 2007; Murphy et al. 2007b; Soffel et al. 2008; Ciufolini 2010). Concerning the Lense-Thirring precessions of the lunar orbit induced by the Earth’s spin, they may remain still undetectable also in the foreseeable future because of overwhelming systematic uncertainties (Iorio 2009a), in spite of the expected mm-level improvements in Earth-Moon ranging with LLR (Murphy et al. 2008).

Several Earth-based laboratory experiments aimed to test the influence of the “intrinsic” terrestrial GM field on classical and quantum objects and electromagnetic waves have been proposed so far (Braginsky et al. 1977, 1984; Cerdonio et al. 1988; Ljubičić and Logan 1992; Camacho and Ahluwalia 2001; Tartaglia and

Ruggiero 2002; Iorio 2003a; Stedman et al. 2003; Iorio 2006a), but they have never been implemented because of several technological difficulties in meeting the stringent requirements in terms of sensitivity and/or accuracy.

As gravitomagnetic effects are, in general, analyzed in the framework of the linearized theory of GTR, they have also an important connection with Gravitational Waves (GWs) (Iorio and Corda 2009, 2010; Baskaran and Grishchuk 2004; Corda 2007b). We recall that the data analysis of interferometric detectors has nowadays been started, and the scientific community awaits a first direct detection of GWs in the near future. For the current status of GW interferometers we refer to Giazotto (2008). Thus, the indirect evidence for the existence of GWs by Hulse and Taylor (1975) might soon be confirmed. Detectors for GWs will be important for a better knowledge of the Universe (Iorio and Corda 2010) and also because the interferometric GWs detection will be the ultimate test for GTR or, alternatively, a strong endorsement for Extended Theories of Gravity (Corda 2009). In fact, if advanced projects on the detection of GWs improve their sensitivity, allowing the scientific community to perform a GW astronomy, accurate angle- and frequency-dependent response functions of interferometers for GWs arising from various theories of gravity will permit to discriminate among GTR and extended theories of gravity. This ultimate test will work because standard GTR admits only two polarizations for GWs, while in all extended theories there exist at least three polarizations states; see Corda (2009) for details. On the other hand, the discovery of GW emission by the compact binary system composed of two Neutron Stars PSR1913+16 (Hulse and Taylor 1975) represents, for scientists working in this research field, the definitive thrust allowing to reach the extremely sophisticated technology needed for investigating in this field of research (Iorio and Corda 2010). GWs are a consequence of Einstein’s GTR (Einstein 1915), which presupposes GWs to be ripples in the spacetime curvature traveling at light speed (Einstein 1916, 1918; Iorio and Corda 2010). The importance of gravitomagnetic effects in the field of a GW has been emphasized by Baskaran and Grishchuk (2004). For a complete review of such a topic, see Iorio and Corda (2010). Recently, the analysis has been extended to gravitomagnetic effects in the field of GWs arising by Scalar Tensor Gravity too (Corda et al. 2010; Iorio and Corda 2010).

1.1 The Lense-Thirring effect

After the birth of the Einstein’s Special Theory of Relativity (STR) in 1905, the problem of a “magnetic”-type

component of the gravitational field of non-static mass distributions was tackled in the framework of the search for a consistent relativistic theory of gravitation (Einstein 1913).

With a preliminary and still incorrect version of GTR, Einstein and Besso in 1913 (Klein et al. 1955) calculated the node precession of planets in the field of the rotating Sun; the figures they obtained for Mercury and Venus were incorrect also because they used a wrong value for the solar mass. Soon after GTR was put forth by Einstein in 1915, de Sitter (1916) worked out the corresponding shifts of the planet's perihelia for ecliptic orbits due to the rotation of the Sun; however, his result for Mercury (-0.01 arcseconds per century) was too large by one order of magnitude because he assumed a homogenous and uniformly rotating Sun. In 1918 Thirring (1918a) analyzed in a short article the formal analogies between the Maxwell equations and the linearized Einstein equations. Later, Thirring (1918a,b, 1921) computed the centrifugal and Coriolis-like gravitomagnetic forces occurring inside a rotating massive shell. Lense and Thirring (1918)³ worked out the gravitomagnetic effects on the orbital motions of test particles outside a slowly rotating mass; in particular, they computed the gravitomagnetic rates for the two satellites of Mars (Phobos and Deimos), and for some of the moons of the giant gaseous planets. They found for the longitude of the ascending node Ω and the argument of pericenter ω a pro- and retrograde precession, respectively, according to⁴

$$\dot{\Omega}_{\text{LT}} = \frac{2GS}{c^2 a^3 (1-e^2)^{3/2}}, \quad \dot{\omega}_{\text{LT}} = -\frac{6GS \cos I}{c^2 a^3 (1-e^2)^{3/2}}, \quad (3)$$

where a, e, I are the semimajor axis, the eccentricity and the inclination of the test particle's orbital plane to the central body's equator, respectively. Later, the Lense-Thirring effect was re-derived in a number of different approaches; see, e.g., Bogorodskii (1959); Zel'dovich and Novikov (1971); Barker and O'Connell (1974); Landau and Lifshitz (1975); Ashby and Allison (1993); Iorio (2001a); Lämmerzahl and Neugebauer (2001); Chashchina et al. (2009). In the following we give some more physical insights about the derivation and the characteristics of eq. (1)-eq. (2) and, conse-

quently, of eq. (3). In the standard parameterized post-Newtonian⁵ (PPN) framework for an isolated, weakly gravitating and slowly rotating body, the PPN space-time metric coefficients involving its angular momentum are the off-diagonal terms

$$g_{0i} = -\frac{(\gamma+1)}{c^2} \mathcal{V}_i, \quad i = 1, 2, 3, \quad (4)$$

with

$$\vec{\mathcal{V}} \doteq \frac{G}{c} \frac{\vec{S} \times \vec{r}}{r^3}. \quad (5)$$

In eq. (4) γ is the PPN parameter accounting for the spatial curvature caused by a unit mass; in GTR $\gamma = 1$. Thus, in the PPN approximation the resulting Christoffel symbols including \mathcal{V}_i , $i = 1, 2, 3$ and entering the geodesic equation of motion are (Soffel 1989)

$$\Gamma_{0j}^i = -\frac{(\gamma+1)}{c^2} \left(\frac{\partial \mathcal{V}_i}{\partial x^j} - \frac{\partial \mathcal{V}_j}{\partial x^i} \right), \quad i, j = 1, 2, 3; \quad (6)$$

they give rise to eq. (1)-eq. (2) for $\gamma = 1$. It is interesting and useful to emphasize the complete analogy of eq. (2) with the Lorentz force of electromagnetism provided that the factor -2 entering eq. (2) can be formally thought as a gravitomagnetic charge-to-mass ratio q_g/m . As originally done by Lense and Thirring (1918), the orbital precessions of the node Ω and the pericenter ω of eq. (3) can be straightforwardly worked out with, e.g., the Gauss equations for the variation of the Keplerian orbital elements (Soffel 1989; Roy 2005) by treating the gravitomagnetic force eq. (2) as a small perturbation of the Newtonian monopole. The Gauss equations for Ω and ω are (Soffel 1989; Roy 2005)

$$\frac{d\Omega}{dt} = \frac{1}{na \sin I \sqrt{1-e^2}} A_\nu \left(\frac{r}{a} \right) \sin u, \quad (7)$$

$$\begin{aligned} \frac{d\omega}{dt} &= \frac{\sqrt{1-e^2}}{nae} \left[-A_r \cos f + A_\tau \left(1 + \frac{r}{p} \right) \sin f \right] - \\ &- \cos I \frac{d\Omega}{dt}, \end{aligned} \quad (8)$$

³However, in August 1917 Einstein (Schulmann et al. 1998) wrote to Thirring that he calculated the Coriolis-type field of the rotating Earth and Sun, and its influence on the orbital elements of planets (and moons). A detailed history of the formulation of the so-called Lense-Thirring effect has recently been outlined by Pfister (2007); according to him, it would be more fair to speak about an Einstein-Thirring-Lense effect.

⁴In fact, Lense and Thirring (1918) considered the longitude of pericenter $\varpi \doteq \Omega + \omega$.

⁵The post-Newtonian formalism allows to approximate the non-linear Einstein field equations for weak fields and slow motions in terms of the lowest order deviations from the Newton's theory. In the framework of the parameterized post-Newtonian formalism (Eddington 1922; Ni 1972; Nordtvedt 1968, 1969; Will 1971), such departures from classical gravity are expressed in terms of a set of ten parameters to discriminate between competing metric theories of relativistic gravity. The modern notation is due to Will and Nordtvedt (1972). For a comprehensive review, see Will (1993).

where $n \doteq \sqrt{GM/a^3}$ is the Keplerian mean motion, $u \doteq \omega + f$ is the argument of latitude in which f is the true anomaly, and A_r, A_τ, A_ν are the projections of the perturbing acceleration onto the radial, transverse and normal components of an orthonormal frame co-moving with the test particle. In the case of eq. (2) these projections correspond to (Soffel 1989)

$$A_r^{\text{LT}} = \eta \cos I (1 + e \cos f), \quad (9)$$

$$A_\tau^{\text{LT}} = -\eta e \cos I \sin f, \quad (10)$$

$$A_\nu^{\text{LT}} = \eta \sin I (1 + e \cos f) \left[2 \sin u + e \left(\frac{\sin f \cos u}{1 + e \cos f} \right) \right], \quad (11)$$

with

$$\eta \doteq \frac{\chi n}{a^2 (1 - e^2)^{7/2}} (1 + e \cos f)^3, \quad (12)$$

and

$$\chi \doteq \frac{2GS}{c^2}. \quad (13)$$

It is immediately seen from eq. (9)–eq. (11) that for polar orbits (i.e. $I = 90$ deg), both the radial and the transverse components vanish, contrary to the out-of-plane component. This fact can easily be inferred also from the dipolar field structure and the Lorentz-type force, i.e. eq. (1)–eq. (2). Indeed, if \vec{S} lies in the orbital plane, the latter one contains \vec{B}_g as well, so that, according to eq. (2), \vec{A}_{GM} is entirely out-of-plane. In that case there is also no pericenter precession, as indicated by eq. (3) since all terms in eq. (8) vanish for $I = 90$ deg. By analogous reasoning it is easy to figure out that for equatorial orbits (i.e. $I = 0$ deg) A_{GM} completely lies in the orbital plane which is in agreement with eq. (9)–eq. (11). If the orbit is circular in addition, A_{GM} , which is perpendicular to \vec{S} and \vec{v} , becomes entirely radial, as confirmed by eq. (9)–eq. (10). Finally, since the factor $\sin I$ cancels in eq. (7) and eq. (11) the Lense-Thirring node precession is independent of I , as stated by eq. (3).

1.2 The gyroscope precession

Another well known GM effect consists of the precession of a gyroscope moving in the field of a slowly rotating body. It was worked out in 1959 by Pugh (1959) and in 1960 by Schiff (1960a,b,c) on the basis of the Mathisson (1937) and Papapetrou (1951) equation and became known as the Schiff effect. More recent derivations, based on a quantum mechanical approach

to gravitation, can be found in Barker and O’Connell (1970, 1972).

In order to yield a direct, physical insight of such a phenomenon, let us recall the following basic facts of Maxwellian electromagnetism. A charged spinning particle with electric charge q , mass m and spin $\vec{\sigma}$ has a magnetic moment

$$\vec{\mu} = \left(\frac{q}{2mc} \right) \vec{\sigma}, \quad (14)$$

so that it precesses in an external magnetic field \vec{B} according to

$$\frac{d\vec{\sigma}}{dt} = \vec{\mu} \times \vec{B} = - \left(\frac{q}{2mc} \right) \vec{B} \times \vec{\sigma} \doteq \vec{\mathfrak{D}} \times \vec{\sigma} \quad (15)$$

with the precessional frequency

$$\vec{\mathfrak{D}} \doteq - \left(\frac{q}{2mc} \right) \vec{B}. \quad (16)$$

Moving now to the weak-field and slow-motion approximation of linearized gravitomagnetism and recalling that the gravitomagnetic charge-to-mass ratio is $q_g/m \doteq -2$, according to eq. (14) a spinning particle like a gyroscope is endowed with a gravitomagnetic dipole moment

$$\vec{\mu}_g \doteq - \frac{\vec{\sigma}}{c}, \quad (17)$$

so that it undergoes a precession during its motion in an external gravitomagnetic field \vec{B}_g with frequency

$$\vec{\mathfrak{D}}_g \doteq \frac{\vec{B}_g}{c}. \quad (18)$$

Since the GM-field of a distant rotating astronomical body is given by eq. (1), the precession frequency becomes

$$\vec{\mathfrak{D}}_g = - \frac{G}{c^2 r^3} \left[\vec{S} - 3 \left(\vec{S} \cdot \hat{r} \right) \hat{r} \right]. \quad (19)$$

If the gyroscope moves along an equatorial orbit⁶, then

$$\frac{d\vec{\sigma}}{dt} = - \frac{G}{c^2 r^3} \vec{S} \times \vec{\sigma} \quad (20)$$

and there is no precession of the orbit in case the two spins are aligned. If the orbit of the gyroscope is polar, then, by choosing a plane $\{xz\}$ reference frame with, say,

$$\vec{S} = S \hat{z} \quad (21)$$

⁶For simplicity, we will assume it circular.

and

$$\hat{r} = \cos nt \hat{x} + \sin nt \hat{z} \quad (22)$$

it is easy to show that the averaged precession vanishes if $\vec{\sigma}$ and \vec{S} are parallel or antiparallel, i.e. for

$$\vec{\sigma} = \pm \sigma \hat{z}. \quad (23)$$

Finally, if $\vec{\sigma}$ is orthogonal to \vec{S} and to the orbital plane, i.e.

$$\vec{\sigma} = \pm \sigma \hat{y}, \quad (24)$$

then there is a net spin precession given by

$$\left\langle \frac{d\vec{s}}{dt} \right\rangle = \frac{G}{2c^2 r^3} \vec{S} \times \vec{\sigma}. \quad (25)$$

Soon after the formulation of the Schiff effect, in 1961 Fairbank and Schiff (1961) submitted to NASA a proposal for a dedicated space-based project aimed to directly measure the precession of eq. (25) in a dedicated, controlled experiment. Such an extraordinary and extremely sophisticated mission, later named Gravity Probe B (GP-B) (Everitt 1974; Everitt et al. 2001), consisted of a drag-free, liquid helium-cooled spacecraft moving in a polar, low⁷ orbit around the Earth and carrying onboard four superconducting gyroscopes whose GM precessions of 39 milliarcseconds per year (mas yr⁻¹ in the following) should have been detected by Superconducting Quantum Interference Devices (SQUID) with an expected accuracy of 1% or better. It took 43 years to be implemented before GP-B was finally launched on 20 April 2004; the science data collection lasted from 27 August 2004 to 29 September 2005, while the data analysis is still ongoing (Conklin et al. 2008; Everitt et al. 2009). It seems that the final accuracy obtainable will be less than initially expected because of the occurrence of unexpected systematic errors (Muhlfelder et al. 2009; Keiser et al. 2009; Silbergleit et al. 2009). At present, the GP-B team reports⁸ evidence of the gravitomagnetic spin precessions as predicted by GTR, with a statistical error of $\approx 14\%$ and systematic uncertainty of $\approx 10\%$.

In 1975 Haas and Ross (1975) proposed to measure the angular momenta of the Sun and Jupiter by exploiting the Schiff effect with dedicated spacecraft-based missions, but such a proposal was not carried out so far.

1.3 The gravitomagnetic clock effect

Zel'dovich (1965) discovered that the gravitational field of a rotating mass of radius R and angular momentum S splits the line emitted by an atom with frequency f_0 into two components with opposite circular polarizations and frequencies $f_0 \pm \Delta f$, where

$$\Delta f = \frac{2GS}{c^2 R^3} \quad (26)$$

for an electromagnetic signal emitted on the body's surface at the pole. It is a gravitational analog of the electromagnetic Zeeman effect and, as such, it does not depend on the specific properties of the system emitting the electromagnetic radiation, thus being the same for an atom or a molecule and independent from the emitted frequency. A similar effect for the orbital motion of test particles around a spinning body of mass M and angular momentum S was discovered later by Vladimirov et al. (1987). They noted that in the equatorial plane of a rotating mass the gravitomagnetic force becomes purely radial (if the motion occurs at a constant distance r), and acts as a supplement to the centripetal Newtonian monopole; it is clearly elucidated by eq. (9)-eq. (10). Such an additional term, may be either positive, i.e. directed outward so that it weakens the overall gravitational force, if the particle's motion coincides with the direction of rotation of the central body, or negative, thus enhancing the force of gravity, if the motion is opposite to the rotation. As a consequence, the orbital period of a particle moving along a circular and equatorial orbit in the Lense-Thirring metric is longer in the first case and shorter in the second⁹. This fact contradicts the idea of frame-dragging where it is conceived that a moving object is “dragged” by spacetime which in turn is “twisted” by the rotation of the central mass. If this were the case, the “dragged” test particle should move faster when co-rotating with the central body and should thus have a shorter period. Interestingly, such a change in the period of the particle's orbit is a universal and structurally very simple quantity, given by

$$T_{\text{GM}} = \pm 2\pi \frac{S}{Mc^2}. \quad (27)$$

It is amazing that eq. (27) is independent of both the Newtonian gravitational constant G and the orbital radius. Cohen and Mashhoon (1993) suggested to consider the difference between the orbital periods of two

⁷Its altitude was 642 km.

⁸See on the WEB: <http://einstein.stanford.edu/>

⁹Remember that the period of a pendulum's oscillations decreases as the force acting on it increases

counter-orbiting clocks moving around a rotating astronomical body along circular and equatorial orbits because it cancels the common Keplerian terms and enhances the gravitomagnetic ones by adding them up. This is the so-called gravitomagnetic clock effect (Mashhoon et al. 1999, 2001a). Theiss (1985) worked out the case of circular orbits with arbitrary inclinations showing that the time difference decreases with increasing inclination; for a polar orbit the effect vanishes as it is expected because of symmetry. The general case for arbitrary values of the eccentricity and the inclination was treated by Mashhoon et al. (2001b) and Lichtenegger and Iorio (2007). If one considers two satellites orbiting a slowly rotating mass M in opposite directions, their common initial position in the orbital plane is given by the argument of latitude $u_0 \doteq \omega_0 + f_0$. In taking the difference of the sidereal periods of the satellites, the gravitoelectric perturbations cancel, leaving

$$\Delta T^{\text{sid}} = \frac{4\pi S \cos I}{c^2 M} \left[-\frac{3}{\sqrt{1-e^2}} + \frac{2(2 - \tan^2 I \cos^2 u_0)}{(1 + e \cos f_0)^2} \right] \quad (28)$$

which reduces to the difference of the GM corrections T_{GM} for counter-orbiting particles of (27) in case of $e = I = 0$. It is interesting to note that this clock effect can reveal a relatively large value by a careful choice of the initial parameters (Lichtenegger and Iorio 2007).

Based on various approaches (e.g., analogies with electromagnetism, spacetime geometric properties), derivations of the gravitomagnetic clock effect for the circular and equatorial cases can be found in (You 1998; Iorio et al. 2002b; Tartaglia 2000a). Gronwald et al. (1997) proposed to detect the gravitomagnetic clock effect with a space-based mission – dubbed Gravity Probe C – in the gravitational field of the Earth where such an effect would be as large as 10^{-7} s. In view of the challenging difficulties of implementing such a demanding experiment, a number of studies were performed to mainly investigate the impact of several competing dynamical effects acting as sources of insidious systematical uncertainty (Lichtenegger et al. 2000; Iorio 2001b,c; Iorio and Lichtenegger 2005; Lichtenegger et al. 2006). Tartaglia (2000b) preliminarily looked at the possibilities offered by other Solar System scenarios finding that, in principle, the less unfavorable situation occurs for the Sun and Jupiter.

1.4 Motivations for attempting to directly measure the Lense-Thirring effect

GTR is a basic pillar of our knowledge of Nature since it currently represents our best theory of gravi-

tation, which is one of the four fundamental interactions governing the physical world. The simplicity, the internal coherence and the mathematical elegance of GTR are remarkable, but the level of its empirical corroboration, although certainly satisfactorily up to now (Will 2006), is not comparable to that of the other theories describing the remaining fundamental interactions. This applies both to the number of successfully tested predictions of GTR as well as to the level of accuracy reached. Notably the level of empirical corroboration of GM, which is a constitutive, fundamental aspect of GTR is to date extraordinarily poor. It is therefore desirable to expand and strengthen the empirical basis of the theory by testing as many diverse aspects and predictions as possible using different methods and techniques. It is also necessary, however, to devise observational/experimental tests in those extreme regimes in which the theory in its currently accepted form is believed to experience failures. This is particularly important in order to gain possible hints on a future quantum gravity theory which should combine both gravitational and quantum phenomena.

Concerning the GP-B mission, aimed to test a well defined GM prediction using the gravitational field of the Earth, although different teams may have the possibility to repeat the analysis of the currently available data record with various approaches and techniques, the results of the mission are likely doomed to remain unique since it will be impossible to replicate the entire experiment in any foreseeable future. For the moment, its level of accuracy is more or less comparable to or better than that reached in the non-dedicated¹⁰ tests of the Lense-Thirring effect with the terrestrial LAGEOS satellites. Thus, it becomes of the utmost importance not only to reliably assess the total accuracy in such attempts but also to look for other possibilities offered by different astronomical scenarios by exploiting future planned/proposed spacecraft-based missions and expected improvements in ranging techniques. Such an effort has the merit, among other things, to realistically establish the limits which may likely be reached in such an endeavor. Moreover, as a non-negligible by-product, the knowledge of several classical effects, regarded in the present context as sources of unwanted systematic biases but interesting if considered from different points of view, will turn out to be greatly improved by the tireless efforts towards the measurement of such a tiny relativistic feature of motion. Last but not least, it should be recalled that reaching a satisfying level of knowledge of GM has important consequences in the

¹⁰LAGEOS and LAGEOS II were originally launched for other purposes.

study of extreme astrophysical scenarios in which, as we know, GM may play a very important role (Thorne et al. 1986; Thorne 1988; Williams 1995, 2004; Arvanitaki and Dubovsky 2010).

Another source of motivation to exploit gravitomagnetic effects is their possible relation with Mach’s principle. While GTR as a whole – despite its name – appears not to fulfill Machian expectations of a description of motion with only relative concepts, some special GM phenomena seem to be in accordance with Machian ideas. In particular dragging effects are considered to be the most direct manifestations of Mach’s principle in general relativity because they indicate that local inertial frames are at least partially determined by the distribution and currents of mass-energy in the universe. Thus the study of gravitomagnetism may provide a deeper insight into the presumed intimate connection between inertial properties and matter.

2 Measuring the Lense-Thirring effect in the gravitational field of the Earth

Soon after the dawn of the space age with the launch of Sputnik in 1957 Soviet scientists proposed to directly test the general relativistic Lense-Thirring effect with artificial satellites orbiting the Earth. In particular, Ginzburg (1957, 1959, 1962) proposed to use the perigee of a terrestrial spacecraft in a highly elliptic orbit, while Bogorodskii (1959) considered also the node. Yilmaz (1959), aware of the aliasing effect of the much larger classical precessions induced by the non-sphericity of the Earth, proposed to launch a satellite in a polar orbit to cancel them. About twenty years later, Van Patten and Everitt (1976a); van Patten and Everitt (1976b) suggested to use a pair of drag-free, counter-orbiting terrestrial spacecraft in nearly polar orbits to detect their combined Lense-Thirring node precessions. Almost contemporaneously, Cugusi and Proverbio (1977, 1978) suggested to use the passive geodetic satellite LAGEOS, in orbit around the Earth since 1976 and tracked with the Satellite Laser Ranging (SLR) technique (Degnan 1985), along with the other existing laser-ranged targets to measure the Lense-Thirring node precession. About ten years later, Ciufolini (1986) proposed a somewhat simpler version of the van Patten-Everitt mission consisting of looking at the sum of the nodes of LAGEOS and of another SLR satellite to be launched in the same orbit, apart from the inclination which should be switched by 180 deg in order to minimize the competing classical precessions due to the centrifugal oblateness of the Earth. Iorio (2003b) showed that such an orbital configuration would allow, in principle, to use the difference of the perigees as well. Test calculations were performed

by Ciufolini et al. (1996, 1997a) with the LAGEOS and LAGEOS II satellites, according to a strategy by Ciufolini (1996) involving the use of a suitable linear combination of the nodes Ω of both satellites and the perigee ω of LAGEOS II in order to remove the impact of the first two multipoles of the non-spherical gravitational potential of the Earth. Latest tests have been reported by Ciufolini and Pavlis (2004), Ciufolini et al. (2006), Ciufolini (2007), Ciufolini et al. (2009), Lucchesi (2007a), and Ries et al. (2008); Ries (2009) with only the nodes of both satellites according to a combination of them explicitly proposed by Iorio and Morea (2004). The total uncertainty reached is still a matter of debate (Iorio 2005a; Ciufolini and Pavlis 2005; Lucchesi 2005; Iorio 2006b, 2007d, 2009c, 2010a; Ciufolini et al. 2009) because of the lingering uncertainties in the Earth’s multipoles and in how to evaluate their biasing impact; it may be as large as $\approx 20 - 30\%$ according to conservative evaluations (Iorio 2005a, 2006b, 2007d, 2009c, 2010a), while more optimistic views (Ciufolini and Pavlis 2004, 2005; Ciufolini et al. 2006; Ries et al. 2008; Ries 2009; Ciufolini et al. 2009) point towards $\approx 10 - 15\%$.

2.1 The LAGEOS-LAGEOS II tests

LAGEOS (Cohen and Smith 1985) was put into orbit in March 1976, followed by its twin LAGEOS II (Zerbini 1989) in October 1992; they are passive, spherical spacecraft entirely covered by retroreflectors which allow for their accurate tracking through laser pulses sent from Earth-based ground stations. They orbit at altitudes of about 6000 km in nearly circular paths markedly inclined to the Earth’s equator; see Table 1 for their orbital geometries and Lense-Thirring node precessions¹¹. The corresponding linear shifts amount to about 1.7 m yr^{-1} in the cross-track direction¹² at the LAGEOS altitudes.

Since earlier studies (Bogorodskii 1959; Cugusi and Proverbio 1978), researchers were aware that a major source of systematic errors is represented by the even

¹¹Cugusi and Proverbio (1978) quoted 40 mas yr^{-1} for the Lense-Thirring node precession of LAGEOS by modeling the Earth as a spinning homogeneous sphere. The correct value for the Lense-Thirring node precession of LAGEOS was obtained by Ciufolini (1986).

¹²A perturbing acceleration like \vec{A}_{GM} is customarily projected onto the radial \hat{r} , transverse $\hat{\tau}$ and cross-track $\hat{\nu}$ directions of an orthogonal frame comoving with the satellite (Soffel 1989); it turns out that the Lense-Thirring node precession affects the cross-track component of the orbit according to $\Delta\nu_{\text{LT}} \approx a \sin I \Delta\Omega_{\text{LT}}$ (eq. (A65), p. 6233 in (Christodoulidis et al. 1988)).

Table 1 Orbital parameters and Lense-Thirring node precessions of LAGEOS, LAGEOS II, LARES and GRACE for $S_{\oplus} = 5.86 \times 10^{33} \text{ kg m}^2 \text{ s}^{-1}$ (McCarthy and Petit 2004). The semimajor axis a is in km, the inclination I is in deg, and the Lense-Thirring rate $\dot{\Omega}_{\text{LT}}$ is in mas yr^{-1} .

Satellite	a	e	I	$\dot{\Omega}_{\text{LT}}$
LAGEOS	12270	0.0045	109.9	30.7
LAGEOS II	12163	0.014	52.65	31.5
LARES	7828	0.0	71.5	118.1
GRACE	6835	0.001	89.02	177.4

($\ell = 2, 4, 6, \dots$) zonal ($m = 0$) harmonic coefficients¹³ J_{ℓ} , $\ell = 2, 4, 6$ of the multipolar expansion of the classical part of the terrestrial gravitational potential, accounting for its departures from spherical symmetry due to the Earth's diurnal rotation, induce competing secular precessions¹⁴ of the node and the perigee of satellites (Kaula 1966) whose nominal sizes are several orders of magnitude larger than the Lense-Thirring ones. They cannot be removed from the time series of data without affecting the Lense-Thirring pattern itself as well. The only thing that can be done is to model such a corrupting effect as most accurately as possible and assessing the impact of the residual mismodelling on the measurement of the gravitomagnetic effect. In the case of the node, the secular precessions induced by the even zonals of the geopotential can be written as

$$\dot{\Omega}^{\text{geopot}} = \sum_{\ell=2} \dot{\Omega}_{\ell} J_{\ell}, \quad (29)$$

where the coefficients $\dot{\Omega}_{\ell}$, $\ell = 2, 4, 6, \dots$ depend on the parameters of the Earth (GM and the equatorial radius R) and on the semimajor axis a , the inclination I and the eccentricity e of the satellite. For example, for $\ell = 2$ the largest precession is due to the first even zonal harmonic J_2 which, in the small eccentricity approximation valid for geodetic satellites, is given by

$$\dot{\Omega}_{J_2} = -\frac{3}{2}n \left(\frac{R_{\oplus}}{a} \right)^2 \frac{\cos I J_2}{(1-e^2)^2}. \quad (30)$$

The mismodelling in the geopotential-induced precessions can be written as

$$\delta \dot{\Omega}^{\text{geopot}} \leq \sum_{\ell=2} |\dot{\Omega}_{\ell}| \delta J_{\ell}, \quad (31)$$

¹³The relation among the even zonals J_{ℓ} and the normalized Stokes gravity coefficients $\bar{C}_{\ell 0}$, which are customarily determined in the global Earth's gravity solutions, is $J_{\ell} \doteq -\sqrt{2\ell+1} \bar{C}_{\ell 0}$.

¹⁴Also the mean anomaly \mathcal{M} experiences secular precession due to the even zonals, but it is not involved in the measurement of the Lense-Thirring effect with the LAGEOS satellites.

where δJ_{ℓ} represents our uncertainty in the knowledge of the even zonals J_{ℓ} . The coefficients $\dot{\Omega}_{\ell}$ of the aliasing classical node precessions (Kaula 1966) $\dot{\Omega}^{\text{geopot}}$ induced by the even zonals have been analytically worked out up to $\ell = 20$ in the small eccentricity approximation by, e.g. Iorio (2003c).

The three-elements combination used by Ciufolini et al. (1996) allowed for removing the uncertainties in J_2 and J_4 . In Ciufolini et al. (1998a) a $\approx 20\%$ test was reported by using the¹⁵ EGM96 Earth gravity model (Lemoine et al. 1998); subsequent detailed analyses showed that such an evaluation of the total error budget was overly optimistic in view of the likely unreliable computation of the total bias due to the even zonals (Iorio 2003c; Ries et al. 2003a,b). An analogous, huge underestimation turned out to hold also for the effect of the non-gravitational perturbations (Milani et al. 1987) like the direct solar radiation pressure, the Earth's albedo, various subtle thermal effects depending on the physical properties of the satellites' surfaces and their rotational state (Inversi and Vespe 1994; Vespe 1999; Lucchesi 2001, 2002, 2003, 2004; Lucchesi et al. 2004; Ries et al. 2003a), which the perigees of LAGEOS-like satellites are particularly sensitive to. As a result, the realistic total error budget in the test reported in (Ciufolini et al. 1998a) might be as large as 60 – 90% or (by considering EGM96 only) even more.

The observable used by Ciufolini and Pavlis (2004) with the EIGEN-GRACE02S model (Reigber et al. 2005) and by Ries et al. (2008) with other more recent Earth gravity models was a linear combination¹⁶ of the nodes of LAGEOS and LAGEOS II

$$f \doteq \dot{\Omega}^{\text{LAGEOS}} + c_1 \dot{\Omega}^{\text{LAGEOS II}}, \quad (32)$$

which was explicitly computed by Iorio and Morea (2004) following the approach put forth by Ciufolini (1996). Here,

$$c_1 \doteq -\frac{\dot{\Omega}_{2.2}^{\text{LAGEOS}}}{\dot{\Omega}_{2.2}^{\text{LAGEOS II}}}, \quad (33)$$

and by means of eq. (30) we find

$$c_1 = -\frac{\cos I_{\text{LAGEOS}}}{\cos I_{\text{LAGEOS II}}} \left(\frac{1 - e_{\text{LAGEOS II}}^2}{1 - e_{\text{LAGEOS}}^2} \right)^2 \left(\frac{a_{\text{LAGEOS II}}}{a_{\text{LAGEOS}}} \right)^{\frac{7}{2}},$$

¹⁵Contrary to the subsequent models based on the dedicated satellites CHAMP (<http://www-app2.gfz-potsdam.de/pb1/op/champ/>) and GRACE (http://www-app2.gfz-potsdam.de/pb1/op/grace/index_GRACE.html), EGM96 relies upon multidecadal tracking of SLR data of a constellation of geodetic satellites including LAGEOS and LAGEOS II as well; thus the possibility of a sort of *a-priori* 'imprinting' of the Lense-Thirring effect itself, not solved-for in EGM96, cannot be neglected.

¹⁶See also (Pavlis 2002; Ries et al. 2003a,b).

(34)

where the values of Table 1 approximately yield $c_1 = 0.544$. The Lense-Thirring signature of eq. (32) amounts to 47.8 mas yr^{-1} . The combination of eq. (32) allows, by construction, to remove the aliasing effects due to the static and time-varying parts of the first even zonal J_2 . The nominal (i.e. computed with the estimated values of J_ℓ , $\ell = 4, 6, \dots$) bias due to the remaining higher degree even zonals would amount to about 10^5 mas yr^{-1} ; the need for a careful and reliable modeling of such an important source of systematic bias is thus quite apparent. Conversely, the nodes of the LAGEOS-type spacecraft are directly affected by the non-gravitational accelerations at a $\approx 1\%$ level of the Lense-Thirring effect (Lucchesi 2001, 2002, 2003, 2004; Lucchesi et al. 2004). For a comprehensive, up-to-date overview of the numerous and subtle issues concerning the measurement of the Lense-Thirring effect see, e.g., (Iorio 2007a).

2.1.1 Conservative evaluation of the impact of the mismodelling in the even zonal harmonics

A common feature of all the competing evaluations so far published is that the systematic bias due to the static component of the geopotential was always calculated by using the released (more or less accurately calibrated) sigmas σ_{J_ℓ} of one Earth gravity model solution at a time for the uncertainties δJ_ℓ . Thus, it was said that the model X yields a $x\%$ error, the model Y yields a $y\%$ error, and so on.

Since a trustable calibration of the formal, statistical uncertainties in the estimated zonals of the covariance matrix of a global solution is always a difficult task to be implemented in a reliable way, a much more realistic and conservative approach consists, instead, of taking the difference¹⁷

$$\Delta J_\ell = |J_\ell(X) - J_\ell(Y)|, \ell = 2, 4, 6, \dots \quad (35)$$

of the estimated even zonals for different pairs of Earth gravity field solutions as representative of the real uncertainty δJ_ℓ in the zonals (Lerch et al. 1994). In Tables 2–13 we present our results for the most recent GRACE-based models released so far by different institutions and retrievable in the Internet at¹⁸ <http://icgem.gfz-potsdam.de/ICGEM/>. The models used are EIGEN-GRACE02S (Reigber et al. 2005)

from GFZ (Potsdam, Germany), GGM02S (Tapley et al. 2005) and GGM03S (Tapley et al. 2007) from CSR (Austin, Texas), ITG-Grace02s (Mayer-Gürr et al. 2006), ITG-Grace03s (Mayer-Gürr 2007) and ITG-Grace2010s (Mayer-Gürr et al. 2010) from IGG (Bonn, Germany), JEM01-RL03B from JPL (NASA, USA), AIUB-GRACE01S (Jäggi et al. 2008) and AIUB-GRACE02S (Jäggi et al. 2009) from AIUB (Switzerland). This approach was explicitly followed also, e.g., by Milani et al. (1987) with the GEM-L2 and GEM 9 models, and by Ciufolini (1996) with the JGM3 and GEMT-2 models. Note that we do not consider models including data from CHAMP, LAGEOS itself¹⁹ and Earth-based data. In Tables 2–13 we quote both the sum $\sum_{\ell=4}^{20} f_\ell$ of the absolute values of the individual mismodelled terms (denoted by SAV)

$$f_\ell \doteq \left| \dot{\Omega}_\ell^{\text{LAGEOS}} + c_1 \dot{\Omega}_\ell^{\text{LAGEOS II}} \right| \Delta J_\ell \quad (36)$$

and the square root of the sum of their squares $\sqrt{\sum_{\ell=4}^{20} f_\ell^2}$ (RSS); in both cases we normalized them to the combined Lense-Thirring total precession of 47.8 mas yr^{-1} .

The systematic bias evaluated with a more realistic approach is about 3 to 4 times larger than the one obtained by using only a single particular model. The scatter is still quite large and far from the 5 – 10% claimed in Ciufolini and Pavlis (2004). In particular, it appears that J_4 , J_6 , and to a lesser extent J_8 , which are just the most relevant zonals for us because of their impact on the combination of eq. (32), are the most uncertain ones, with discrepancies ΔJ_ℓ between different models, in general, larger than the sum of their sigmas σ_{J_ℓ} , whether calibrated or not.

Such an approach has been criticized by Ciufolini et al. (2009) by writing that one should not compare models with different intrinsic accuracies. Moreover, Ciufolini et al. (2009) claim that our method would be exactly equivalent to compare a modern value of the Newtonian gravitational constant G , accurate to 10^{-5} , to the earlier results obtained in the 18th century, accurate to 10^{-2} , and conclude that the present-day accuracy would be wrong by a factor 1000. Such criticisms are incorrect for the following reasons. According to CODATA²⁰, the present-day relative accuracy in G is $1.0 \times 10^{-4} = 0.01\%$, not 0.0015%, corresponding to

¹⁷See Fig.5 of Lucchesi (2007b) for a comparison of the estimated \bar{C}_{40} in different models.

¹⁸L. I. thanks M Watkins (JPL) for having provided me with the even zonals and their sigmas of the JEM01-RL03B model.

¹⁹It is just one of the devices with which the Lense-Thirring effect is measured: using Earth's gravity models including its data would yield a-priori “imprint” of GTR itself. Note that the latest models by GFZ are unsuitable for our purposes because they make use of LAGEOS data.

²⁰See <http://physics.nist.gov/cuu/Constants/> on the WEB.

Table 2 Impact of the mismodelling in the even zonal harmonics on $f_\ell = |\dot{\Omega}_\ell^{\text{LAGEOS}} + c_1 \dot{\Omega}_{\ell}^{\text{LAGEOS II}}| \Delta J_\ell$, $\ell = 4, \dots, 20$, in mas yr⁻¹. Recall that $J_\ell = -\sqrt{2\ell+1} \bar{C}_{\ell 0}$; for the uncertainty in the even zonals we have taken here the difference $\Delta \bar{C}_{\ell 0} = |\bar{C}_{\ell 0}^{(X)} - \bar{C}_{\ell 0}^{(Y)}|$ between the model X=GGM02S (Tapley et al. 2005) and the model Y=ITG-Grace02s (Mayer-Gürr et al. 2006). GGM02S is based on 363 days of GRACE-only data (GPS and intersatellite tracking, neither constraints nor regularization applied) spread between April 4, 2002 and Dec 31, 2003. The σ are formal for both models. $\Delta \bar{C}_{\ell 0}$ are always larger than the linearly added sigmas, apart from $\ell = 12$ and $\ell = 18$. Values of f_ℓ smaller than 0.1 mas yr⁻¹ have not been quoted. The Lense-Thirring precession of the combination of eq. (32) amounts to 47.8 mas yr⁻¹. The percent bias $\delta\mu$ have been computed by normalizing the linear sum of f_ℓ , $\ell = 4, \dots, 20$ (SAV) and the square root of the sum of f_ℓ^2 , $\ell = 4, \dots, 20$ to the Lense-Thirring combined precessions.

ℓ	$\Delta \bar{C}_{\ell 0}$ (GGM02S-ITG-Grace02s)	$\sigma_X + \sigma_Y$	f_ℓ (mas yr ⁻¹)
4	1.9×10^{-11}	8.7×10^{-12}	7.2
6	2.1×10^{-11}	4.6×10^{-12}	4.6
8	5.7×10^{-12}	2.8×10^{-12}	0.2
10	4.5×10^{-12}	2.0×10^{-12}	-
12	1.5×10^{-12}	1.8×10^{-12}	-
14	6.6×10^{-12}	1.6×10^{-12}	-
16	2.9×10^{-12}	1.6×10^{-12}	-
18	1.4×10^{-12}	1.6×10^{-12}	-
20	2.0×10^{-12}	1.6×10^{-12}	-
$\delta\mu = 25\%$ (SAV)		$\delta\mu = 18\%$ (RSS)	

Table 3 Bias due to the mismodelling in the even zonals of the models X=ITG-Grace03s (Mayer-Gürr 2007), based on GRACE-only accumulated normal equations from data out of September 2002-April 2007 (neither apriori information nor regularization used), and Y=GGM02S (Tapley et al. 2005). The σ for both models are formal. $\Delta \bar{C}_{\ell 0}$ are always larger than the linearly added sigmas, apart from $\ell = 12$ and $\ell = 18$.

ℓ	$\Delta \bar{C}_{\ell 0}$ (ITG-Grace03s-GGM02S)	$\sigma_X + \sigma_Y$	f_ℓ (mas yr ⁻¹)
4	2.58×10^{-11}	8.6×10^{-12}	9.6
6	1.39×10^{-11}	4.7×10^{-12}	3.1
8	5.6×10^{-12}	2.9×10^{-12}	0.2
10	1.03×10^{-11}	2×10^{-12}	-
12	7×10^{-13}	1.8×10^{-12}	-
14	7.3×10^{-12}	1.6×10^{-12}	-
16	2.6×10^{-12}	1.6×10^{-12}	-
18	8×10^{-13}	1.6×10^{-12}	-
20	2.4×10^{-12}	1.6×10^{-12}	-
$\delta\mu = 27\%$ (SAV)		$\delta\mu = 21\%$ (RSS)	

1.5×10^{-5} , as claimed by Ciufolini et al. (2009); thus, according to their reasoning corrected for this error, our approach would be exactly equivalent to state that the present-day accuracy in G would be wrong by a factor of 100. Moreover, the relative uncertainties in the Earth’s gravity models considered are, in fact, all of the same order of magnitude; for example, the relative uncertainty in \bar{C}_{40} is 7.2×10^{-6} from EIGEN-GRACE02S (Reigber et al. 2005) and 7.8×10^{-6} in the more recent GGM03S model²¹ (Tapley et al. 2007). Thus, the comparison drawn by Ciufolini et al. (2009) between G and the even zonals is misleading. Even more important, it is well known that the rejection of a “suspect” exper-

imental result from a sample of data is always a very delicate matter (Taylor 1997), and quantitative criteria are needed to reject one or more outliers (Peirce 1852; Chauvenet 1863). Instead, Ciufolini et al. (2009) do not apply any of them to support their claims against the comparison of various geopotential models. The most famous rejection criterion is perhaps the one devised by Chauvenet (1863). Anyway, it relies upon an arbitrary assumption that a measurement may be rejected if the probability of obtaining the deviation from the mean for that value is less than the inverse of twice the number of measurements; moreover, it makes no distinction between the case of one or several suspicious data values. The criterion by Peirce (1852), instead, is a rigorous theory that can be easily applied in the case of several suspicious data values using the table in Ross (2003). Let us apply it to the case of G . If we consider

²¹The relative uncertainty in \bar{C}_{40} is 2×10^{-7} for ITG-Grace2010s (Mayer-Gürr et al. 2010), but it must be recalled that for such a model the available errors are the formal, statistical ones.

Table 4 Bias due to the mismodelling in the even zonals of the models X = GGM02S (Tapley et al. 2005) and Y = GGM03S (Tapley et al. 2007) retrieved from data spanning January 2003 to December 2006. The σ for GGM03S are calibrated. $\Delta\bar{C}_{\ell 0}$ are larger than the linearly added sigmas for $\ell = 4, 6$. (The other zonals are of no concern)

ℓ	$\Delta\bar{C}_{\ell 0}$ (GGM02S-GGM03S)	$\sigma_X + \sigma_Y$	f_ℓ (mas yr $^{-1}$)
4	1.87×10^{-11}	1.25×10^{-11}	6.9
6	1.96×10^{-11}	6.7×10^{-12}	4.2
8	3.8×10^{-12}	4.3×10^{-12}	0.1
10	8.9×10^{-12}	2.8×10^{-12}	0.1
12	6×10^{-13}	2.4×10^{-12}	-
14	6.6×10^{-12}	2.1×10^{-12}	-
16	2.1×10^{-12}	2.0×10^{-12}	-
18	1.8×10^{-12}	2.0×10^{-12}	-
20	2.2×10^{-12}	1.9×10^{-12}	-
$\delta\mu = 24\%$ (SAV)		$\delta\mu = 17\%$ (RSS)	

Table 5 Bias due to the mismodelling in the even zonals of the models X = EIGEN-GRACE02S (Reigber et al. 2005) and Y = GGM03S (Tapley et al. 2007). The σ for both models are calibrated. $\Delta\bar{C}_{\ell 0}$ are always larger than the linearly added sigmas apart from $\ell = 14, 18$.

ℓ	$\Delta\bar{C}_{\ell 0}$ (EIGEN-GRACE02S-GGM03S)	$\sigma_X + \sigma_Y$	f_ℓ (mas yr $^{-1}$)
4	2.00×10^{-11}	8.1×10^{-12}	7.4
6	2.92×10^{-11}	4.3×10^{-12}	6.3
8	1.05×10^{-11}	3.0×10^{-12}	0.4
10	7.8×10^{-12}	2.9×10^{-12}	0.1
12	3.9×10^{-12}	1.8×10^{-12}	-
14	5×10^{-13}	1.7×10^{-12}	-
16	1.7×10^{-12}	1.4×10^{-12}	-
18	2×10^{-13}	1.4×10^{-12}	-
20	2.5×10^{-12}	1.4×10^{-12}	-
$\delta\mu = 30\%$ (SAV)		$\delta\mu = 20\%$ (RSS)	

the set of modern measurements in Table 13 of Mohr and Taylor (1999), accurate to $10^{-3} - 10^{-4}$, and the result by Cavendish (1798), accurate to 10^{-2} , reported by de Boer (1984) and Ohanian and Ruffini (1994), it turns out that, according to the Peirce (1852) criterion, the oldest value must be rejected. On the contrary, if we apply the Peirce (1852) criterion to all the values of, e.g., \bar{C}_{40} from the models considered, no one of them has to be rejected. Interestingly, if we also considered models including CHAMP, LAGEOS and Earth-based data, and even the latest SLR-based solutions, the result would not change: indeed, concerning \bar{C}_{40} , only the CHAMP-based TUM-2S model (Wermuth et al. 2004) would not pass the Peirce (1852) criterion. Thus, we do not see any founded, quantitative reasons to decline the comparison among different Earth’s gravity models followed here.

Another way to evaluate the uncertainty in the LAGEOS-LAGEOS II node test may consist of computing the nominal values of the total combined precessions for different models and comparing them, i.e.

by taking

$$\left| \sum_{\ell=4} \left(\dot{\Omega}_{\ell}^{\text{LAGEOS}} + c_1 \dot{\Omega}_{\ell}^{\text{LAGEOS II}} \right) [J_\ell(X) - J_\ell(Y)] \right|. \quad (37)$$

The results for each pair of models are shown in Table 14. Their average is about 17%.

A further, different approach that could be followed to take into account the scatter among the various solutions consists in computing mean and standard deviation of the entire set of values of the even zonals for the models considered so far, degree by degree, and taking the standard deviations as representative of the uncertainties δJ_ℓ , $\ell = 4, 6, 8, \dots$. It yields $\delta\mu = 15\%$, a figure slightly larger than that by Ries et al. (2008). Anyway, in evaluating mean and standard deviation for each even zonals, Ries et al. (2008) also used global gravity solutions like EIGEN-GL04C (Förste et al. 2006) and EIGEN-GL05C (Förste et al. 2008) which include data from the LAGEOS satellite itself; this may likely have introduced a sort of favorable a priori “imprint”

Table 6 Bias due to the mismodelling in the even zonals of the models X = JEM01-RL03B, based on 49 months of GRACE-only data, and Y = GGM03S (Tapley et al. 2007). The σ for GGM03S are calibrated. $\Delta\bar{C}_{\ell 0}$ are always larger than the linearly added sigmas apart from $\ell = 16$.

ℓ	$\Delta\bar{C}_{\ell 0}$ (JEM01-RL03B-GGM03S)	$\sigma_X + \sigma_Y$	f_ℓ (mas yr $^{-1}$)
4	1.97×10^{-11}	4.3×10^{-12}	7.3
6	2.7×10^{-12}	2.3×10^{-12}	0.6
8	1.7×10^{-12}	1.6×10^{-12}	-
10	2.3×10^{-12}	8×10^{-13}	-
12	7×10^{-13}	7×10^{-13}	-
14	1.0×10^{-12}	6×10^{-13}	-
16	2×10^{-13}	5×10^{-13}	-
18	7×10^{-13}	5×10^{-13}	-
20	5×10^{-13}	4×10^{-13}	-
$\delta\mu = 17\%$ (SAV)		$\delta\mu = 15\%$ (RSS)	

Table 7 Bias due to the mismodelling in the even zonals of the models X = JEM01-RL03B and Y = ITG-Grace03s (Mayer-Gürr 2007). The σ for ITG-Grace03s are formal. $\Delta\bar{C}_{\ell 0}$ are always larger than the linearly added sigmas.

ℓ	$\Delta\bar{C}_{\ell 0}$ (JEM01-RL03B-ITG-Grace03s)	$\sigma_X + \sigma_Y$	f_ℓ (mas yr $^{-1}$)
4	2.68×10^{-11}	4×10^{-13}	9.9
6	3.0×10^{-12}	2×10^{-13}	0.6
8	3.4×10^{-12}	1×10^{-13}	0.1
10	3.6×10^{-12}	1×10^{-13}	-
12	6×10^{-13}	9×10^{-14}	-
14	1.7×10^{-12}	9×10^{-14}	-
16	4×10^{-13}	8×10^{-14}	-
18	4×10^{-13}	8×10^{-14}	-
20	7×10^{-13}	8×10^{-14}	-
$\delta\mu = 22\%$ (SAV)		$\delta\mu = 10\%$ (RSS)	

of the Lense-Thirring effect itself. Moreover, Ries et al. (2008) gave only a RSS evaluation of the total bias.

It should be recalled that also the further bias due to the cross-coupling between J_2 and the orbit inclination, evaluated to be about 9% in Iorio (2007d), must be added.

2.1.2 An a-priori, “imprinting” effect?

GRACE recovers the spherical harmonic coefficients of the geopotential from the tracking of both satellites by GPS and from the observed intersatellite distance variations (Reigber et al. 2005). A potential critical issue is, thus, a possible “memory” effect of the gravitomagnetic force. Its impact in the satellite-to-satellite tracking was preliminarily addressed in Iorio (2005a); here we will focus on the “imprint” coming from the GRACE orbits which is more important for us because it mainly resides in the low degree even zonals (Iorio 2010b).

Concerning that issue, Ciufolini and Pavlis (2005) write that such a kind of leakage of the Lense-Thirring signal itself into the even zonals retrieved by GRACE is completely negligible because the GRACE satellites move along (almost) polar orbits. Indeed, for perfectly polar ($I = 90$ deg) trajectories, the gravitomagnetic

force is entirely out-of-plane, while the perturbing action of the even zonals is confined to the orbital plane itself. According to Ciufolini and Pavlis (2005), the deviations of the orbit of GRACE from the ideal polar orbital configuration would have negligible consequences on the “imprint” issue. In particular, they write: “the values of the even zonal harmonics determined by the GRACE orbital perturbations are substantially independent on the a priori value of the LenseThirring effect. [...] The small deviation from a polar orbit of the GRACE satellite, that is 1.7×10^{-2} rad, gives only rise, *at most*, to a very small correlation with a factor 1.7×10^{-2} ”. The meaning of such a statement is unclear; anyway, we will show below that such a conclusion is incorrect.

The relevant orbital parameters of GRACE are quoted in Table 1; variations of the orders of about 10 km in the semimajor axis a and 0.001 deg in the inclination I may occur, but it turns out that they are irrelevant in our discussion (<http://www.csr.utexas.edu/grace/ground/globe.html>). The orbital plane of GRACE is, in fact, shifted by 0.98 deg from the ideal polar configuration, and, contrary to what is claimed in Ciufolini and Pavlis (2005), this does matter because its classical secular node precessions are far from be-

Table 8 Aliasing effect of the mismodelling in the even zonal harmonics estimated in the X=ITG-Grace03s (Mayer-Gürr 2007) and the Y=EIGEN-GRACE02S (Reigber et al. 2005) models. The covariance matrix σ for ITG-Grace03s are formal, while the ones of EIGEN-GRACE02S are calibrated. $\Delta\overline{C}_{\ell 0}$ are larger than the linearly added sigmas for $\ell = 4, \dots, 20$, apart from $\ell = 18$.

ℓ	$\Delta\overline{C}_{\ell 0}$ (ITG-Grace03s-EIGEN-GRACE02S)	$\sigma_X + \sigma_Y$	f_ℓ (mas yr ⁻¹)
4	2.72×10^{-11}	3.9×10^{-12}	10.1
6	2.35×10^{-11}	2.0×10^{-12}	5.1
8	1.23×10^{-11}	1.5×10^{-12}	0.4
10	9.2×10^{-12}	2.1×10^{-12}	0.1
12	4.1×10^{-12}	1.2×10^{-12}	-
14	5.8×10^{-12}	1.2×10^{-12}	-
16	3.4×10^{-12}	9×10^{-13}	-
18	5×10^{-13}	1.0×10^{-12}	-
20	1.8×10^{-12}	1.1×10^{-12}	-
$\delta\mu = 37\%$ (SAV)		$\delta\mu = 24\%$ (RSS)	

Table 9 Bias due to the mismodelling in the even zonals of the models X = JEM01-RL03B, based on 49 months of GRACE-only data, and Y = AIUB-GRACE01S (Jäggi et al. 2008). The latter one was obtained from GPS satellite-to-satellite tracking data and K-band range-rate data out of the period January 2003 to December 2003 using the Celestial Mechanics Approach. No accelerometer data, no de-aliasing products, and no regularisation was applied. The σ for AIUB-GRACE01S are formal. $\Delta\overline{C}_{\ell 0}$ are always larger than the linearly added sigmas.

ℓ	$\Delta\overline{C}_{\ell 0}$ (JEM01-RL03B-AIUB-GRACE01S)	$\sigma_X + \sigma_Y$	f_ℓ (mas yr ⁻¹)
4	2.95×10^{-11}	2.1×10^{-12}	11
6	3.5×10^{-12}	1.3×10^{-12}	0.8
8	2.14×10^{-11}	5×10^{-13}	0.7
10	4.8×10^{-12}	5×10^{-13}	-
12	4.2×10^{-12}	5×10^{-13}	-
14	3.6×10^{-12}	5×10^{-13}	-
16	8×10^{-13}	5×10^{-13}	-
18	7×10^{-13}	5×10^{-13}	-
20	1.0×10^{-12}	5×10^{-13}	-
$\delta\mu = 26\%$ (SAV)		$\delta\mu = 23\%$ (RSS)	

ing negligible with respect to our issue. The impact of the Earth’s gravitomagnetic force on the even zonals retrieved by GRACE can be quantitatively evaluated by computing the “effective” value $\overline{C}_{\ell 0}^{LT}$ of the normalized even zonal gravity coefficients which would induce classical secular node precessions for GRACE as large as those due to its Lense-Thirring effect, which is independent of the inclination I . To be more precise, $\overline{C}_{\ell 0}^{LT}$ comes from solving the following equation which connects the classical even zonal precession of degree ℓ $\dot{\Omega}_{J_\ell} \doteq \dot{\Omega}_{\ell} J_\ell$ to the Lense-Thirring node precession $\dot{\Omega}_{LT}$

$$\dot{\Omega}_{\ell} J_\ell = \dot{\Omega}_{LT}. \quad (38)$$

Table 15 lists $\overline{C}_{\ell 0}^{LT}$ for degrees $\ell = 4, 6$, which are the most effective in affecting the combination of eq. (32). Thus, the gravitomagnetic field of the Earth contributes to the value of the second even zonal of the geopotential retrieved from the orbital motions of GRACE by an amount of the order of 2×10^{-10} , while for $\ell = 6$ the imprint is one order of magnitude smaller. Given

the present-day level of accuracy of the latest GRACE-based solutions, which is of the order of 10^{-12} , effects as large as those of Table 15 cannot be neglected. Thus, we conclude that the influence of the Earth’s gravitomagnetic field on the low-degree even zonal harmonics of the global gravity solutions from GRACE may exist, falling well within the present-day level of measurability.

A further, crucial step consists of evaluating the impact of such an a-priori “imprint” on the test conducted with the LAGEOS satellites and the combination of eq. (32): if the LAGEOS-LAGEOS II uncanceled combined classical geopotential precession computed with the GRACE-based a-priori “imprinted” even zonals of Table 15 is a relevant part of – or even larger than – the combined Lense-Thirring precession, it will be demonstrated that the doubts concerning the a-priori gravitomagnetic “memory” effect are founded. It turns out that this is just the case because eq. (32) and Table 15 yield a combined geopotential precession whose magnitude is 77.8 mas yr^{-1} ($-82.9 \text{ mas yr}^{-1}$ for $\ell = 4$ and

Table 10 Bias due to the mismodelling in the even zonals of the models X = EIGEN-GRACE02S (Reigber et al. 2005) and Y = AIUB-GRACE01S (Jäggi et al. 2008). The σ for AIUB-GRACE01S are formal, while those of EIGEN-GRACE02S are calibrated. $\Delta\overline{C}_{\ell 0}$ are larger than the linearly added sigmas for $\ell = 4, 6, 8, 16$.

ℓ	$\Delta\overline{C}_{\ell 0}$ (EIGEN-GRACE02S–AIUB-GRACE01S)	$\sigma_X + \sigma_Y$	f_ℓ (mas yr ⁻¹)
4	2.98×10^{-11}	6.0×10^{-12}	11.1
6	2.29×10^{-11}	3.3×10^{-12}	5.0
8	1.26×10^{-11}	1.9×10^{-12}	0.4
10	6×10^{-13}	2.5×10^{-12}	-
12	5×10^{-13}	1.6×10^{-12}	-
14	5×10^{-13}	1.6×10^{-12}	-
16	2.9×10^{-12}	1.4×10^{-12}	-
18	6×10^{-13}	1.4×10^{-12}	-
20	2×10^{-13}	1.5×10^{-12}	-
$\delta\mu = 34\%$ (SAV)		$\delta\mu = 25\%$ (RSS)	

Table 11 Bias due to the mismodelling in the even zonals of the models X = JEM01-RL03B and Y = AIUB-GRACE02S (Jäggi et al. 2009). The σ for both AIUB-GRACE02S and JEM01-RL03B are formal. $\Delta\overline{C}_{\ell 0}$ are larger than the linearly added sigmas for $\ell = 4 - 20$.

ℓ	$\Delta\overline{C}_{\ell 0}$ (JEM01-RL03B–AIUB-GRACE02S)	$\sigma_X + \sigma_Y$	f_ℓ (mas yr ⁻¹)
4	1.58×10^{-11}	2×10^{-13}	5.9
6	5.9×10^{-12}	1×10^{-13}	1.3
8	5.8×10^{-12}	1×10^{-13}	0.2
10	1.27×10^{-11}	1×10^{-13}	0.1
12	4.3×10^{-12}	1×10^{-13}	-
14	2.7×10^{-12}	1×10^{-13}	-
16	1.6×10^{-12}	1×10^{-13}	-
18	1.8×10^{-12}	1×10^{-13}	-
20	1.9×10^{-12}	1×10^{-13}	-
$\delta\mu = 16\%$ (SAV)		$\delta\mu = 13\%$ (RSS)	

5.1 mas yr⁻¹ for $\ell = 6$), i.e. just 1.6 times the Lense-Thirring signal itself. This means that the part of the LAGEOS-LAGEOS II uncanceled classical combined node precessions which is affected by the “imprinting” of the Lense-Thirring force through the GRACE-based geopotential’s spherical harmonics is as large as the LAGEOS-LAGEOS II combined gravitomagnetic signal itself.

We, now, comment on how Ciufolini and Pavlis (2005) reach a different conclusion. They write: “However, the Lense-Thirring effect depends on the third power of the inverse of the distance from the central body, i.e., $(1/r)^3$, and the J_2, J_4, J_6, \dots effects depend on the powers $(1/r)^{3.5}, (1/r)^{5.5}, (1/r)^{7.5}, \dots$ of the distance; then, since the ratio of the semimajor axes of the GRACE satellites to the LAGEOS’ satellites is $\sim \frac{6780}{12270} \cong 1.8$, any conceivable “Lense-Thirring imprint” on the spherical harmonics at the GRACE altitude becomes quickly, with increasing distance, a negligible effect, especially for higher harmonics of degree $l > 4$. Therefore, any conceivable “Lense-Thirring imprint” is negligible at the LAGEOS’ satellites altitude.” From such statements it seems that they compare the classical GRACE precessions with the gravitomagnetic

LAGEOS’ ones. This is meaningless since, as we have shown, one has, first, to compare the classical and relativistic precessions of GRACE itself, with which the Earth’s gravity field is solved for and only after to compute the impact of the relativistically “imprinted” part of the GRACE-based even zonals on the combined LAGEOS nodes. These two stages have to be kept separate, with the first one which is fundamental; if different satellite(s) Y were to be used to measure the gravitomagnetic field of the Earth, the impact of the Lense-Thirring effect itself on them should be evaluated by using the “imprinted” even zonals evaluated in the first stage. Finally, in their latest statement Ciufolini and Pavlis (2005) write: “In addition, in (Ciufolini et al. 1997b), it was proved with several simulations that by far the largest part of this “imprint” effect is absorbed in the by far largest coefficient J_2 .” Also such a statement, in the present context, has no validity since the cited work refers to a pre-GRACE era. Moreover, no quantitative details at all were explicitly released concerning the quoted simulations, so that it is impossible to form an opinion.

Table 12 Bias due to the mismodelling in the even zonals of the models X = ITG-Grace2010s (Mayer-Gürr et al. 2010) and Y = AIUB-GRACE02S (Jäggi et al. 2009). The ITG-Grace2010s model has been obtained by processing 7 yr (2002-2009) of GRACE data. The σ for both models are formal. $\Delta\overline{C}_{\ell 0}$ are larger than the linearly added sigmas for all the degrees considered.

ℓ	$\Delta\overline{C}_{\ell 0}$ (ITG-Grace2010s–AIUB-GRACE02S)	$\sigma_X + \sigma_Y$	f_ℓ (mas yr ⁻¹)
4	2.665×10^{-11}	1.9×10^{-13}	9.9
6	4.66×10^{-12}	1.1×10^{-13}	1.0
8	3.86×10^{-12}	9×10^{-14}	0.1
10	9.50×10^{-12}	8×10^{-14}	0.1
12	1.67×10^{-12}	7×10^{-14}	-
14	2.36×10^{-12}	7×10^{-14}	-
16	8.7×10^{-13}	6×10^{-14}	-
18	8.0×10^{-13}	6×10^{-14}	-
20	1.09×10^{-12}	7×10^{-14}	-
$\delta\mu = 23\%$ (SAV)		$\delta\mu = 21\%$ (RSS)	

Table 13 Bias due to the mismodelling in the even zonals of the models X = ITG-Grace2010s (Mayer-Gürr et al. 2010) and Y = GGM03S (Tapley et al. 2007). The σ of ITG-Grace2010s are formal, while those for GGM03S are calibrated. $\Delta\overline{C}_{\ell 0}$ are larger than the linearly added sigmas for $\ell = 4, 10, 12, 16, 18$.

ℓ	$\Delta\overline{C}_{\ell 0}$ (ITG-Grace2010s–GGM03S)	$\sigma_X + \sigma_Y$	f_ℓ (mas yr ⁻¹)
4	3.05×10^{-11}	4.3×10^{-12}	11.3
6	1.4×10^{-12}	2.3×10^{-12}	0.3
8	3×10^{-13}	1.6×10^{-12}	-
10	9×10^{-13}	8×10^{-13}	-
12	1.9×10^{-12}	6×10^{-13}	-
14	6×10^{-13}	6×10^{-13}	-
16	9×10^{-13}	4×10^{-13}	-
18	1.7×10^{-12}	4×10^{-13}	-
20	2×10^{-13}	4×10^{-13}	-
$\delta\mu = 25\%$ (SAV)		$\delta\mu = 24\%$ (RSS)	

2.1.3 A new approach to extract the Lense-Thirring signature from the data

The technique adopted so far by Ciufolini and Pavlis (2004) and Ries et al. (2008) to extract the gravitomagnetic signal from the LAGEOS and LAGEOS II data is described in detail in (Lucchesi and Balmino 2006; Lucchesi 2007b). In both approaches the Lense-Thirring force is not included in the dynamical force models used to fit the satellites’ data. In the data reduction process no dedicated gravitomagnetic parameter is estimated, contrary to, e.g., station coordinates, state vector, satellite drag and radiation coefficients C_D and C_R , respectively, etc.; its effect is retrieved with a sort of post-post-fit analysis in which the time series of the computed²² “residuals” of the nodes with the difference between the orbital elements of consecutive arcs, combined with eq. (32), is fitted with a straight line.

²²The expression “residuals of the nodes” is used, strictly speaking, in an improper sense because the Keplerian orbital elements are not directly measured.

In regard to possible other approaches which could be followed, it would be useful to, e.g., estimate (in the least square sense), among other solve-for parameters, purely phenomenological corrections $\Delta\dot{\Omega}$ to the LAGEOS/LAGEOS II node precessions as well, without modelling the Lense-Thirring effect itself, so that it will be, in principle, contained in $\Delta\dot{\Omega}$, and combine them according to eq. (32). Something similar has been done – although for different scopes – for the perihelia of the inner planets of the solar system (Pitjeva 2005a) (see Section 3) and the periastron of the pulsars (Kramer et al. 2006). To be more definite, various solutions with a complete suite of dynamical models, apart from the gravitomagnetic force itself, should be produced in which one inserts a further solve-for parameter, i.e. a correction $\Delta\dot{\Omega}$ to the standard Newtonian modelled precessions. One could see how the outcome varies by changing the data sets and/or the parameters to be solved for. Maybe it could be done for each arc, so to have a collection of such node extra-rates. Such a strategy would be much more model-independent.

As previously suggested by Nordtvedt (2001), another way to tackle the problem consists of looking at

Table 14 Systematic uncertainty $\delta\mu$ in the LAGEOS-LAGEOS II test evaluated by taking the absolute value of the difference between the nominal values of the total combined node precessions due to the even zonals for different models X and Y, i.e. $|\dot{\Omega}^{\text{geopot}}(\text{X}) - \dot{\Omega}^{\text{geopot}}(\text{Y})|$. The average is $\approx 17\%$.

Models compared	$\delta\mu$
ITG-Grace2010s–JEM01-RL03B	7%
ITG-Grace2010s–GGM02S	0.3%
ITG-Grace2010s–GGM03S	24%
ITG-Grace2010s–ITG-Grace02	25%
ITG-Grace2010s–ITG-Grace03	27%
ITG-Grace2010s–AIUB-GRACE02S	23%
ITG-Grace2010s–AIUB-GRACE01S	27%
ITG-Grace2010s–EIGEN-GRACE02S	5%
AIUB-GRACE02S–JEM01-RL03B	16%
AIUB-GRACE02S–GGM02S	23%
AIUB-GRACE02S–GGM03S	17%
AIUB-GRACE02S–ITG-Grace02	2%
AIUB-GRACE02S–ITG-Grace03	13%
AIUB-GRACE02S–EIGEN-GRACE02S	28%
AIUB-GRACE01S–JEM01-RL03B	20%
AIUB-GRACE01S–GGM02S	27%
AIUB-GRACE01S–GGM03S	3%
AIUB-GRACE01S–ITG-Grace02	2%
AIUB-GRACE01S–ITG-Grace03	0.1%
AIUB-GRACE01S–EIGEN-GRACE02S	33%
JEM01-RL03B–GGM02S	7%
JEM01-RL03B–GGM03S	17%
JEM01-RL03B–ITG-Grace02	18%
JEM01-RL03B–ITG-Grace03s	20%
JEM01-RL03B–EIGEN-GRACE02S	13%
GGM02S–GGM03S	24%
GGM02S–ITG-Grace02	25%
GGM02S–ITG-Grace03s	27%
GGM02S–EIGEN-GRACE02S	6%
GGM03S–ITG-Grace02	1%
GGM03S–ITG-Grace03s	3%
GGM03S–EIGEN-GRACE02S	30%
ITG-Grace02–ITG-Grace03s	2%
ITG-Grace02–EIGEN-GRACE02S	31%
ITG-Grace03s–EIGEN-GRACE02S	33%

a Lense-Thirring-dedicated parameter to be estimated along with all the zonals in a new global solution for the gravity field incorporating the gravitomagnetic component as well; instead, in all the so far produced global gravity solutions no relativistic parameter(s) have been included in the set of the estimated ones. As shown in Section 2.1.2, this would also cure the impact of possible forms of a-priori “imprinting” effects.

A first, tentative step towards the implementation of the strategy of the first point mentioned above with the LAGEOS satellites in terms of the PPN parameter γ has been recently taken by Combrinck (2008).

2.2 The LARES mission

Van Patten and Everitt (1976a) proposed to measure the Lense-Thirring precession of the nodes Ω of a pair of counter-orbiting spacecraft to be launched in terrestrial polar orbits and endowed with a drag-free apparatus. A somewhat equivalent, cheaper version of such an idea was put forth ten years later by Ciufolini (1986, 1989) who proposed to launch a passive, geodetic satellite in an orbit identical to that of LAGEOS apart from the orbital planes which should have been displaced by 180 deg apart. The measurable quantity was, in the case of the proposal by Ciufolini (1986), the sum of the nodes of LAGEOS and of the new spacecraft, later named LAGEOS III (Ciufolini 1994), LARES (Ciufolini et al.

Table 15 $\overline{C}_{\ell 0}^{\text{LT}}$: effective “gravitomagnetic” normalized gravity coefficients for GRACE ($\ell = 4, 6$; $m = 0$). They have been obtained by comparing the GRACE classical node precessions to the Lense-Thirring rate. Thus, they may be viewed as a quantitative measure of the leakage of the Lense-Thirring effect itself into the second and third even zonal harmonics of the global gravity solutions from GRACE. Compare them with the much smaller calibrated errors $\sigma_{\overline{C}_{\ell 0}}$ in \overline{C}_{40} and \overline{C}_{60} of the GGM03S model (Tapley et al. 2007).

$\overline{C}_{40}^{\text{LT}}$	$\overline{C}_{60}^{\text{LT}}$	$\sigma_{\overline{C}_{40}}$	$\sigma_{\overline{C}_{60}}$
2.23×10^{-10}	-2.3×10^{-11}	4×10^{-12}	2×10^{-12}

1998b), and WEBER-SAT²³, in order to cancel to a high level of accuracy the corrupting effect of the multipoles of the Newtonian part of the terrestrial gravitational potential which represent the major source of systematic errors. Although extensively studied by various groups (Ries et al. 1989; Ciufolini et al. 1998b), such an idea was not implemented for many years. Iorio et al. (2002a) proposed to include also the data from LAGEOS II by using a different observable. Such an approach was proven in Iorio (2005b) to be, in principle, potentially useful in making the constraints on the orbital configuration of the new SLR satellite less stringent than it was originally required in view of the recent improvements in our knowledge of the classical part of the terrestrial gravitational potential due to the dedicated CHAMP and, especially, GRACE missions.

Since reaching high altitudes and minimizing the unavoidable orbital injection errors is expensive, the possibility of discarding LAGEOS and LAGEOS II using a low-altitude, nearly polar orbit for LARES (Lucchesi and Paolozzi 2001; Ciufolini 2006) was explored. However, in Iorio (2002, 2007b) it was proven that such alternative approaches are not feasible. It was also suggested that LARES would be able to probe alternative theories of gravity (Ciufolini 2004), but also in this case it turned out to be impossible (Iorio 2005c, 2007c).

The stalemate came to an end when ASI recently approved the LARES mission, although with a different orbital geometry with respect to the original configuration: now the orbital altitude is 1450 km corresponding to a semimajor axis $a = 7828$ km (Ciufolini et al. 2009). See Table 1 for the new orbital parameters and the related Lense-Thirring node precession. LARES should be launched in late 2010/early 2011 with the first qualification flight of the VEGA rocket (<http://www.spacenews.com/civil/100115-asi-expects-budget-remain-flat-2010.html>).

The combination that should be used for measuring the Lense-Thirring effect with LAGEOS, LAGEOS II

and LARES is (Iorio 2005b)

$$\dot{\Omega}^{\text{LAGEOS}} + k_1 \dot{\Omega}^{\text{LAGEOS II}} + k_2 \dot{\Omega}^{\text{LARES}}, \quad (39)$$

where the coefficients k_1 and k_2 entering eq. (39) are defined as

$$k_1 = \frac{\dot{\Omega}_2^{\text{LARES}} \dot{\Omega}_4^{\text{LAGEOS}} - \dot{\Omega}_2^{\text{LAGEOS}} \dot{\Omega}_4^{\text{LARES}}}{\dot{\Omega}_2^{\text{LAGEOS II}} \dot{\Omega}_4^{\text{LARES}} - \dot{\Omega}_2^{\text{LARES}} \dot{\Omega}_4^{\text{LAGEOS II}}} = 0.3586,$$

$$k_2 = \frac{\dot{\Omega}_2^{\text{LAGEOS}} \dot{\Omega}_4^{\text{LAGEOS II}} - \dot{\Omega}_2^{\text{LAGEOS II}} \dot{\Omega}_4^{\text{LAGEOS}}}{\dot{\Omega}_2^{\text{LAGEOS II}} \dot{\Omega}_4^{\text{LARES}} - \dot{\Omega}_2^{\text{LARES}} \dot{\Omega}_4^{\text{LAGEOS II}}} = 0.0751. \quad (40)$$

By construction, the combination eq. (39) cancels the impact of the first two even zonals; we have used $a_{\text{LR}} = 7828$ km and $I_{\text{LR}} = 71.5$ deg. The total Lense-Thirring effect, according to eq. (39) and eq. (40), amounts to 50.8 mas yr⁻¹.

2.2.1 A conservative evaluation of the impact of the geopotential on the LARES mission

The systematic error due to the uncanceled even zonals J_6, J_8, \dots can be conservatively evaluated as

$$\delta\mu \leq \sum_{\ell=6} \left| \dot{\Omega}_{\ell}^{\text{LAGEOS}} + k_1 \dot{\Omega}_{\ell}^{\text{LAGEOS II}} + k_2 \dot{\Omega}_{\ell}^{\text{LARES}} \right| \delta J_{\ell} \quad (41)$$

Of crucial importance is how to assess δJ_{ℓ} . By proceeding as in Section 2.1.1 and by using the same models up to degree $\ell = 60$ because of the lower altitude of LARES with respect to LAGEOS and LAGEOS II which brings into play more even zonals, we come up with the results presented in Table 16. They have been obtained with the standard and widely used Kaula approach (Kaula 1966) in the following way. We, first, calibrated our numerical calculation with the analytical ones performed with the explicit expressions for $\dot{\Omega}_{\ell}$ worked out up to $\ell = 20$ in Iorio (2003c); then, after having obtained identical results, we confidently extended our numerical calculation to higher degrees by means of two different softwares (Matlab and MATHEMATICA).

²³In memory of Dr J. Weber, US Naval Academy (USNA) Class of 1940.

Table 16 Systematic percent uncertainty $\delta\mu$ in the combined Lense-Thirring effect with LAGEOS, LAGEOS II and LARES according to eq. (41) and $\delta J_\ell = \Delta J_\ell$ up to degree $\ell = 60$ for the global Earth’s gravity solutions considered here; the approach by (Kaula 1966) has been followed. For LARES we adopted $a_{\text{LR}} = 7828$ km, $I_{\text{LR}} = 71.5$ deg, $e_{\text{LR}} = 0.0$.

Models compared ($\delta J_\ell = \Delta J_\ell$)	$\delta\mu$ (SAV)	$\delta\mu$ (RSS)
ITG-Grace2010s–JEM01-RL03B	4%	2%
ITG-Grace2010s–GGM02S	14%	8%
ITG-Grace2010s–GGM03S	2%	1%
ITG-Grace2010s–ITG-Grace02	2%	1%
ITG-Grace2010s–ITG-Grace03	2%	1%
ITG-Grace2010s–AIUB-GRACE02S	5%	2%
ITG-Grace2010s–AIUB-GRACE01S	22%	14%
ITG-Grace2010s–EIGEN-GRACE02S	24%	13%
AIUB-GRACE02S–JEM01-RL03B	9%	4%
AIUB-GRACE02S–GGM02S	16%	7%
AIUB-GRACE02S–GGM03S	4%	2%
AIUB-GRACE02S–ITG-Grace02	5%	2%
AIUB-GRACE02S–ITG-Grace03	6%	3%
AIUB-GRACE02S–EIGEN-GRACE02S	24%	13%
AIUB-GRACE02S–AIUB-GRACE01S	23%	13%
AIUB-GRACE01S–JEM01-RL03B	23%	16%
AIUB-GRACE01S–GGM02S	16%	8%
AIUB-GRACE01S–GGM03S	22%	13%
AIUB-GRACE01S–ITG-Grace02	24%	15%
AIUB-GRACE01S–ITG-Grace03	22%	14%
AIUB-GRACE01S–EIGEN-GRACE02S	14%	7%
JEM01-RL03B–GGM02S	14%	9%
JEM01-RL03B–GGM03S	5%	3%
JEM01-RL03B–ITG-Grace02	4%	2%
JEM01-RL03B–ITG-Grace03s	5%	2%
JEM01-RL03B–EIGEN-GRACE02S	26%	15%
GGM02S–GGM03S	13%	7%
GGM02S–ITG-Grace02	16%	8%
GGM02S–ITG-Grace03s	14%	7%
GGM02S–EIGEN-GRACE02S	14%	7%
GGM03S–ITG-Grace02	3%	2%
GGM03S–ITG-Grace03s	2%	0.5%
GGM03S–EIGEN-GRACE02S	24%	13%
ITG-Grace02–ITG-Grace03s	3%	2%
ITG-Grace02–EIGEN-GRACE02S	25%	14%
ITG-Grace03s–EIGEN-GRACE02S	24%	13%

It must be stressed that our results may be still optimistic: indeed, computations for $\ell > 60$ become unreliable because of numerical instability of the results.

In Table 17 we repeat the calculation by using for δJ_ℓ the covariance matrix sigmas σ_{J_ℓ} ; also in this case we use the approach by Kaula (1966) up to degree $\ell = 60$.

If, instead, one assumes $\delta J_\ell = \sigma_\ell$, $\ell = 2, 4, 6, \dots$ i.e., the standard deviations of the sets of all the best estimates of J_ℓ for the models considered here the systematic bias, up to $\ell = 60$, amounts to 12% (SAV) and 6% (RSS). Again, also this result may turn out to be optimistic for the same reasons as before.

It must be pointed out that the evaluations presented here rely upon calculations of the coefficients $\dot{\Omega}_\ell$ performed with the well known standard approach

by Kaula (1966); it would be important to try to follow also different computational strategies in order to test them. In regard to this point, Ciufolini et al. (2009) state that, in reality, the bias due to the even zonals is of the order of 1% or less, and repeatedly write that the results of one of us (L. I.) are based on “miscalculations”. In fact, Ciufolini et al. (2009), do not demonstrate their allegations by explicitly disclosing the alleged error(s).

2.2.2 The impact of some non-gravitational perturbations

It is worthwhile noting that also the impact of the subtle non-gravitational perturbations will be different with respect to the original proposal because LARES will fly in a lower orbit and its thermal behavior will

Table 17 Systematic percent uncertainty $\delta\mu$ in the combined Lense-Thirring effect with LAGEOS, LAGEOS II and LARES according to eq. (41) and $\delta J_\ell = \sigma_{J_\ell}$ up to degree $\ell = 60$ for the global Earth’s gravity solutions considered here; the approach by (Kaula 1966) has been followed. For LARES we adopted $a_{\text{LR}} = 7828$ km, $I_{\text{LR}} = 71.5$ deg, $e_{\text{LR}} = 0.0$.

Model ($\delta J_\ell = \sigma_\ell$)	$\delta\mu$ (SAV)	$\delta\mu$ (RSS)
ITG-Grace2010s (formal)	0.2%	0.1%
AIUB-GRACE02S (formal)	1%	0.9%
AIUB-GRACE01S (formal)	11%	9%
JEM01-RL03B (formal)	1%	0.9%
GGM03S (calibrated)	5%	4%
GGM02S (formal)	20%	15%
ITG-Grace03s (formal)	0.3%	0.2%
ITG-Grace02s (formal)	0.4%	0.2%
EIGEN-GRACE02S (calibrated)	21%	17%

probably be different with respect to LAGEOS and LAGEOS II. The reduction of the impact of the thermal accelerations, like the Yarkovsky-Schach effects, should have been reached with two concentric spheres. However, as explained by Andrés (2007), this solution will increase the floating potential of LARES because of the much higher electrical resistivity and, thus, the perturbative effects produced by the charged particle drag. Moreover, the atmospheric drag will increase also because of the lower orbit of the satellite, both in its neutral and charged components. Indeed, although it does not affect directly the node Ω , it induces a secular decrease of the inclination I of a LAGEOS-like satellite (Milani et al. 1987) which translates into a further bias for the node itself according to

$$\delta\dot{\Omega}_{\text{drag}} = \frac{3}{2}n \left(\frac{R}{a}\right)^2 \frac{\sin I}{(1-e^2)^2} J_2 \delta I, \quad (42)$$

in which δI accounts not only for the measurement errors in the inclination, but also for any unmodelled/mismodelled dynamical effect on it. According to (Iorio 2010c), the secular decrease for LARES would amount to

$$\left\langle \frac{dI}{dt} \right\rangle_{\text{LR}} \approx -0.6 \text{ mas yr}^{-1} \quad (43)$$

yielding a systematic uncertainty in the Lense-Thirring signal of eq. (39) of about $3 - 9\% \text{ yr}^{-1}$. An analogous indirect node effect via the inclination could be induced by the thermal Yarkovski-Rubincam force as well (Iorio 2010c). Also the Earth’s albedo, with its anisotropic components, may have a non-negligible effect.

Ciufolini et al. (2009) objected that, in fact, the disturbing effect examined would not appear in the real data analysis procedure because the inclination along with all the other Keplerian orbital elements would be measured arc by arc, so that one should only have to correct the signal for the measured value of the inclination; after all, the same problems, if not even larger,

would occur with the semimajor axes of the LAGEOS satellites, which are known to undergo still unexplained secular decrease of 1.1 mm d^{-1} (Rubincam 1982) and their consequent mappings onto the node rates. The problem is that while a perturbation Δa pertains the in-plane, radial component (Christodoulidis et al. 1988) of the LAGEOS orbits, both the Lense-Thirring node precession and the shifts in the inclination affect the out-of-plane, normal component of the orbit (Christodoulidis et al. 1988); thus, even if repeated corrections to the semimajor axis could be applied without affecting the gravitomagnetic signal of interest, the same would not hold for the inclination. This is particularly true in view of the fact that, for still unexplained reasons, the Lense-Thirring effect itself has never been estimated, either as a short-arc or as a global parameter. Moreover, it has been claimed that the recent improvements in atmospheric refraction modelling would allow to measure the inclination of the LAGEOS satellites at a level of accuracy, on average, of $30 \mu\text{s}$ for LAGEOS and $10 \mu\text{s}$ for LAGEOS II (Ciufolini et al. 2009). Firstly, the tracking of a relatively low satellite is always more difficult than for higher targets, so that caution would be needed in straightforwardly extrapolating results valid for LAGEOS to the still non-existing LARES. Second, it is difficult to understand the exact sense of such claims because they would imply an accuracy $\delta r \approx a\delta I$ in reconstructing the orbits of LAGEOS and LAGEOS II, on average, of 0.2 cm and 0.06 cm , respectively.

Let us point out the following issue as well. At present, it is not yet clear how the data of LAGEOS, LAGEOS II and LARES will be finally used by the proponent team in order to detect the Lense-Thirring effect. This could turn out to be a non-trivial matter because of the non-gravitational perturbations. Indeed,

if, for instance, a combination²⁴

$$\dot{\Omega}^{\text{LARES}} + h_1 \dot{\Omega}^{\text{LAGEOS}} + h_2 \dot{\Omega}^{\text{LAGEOS II}} \quad (44)$$

was adopted instead of that of eq. (39), the coefficients of the nodes of LAGEOS and LAGEOS II, in view of the lower altitude of LARES, would be

$$h_1 = \frac{\dot{\Omega}_2^{\text{LAGEOS II}} \dot{\Omega}_4^{\text{LARES}} - \dot{\Omega}_2^{\text{LARES}} \dot{\Omega}_4^{\text{LAGEOS II}}}{\dot{\Omega}_2^{\text{LARES}} \dot{\Omega}_4^{\text{LAGEOS II}} - \dot{\Omega}_2^{\text{LAGEOS II}} \dot{\Omega}_4^{\text{LARES}}} = 13.3215,$$

$$h_2 = \frac{\dot{\Omega}_2^{\text{LARES}} \dot{\Omega}_4^{\text{LAGEOS}} - \dot{\Omega}_2^{\text{LAGEOS}} \dot{\Omega}_4^{\text{LARES}}}{\dot{\Omega}_2^{\text{LAGEOS}} \dot{\Omega}_4^{\text{LAGEOS II}} - \dot{\Omega}_2^{\text{LAGEOS II}} \dot{\Omega}_4^{\text{LARES}}} = 4.7744. \quad (45)$$

and the combined Lense-Thirring signal would amount to 676.8 mas yr⁻¹. As a consequence, the direct and indirect effects of the non-gravitational²⁵ perturbations on the nodes of LAGEOS and LAGEOS II would be enhanced by such larger coefficients and this may yield a lower total obtainable accuracy.

3 In search of the Sun's gravitomagnetic field

3.1 General considerations

Recent determinations of the Sun's proper angular momentum

$$S_{\odot} = (190.0 \pm 1.5) \times 10^{39} \text{ kg m}^2 \text{ s}^{-1} \quad (46)$$

from helioseismology (Pijpers 1998, 2003), accurate to 0.8%, yield a value about one order of magnitude smaller than that obtained by assuming a homogeneous and uniformly rotating Sun, as done in the pioneering work by de Sitter (1916), and also by Soffel (1989) and Cugusi and Proverbio (1978) who concluded that, at their time, it was not possible to measure the solar Lense-Thirring effect. Despite the reduced magnitude of the solar gravitomagnetic field with respect to the earlier predictions, the present and near future situation seems more promising. The characteristic length with which the accuracy of the determination of the orbits of the particles should be compared is

$$l_g^{\odot} \doteq \frac{S_{\odot}}{M_{\odot} c} = 319 \text{ m}; \quad (47)$$

in the case of gravitoelectric effects, l_g is usually replaced by the Schwarzschild radius $R_g \doteq 2GM/c^2 = 3$

km for the Sun. The present-day accuracy in knowing, e.g., the inner planets' mean orbital radius

$$\langle r \rangle = a \left(1 + \frac{e^2}{2} \right), \quad (48)$$

is shown in Table 18. Such values have been obtained by linearly propagating the formal, statistical errors in a and e according to Table 3 of Pitjeva (2008); even by re-scaling them by a factor of, say, 2 – 5, the gravitomagnetic effects due to the Sun's rotation fall, in principle, within the measurability domain. Another possible way to evaluate the present-day uncertainty in the planetary orbital motions consists of looking at different ephemerides of comparable accuracy. In Table 18 we do that for the EPM2006/EPM2008 (Pitjeva 2008, 2010), and the DE414/DE421 (Standish 2006; Folkner et al. 2008) ephemerides; although, larger than $\delta \langle r \rangle$, the maximum differences between such ephemerides are smaller than the solar gravitomagnetic length l_g^{\odot} .

With regard to the currently collected ranging data to the Venus Express spacecraft²⁶ and in view of the ongoing Messenger (Balogh et al. 2007) and the future BepiColombo²⁷ (Milani et al. 2002; Balogh et al. 2007) missions to Mercury and of the developments in the Planetary Laser Ranging (PLR) technique, the planetary orbit accuracy is likely to be further improved. More specifically, recent years have seen increasing efforts towards the implementation of PLR accurate to cm-level (Smith et al. 2006; Chandler et al. 2004; Neumann et al. 2006; Degnan 2006; Turyshev and Williams 2007; Merkowitz et al. 2007; Degnan 2008; Zuber and Smith 2008). It would allow to reach major improvements in three related fields: solar system dynamics, tests of general relativity and alternative theories of gravity, and physical properties of the target planet itself. In principle, any solar system body endowed with a solid surface and a transparent atmosphere would be a suitable platform for a PLR system, but some targets are more accessible than others. Major efforts have been practically devoted so far to Mercury (Smith et al. 2006) and Mars (Chandler et al. 2004; Turyshev and Williams 2007), although simulations reaching 93 AU or more have been undertaken as well (Degnan 2006, 2008). In 2005 two interplanetary laser transponder experiments were successfully demonstrated by the Goddard Geophysical Astronomical Observatory (GGAO). The first utilized the non-optimized Mercury Laser Al-

²⁴The impact of the geopotential is, by construction, unaffected with respect to the combination of eq. (39).

²⁵The same may hold also for time-dependent gravitational perturbations affecting the nodes of LAGEOS and LAGEOS II, like the tides.

²⁶See on the WEB http://www.esa.int/esaMI/Venus_Express/.

²⁷It is an ESA mission, including two spacecraft, one of which provided by Japan, to be put into orbit around Mercury. The launch is scheduled for 2014. The construction of the instruments is currently ongoing.

Table 18 First line: uncertainties (in m) in the average heliocentric distances of the inner planets obtained by propagating the formal errors in a and e according to Table 3 of Pitjeva (2008); the EPM2006 ephemerides were used by Pitjeva (2008). Second line: maximum differences (in m) between the EPM2006 and the DE414 (Standish 2006) ephemerides for the inner planets in the time interval 1960-2020 according to Table 5 of Pitjeva (2010). Third line: maximum differences (in m) between the EPM2008 (Pitjeva 2010) and the DE421 (Folkner et al. 2008) ephemerides for the inner planets in the time interval 1950-2050 according to Table 5 of Pitjeva (2010). They have to be compared with the characteristic gravitomagnetic length of the Sun $l_g^\odot = 319$ m.

Type of orbit uncertainty	Mercury	Venus	Earth	Mars
$\delta \langle r \rangle$ (EPM2006)	38	3	1	2
EPM2006–DE414	256	131	17.2	78.7
EPM2008–DE421	185	4.6	11.9	233

timeter (MLA) on the Messenger spacecraft (Smith et al. 2006; Neumann et al. 2006), obtaining a formal error in the laser range solution of 0.2 m, or one part in 10^{11} . The second utilized the Mars Orbiting Laser Altimeter (MOLA) on the Mars Global Surveyor spacecraft (Abshire 2006; Neumann et al. 2006). A precise value of the Earth-Mars distance, measured between their centers of mass and taken over an extended period (five years or more), would support, among other things, a better determination of several parameters of the solar system. Sensitivity analyses point towards measurement uncertainties between 1 mm and 100 mm (Chandler et al. 2004). A recent analysis of the future BepiColombo mission to Mercury, aimed to accurately determining, among other things, several key parameters of post-Newtonian gravity and the solar quadrupole moment from Earth-Mercury distance data collected with a multi-frequency radio link (Milani et al. 2002, 2008), points toward a maximum uncertainty of 4.5 – 10 cm in determining the Earth-Mercury range over a multi-year time span (1-8 yr) (Milani et al. 2002; Ashby et al. 2007; Milani et al. 2008). A proposed spacecraft-based mission aimed to accurately measure also the gravitomagnetic field of the Sun and its J_2 along with other PPN parameters like γ and β by means of interplanetary ranging is the Astrodynamical Space Test of Relativity using Optical Devices²⁸ (ASTROD) (Ni 2008). Another space-based mission proposed to accurately test several aspects of the gravitational interaction via interplanetary laser ranging is the Laser Astrometric Test of Relativity (LATOR) (Turyshev et al. 2009).

It is remarkable to note that the currently available estimate of S_\odot from helioseismology is accurate enough to allow, in principle, a genuine Lense-Thirring test. Moreover, it was determined in a relativity-free fashion from astrophysical techniques which do not rely on the

dynamics of planets in the gravitational field of the Sun. Thus, there is no any a priori “memory” effect of general relativity itself in the adopted value of S_\odot .

3.2 The Lense-Thirring perihelion precessions of the planets and their measurability

The action of the solar gravitomagnetic field on Mercury’s longitude of perihelion²⁹ ϖ was calculated for the first time by de Sitter (1916) who, by assuming a homogenous and uniformly rotating Sun, found a secular rate of -0.01 arcseconds per century (arcsec cy^{-1} in the following). This value is also quoted by Soffel (1989); Cugusi and Proverbio (1978) yield -0.02 arcsec cy^{-1} for the argument of perihelion ω of Mercury.

The recent estimate of the Sun’s angular momentum (Pijpers 1998, 2003) from helioseismology implies a precessional effect for Mercury which is one order of magnitude smaller; see Table 19 for the predicted Lense-Thirring precessions $\dot{\varpi}_{\text{LT}}$ of the longitudes of the perihelia of the inner planets which are of the order of $10^{-3} - 10^{-5}$ arcsec cy^{-1} . They are obtained by taking into account the fact that the inclinations I of the planets usually quoted in the literature refer to the mean ecliptic at a given epoch³⁰ (Roy 2005), while the Sun’s equator is tilted by $\epsilon_\odot = 7.15$ deg to the mean ecliptic at J2000 (Beck and Giles 2005). So far, the solar Lense-Thirring effect on the orbits of the inner planets was believed to be too small to be detected (Soffel 1989). However, the situation seems now favorably changing. Iorio (2005d) preliminarily investigated the possibility of measuring such tiny effects in view of recent important developments in the planetary ephemerides generation.

First attempts to measure the Sun’s Lense-Thirring effect have recently been implemented by Iorio (2007e, 2008a) with the Ephemerides of Planets and the Moon

²⁸Its cheaper version ASTROD I makes use of one spacecraft in a Venus-gravity-assisted solar orbit, ranging optically with ground stations (Appourchaux et al. 2009).

²⁹Since Ω and ω do not lie, in general, in the same plane, ϖ is a “dogleg” angle.

³⁰It is J2000 (JD 2451545.0).

Table 19 First line: corrections $\Delta\dot{\omega}$, in 10^{-4} arcsec cy^{-1} ($1 \text{ arcsec } \text{cy}^{-1} = 10 \text{ mas } \text{yr}^{-1} = 1.5 \times 10^{-15} \text{ s}^{-1}$), to the standard Newton/Einstein secular precessions of the perihelia of the inner planets estimated by Pitjeva (2005a) with the EPM2004 ephemerides. The result for Venus (E.V. Pitjeva, private communication, 2008) has been obtained by recently processing radiometric data from Magellan spacecraft with the EPM2006 ephemerides (Pitjeva 2008); it has also been cited in Table 4 of Fienga et al. (2010) and, as far as the uncertainty is concerned, in Table 1 of Biswas and Mani (2008). The errors in square brackets are the $1 - \sigma$ formal, statistical ones. Second line: predicted Lense-Thirring perihelion precessions $\dot{\omega}_{\text{LT}}$, in 10^{-4} arcsec cy^{-1} (Iorio 2007e). Third line: nominal values of the perihelion precessions due to the Sun’s oblateness for $J_2^\odot = 2 \times 10^{-7}$ (Pireaux and Rozelot 2003; Pitjeva 2005a); the current level of uncertainty in it is about 10% (Fienga et al. 2008). Fourth line: nominal values of the perihelion precessions due to the ring of the minor asteroids for $m_{\text{ring}} = 5 \times 10^{-10} M_\odot$ (Krasinsky et al. 2002); the uncertainty in it amounts to $\delta m_{\text{ring}} = 1 \times 10^{-10} M_\odot$ (Krasinsky et al. 2002). Anyway, more recent estimates yield a smaller uncertainty: it is of the order of $\delta m_{\text{ring}} = 0.1 - 0.3 \times 10^{-10} M_\odot$ (Fienga et al. 2009). Fifth line: nominal values of the perihelion precessions due to a massive ring modelling the action of the Classical Kuiper Belt Objects (CKBOs) for $m_{\text{CKBOs}} = 0.052 m_\oplus = 1.562 \times 10^{-7} M_\odot$ (Iorio 2007f). Actually, they may be smaller since direct estimates of the mass of the TNOs, modelled as a ring in the EPM2008 ephemerides, place an upper limit of $5.26 \times 10^{-8} M_\odot$ (Pitjeva 2010).

	Mercury	Venus	Earth	Mars
$\Delta\dot{\omega}$	-36 ± 50 [42]	-4 ± 5 [1]	-2 ± 4 [1]	1 ± 5 [1]
$\dot{\omega}_{\text{LT}}$	-20	-3	-1	-0.3
$\dot{\omega}_{J_2^\odot}$	+254	+26	+8	+2
$\dot{\omega}_{\text{ring}}$	+3	+7	+11	+24
$\dot{\omega}_{\text{CKBOs}}$	+0.2	+0.6	+1	+2

(EPM2004) produced by Pitjeva (2005b). They are based on a data set of more than 317,000 observations (1913–2003) including radiometric measurements of planets and spacecraft, astrometric CCD observations of the outer planets and their satellites, and meridian and photographic observations. Such ephemerides were constructed by the simultaneous numerical integration of the equations of motion for all planets, the Sun, the Moon, and the 301 largest asteroids. The rotations of the Earth and the Moon, the perturbations from the solar quadrupolar mass moment J_2^\odot and that of the asteroid ring that lies in the ecliptic plane and which consists of the remaining smaller asteroids are included. With regard to the post-Newtonian dynamics, only the gravitoelectric, Schwarzschild-like terms of order $\mathcal{O}(c^{-2})$, in the harmonic gauge (Newhall et al. 1983), were included; the gravitomagnetic force of the Sun was not modelled.

The EPM2004 ephemerides were used by Pitjeva (2005a) to phenomenologically estimate corrections $\Delta\dot{\omega}$ to the known standard Newtonian/Einsteinian secular precessions of the longitudes of perihelia of the inner planets as fitted parameters of a particular solution. Table 19 displays these corrections, which are obtained by comparing computer simulations based on the constructed ephemerides with actual observations. In determining such extra-precessions the PPN parameters γ and β and the solar even zonal harmonic coefficient J_2^\odot were not fitted; they were held fixed to their general relativistic and Newtonian values, i.e. $\gamma = \beta = 1$, $J_2^\odot = 2 \times 10^{-7}$. In the EPM2006 ephemerides (Pitjeva 2008), used to accurately estimate the perihelion

precession of Venus as well, were constructed by also modelling the actions of Eris and of the other 20 largest Trans-Neptunian Objects (TNOs); the database was enlarged by including, among other things, ranging data to the Magellan and Cassini spacecraft.

Although the original purpose³¹ of the estimation of the corrections $\Delta\dot{\omega}$ was not the measurement of the Lense-Thirring effect, the results of Table 19 can be used to take first steps towards an observational corroboration of the existence of the solar gravitomagnetic force.

From Table 19 it turns out that the magnitude of the Lense-Thirring perihelion precessions of the inner planets just lies at the edge of the accuracy in determining $\Delta\dot{\omega}$. All the predicted Lense-Thirring precessions are compatible with the estimated corrections $\Delta\dot{\omega}$. It should be noted that for Venus the $1 - \sigma$ formal, statistical error in $\Delta\dot{\omega}$ is smaller than the gravitomagnetic effect.

³¹The goal of Pitjeva (2005a) was to make a test of the quality of the previously obtained general solution in which certain values of β, γ, J_2^\odot were obtained. If the construction of the ephemerides was satisfactory, very small ‘residual’ effects due to such parameters should have been found. She writes: “At present, as a test, we can determine [...] the corrections to the motions of the planetary perihelia, which allows us to judge whether the values of β, γ and J_2^\odot used to construct the ephemerides are valid.” The smallness of the extra-perihelion precessions found in her particular test-solution is interpreted by Pitjeva as follows: “Table 3 [of Pitjeva (2005a)] shows that the parameters $\gamma = \beta = 1, J_2^\odot = 2 \times 10^{-7}$ used to construct the EPM2004 ephemerides are in excellent agreement with the observations.”

Table 20 Corrections $\Delta\dot{\omega}$, in 10^{-4} arcsec cy^{-1} ($1 \text{ arcsec cy}^{-1} = 10 \text{ mas yr}^{-1} = 1.5 \times 10^{-15} \text{ s}^{-1}$), to the standard Newton/Einstein secular precessions of the perihelia of the inner planets estimated by Pitjeva (2010) with the EPM2008 ephemerides including also radiometric data from Venus Express, Cassini and Magellan for Venus. The uncertainties are realistic. Source: Table 8 of Pitjeva (2010). Cfr. with Table 19.

	Mercury	Venus	Earth	Mars
$\Delta\dot{\omega}$	-40 ± 50	240 ± 330	60 ± 70	-70 ± 70

It must be considered that the inclusion of new data sets, modeling of further dynamical effects and new data processing techniques may have an impact on the estimation of the corrections $\Delta\dot{\omega}$. Thus, we are still in a preliminary, ongoing phase. As an example, in Table 20, retrieved from Table 8 of Pitjeva (2010), we show new results for $\Delta\dot{\omega}$ of the inner planets.

Concerning the systematic alias due to the various competing dynamical effects listed in Table 19, the present-day level of their mismodelling would make them not particularly insidious (at $\approx 10\%$ level of accuracy or even less, taking into account the recent improvements in constraining the masses of the rings of the minor asteroids and of the TNOs), at least for Mercury and, especially, Venus, with the exception of the impact of the Sun's oblateness on Mercury. The latter could be removed anyway by suitably designing a linear combination of the perihelia of Mercury and Venus, as done for the LAGEOS satellites. Moreover, an improvement of the determination of J_2^\odot by one order of magnitude with respect to the present-day level of uncertainty is one of the goals of the BepiColombo mission (Milani et al. 2002; Ashby et al. 2007; Milani et al. 2008). At present, it is known with an uncertainty of about 10% (Fienga et al. 2009).

In principle, it would be possible to use also the nodes (Iorio 2005d), if only the corrections $\Delta\dot{\Omega}$ to their standard precessions were available. Once other teams of astronomers have independently estimated their own corrections to the standard perihelion precessions (and, hopefully, to the nodal precessions as well) with different ephemerides, it will be possible to fruitfully repeat the present test.

3.3 The interplanetary ranges

An alternative approach to the perihelion precessions consists of looking at the Earth-planet ranges $|\vec{\rho}|$, which are, among other things, directly observable quantities³². We numerically investigated the solar Lense-Thirring effect on such an observable for the inner planets (Iorio 2010d) by taking the difference between the

perturbed range ($|\vec{\rho}_P|$) and the unperturbed, reference range ($|\vec{\rho}_R|$). The temporal interval of the numerical integrations has been taken equal to $\Delta t = 2 \text{ yr}$ because most of the present-day available time series of range residuals from several spacecraft approximately cover similar temporal extensions; moreover, also the typical operational time spans forecasted for future PLR technique are similar.

3.3.1 Earth-Mercury

At present, the 1-way range residuals of Mercury from radar-ranging span 30 yr (1967-1997) and are at a few km-level (Figure B-2 of Folkner et al. (2008)); the same holds for the 1-way Mercury radar closure residuals covering 8 yr (1989-1997, Figure B-3 a) of Folkner et al. (2008)). There are also a pair of Mariner 10 range residuals in the 70s at Mercury at 0.2 km level (Figure B-3 b) of Folkner et al. (2008)). Ranging to BepiColombo should be accurate to 4.5 – 10 cm (Ashby et al. 2007; Milani et al. 2008) over a few years.

Figure 1 depicts the range perturbation due to the Sun's Lense-Thirring effect, neither considered so far in the dynamical force models of the planetary ephemerides nor in the BepiColombo analyses so far performed. The peak-to-peak amplitude of the Lense-Thirring signal is up to 17.5 m over 2 yr, which, if on the one hand is unmeasurable from currently available radar-ranging to Mercury, on the other hand corresponds to a potential relative accuracy in measuring it with BepiColombo of $2 - 5 \times 10^{-3}$; this clearly shows that the solar gravitomagnetic field should be taken into account in future analyses and data processing. Otherwise, it would alias the recovery of other effects.

Figure 2 shows the nominal signature of the Sun's quadrupolar mass moment on the Mercury range for $J_2^\odot = 2 \times 10^{-7}$. Its action has been modeled as (Vrbik 2005)

$$\vec{A}_{J_2^\odot} = -\frac{3J_2^\odot R_\odot^2 GM_\odot}{2r^4} \left[\hat{r} - 5 \left(\hat{r} \cdot \hat{k} \right)^2 + 2 \left(\hat{r} \cdot \hat{k} \right) \hat{k} \right], \quad (49)$$

where R_\odot is the Sun's mean equatorial radius and \hat{k} is the unit vector of the z axis directed along the body's

³²Recall that the perihelia, like all the other Keplerian orbital elements, cannot be directly measured.

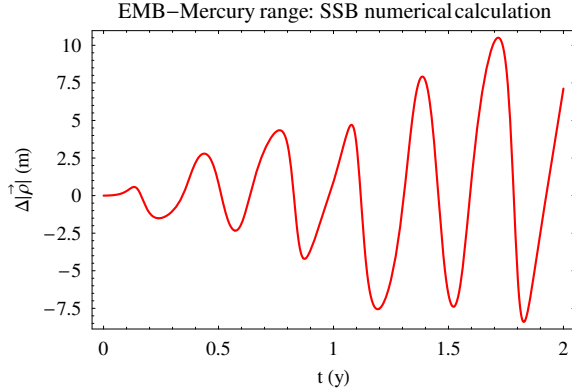


Fig. 1 Difference $\Delta|\vec{\rho}| \doteq |\vec{\rho}_P| - |\vec{\rho}_R|$ in the numerically integrated EMB-Mercury ranges with ($\vec{\rho}_P$) and without ($\vec{\rho}_R$) the perturbation due to the Sun’s Lense-Thirring field over $\Delta t = 2$ yr. The same initial conditions (J2000) have been used for both integrations. The state vectors at the reference epoch have been retrieved from the NASA JPL Horizons system. The integrations have been performed in the ICRF/J2000.0 reference frame, with the mean equinox of the reference epoch and the reference $\{xy\}$ plane rotated from the mean ecliptic of the epoch to the Sun’s equator, centered at the Solar System Barycenter (SSB).

rotation axis. The signal in Figure 2 has a maximum span of 300 m, corresponding to an accuracy measurement of 3×10^{-4} . A measure of the solar J_2^\odot accurate to 10^{-2} is one of the goals of BepiColombo (Milani et al. 2002); knowing precisely J_2^\odot would yield important insights on the internal rotation of the Sun.

Concerning the impact of neglecting the gravitomagnetic field of the Sun in future data analyses, it may affect the determination of J_2^\odot at the 12% level. On the other hand, in order to allow for a determination of the Lense-Thirring effect, the Sun’s quadrupole mass moment should be known with an accuracy better than at present by at least one order of magnitude; this is just one of the goals of BepiColombo. Anyway, also the time signatures of the two signals would play a role.

3.3.2 Earth-Venus

Although at present, contrary to Mercury and Mars, no tests of interplanetary ranging to Venus have been practically performed, we include this case not only for completeness but also because simulations of interplanetary transponder and laser communications experiments via dual station ranging to SLR satellites covering also Venus have been implemented (Degnan 2006, 2008). Currently available radar-ranging normal points to Venus cover about 33 yr, from 1962 to 1995. The range residuals are depicted in Figure B-6 of Folkner et al. (2008); after having been as large as 15 km in the first 10 yr, they have dropped below 5 km since. Figure

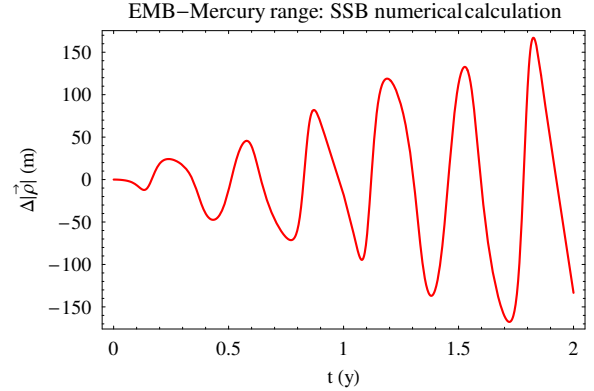


Fig. 2 Difference $\Delta|\vec{\rho}| \doteq |\vec{\rho}_P| - |\vec{\rho}_R|$ in the numerically integrated EMB-Mercury ranges with ($\vec{\rho}_P$) and without ($\vec{\rho}_R$) the nominal perturbation due to the Sun’s quadrupole mass moment $J_2^\odot = 2.0 \times 10^{-7}$ over $\Delta t = 2$ yr. The same initial conditions (J2000) have been used for both integrations. The state vectors at the reference epoch have been retrieved from the NASA JPL Horizons system. The integrations have been performed in the ICRF/J2000.0 reference frame, with the mean equinox of the reference epoch and the reference $\{xy\}$ plane rotated from the mean ecliptic of the epoch to the Sun’s equator, centered at the Solar System Barycenter (SSB).

B-4 of Folkner et al. (2008) shows the range residuals to Venus Express at Venus from 2006 to 2008; the are below the 10 m level.

Figure 3 shows the Lense-Thirring perturbation of the Venus range, integrated in a frame aligned with the Sun’s equator. The peak-to-peak amplitude is 2 m, which would be measurable with a future accurate cm-level ranging device with a relative accuracy of $2 - 5 \times 10^{-2}$. The Lense-Thirring signature is still too small to be detected nowadays with the current spacecraft ranging.

The range perturbation due to the Sun’s oblateness is depicted in Figure 4 for the nominal value $J_2^\odot = 2 \times 10^{-7}$. Also in this case a barycentric frame rotated to the Sun’s equator has been adopted. The nominal maximum shift is 40 m, so that a measure accurate to 2.5×10^{-3} would be possible with a future 10 cm-level ranging technique.

If not modeled, the Sun’s gravitomagnetic field would impact a determination of J_2^\odot at the 5% level. Conversely, the present-day 10% uncertainty in the Sun’s oblateness would yield a mismodeled signal two times larger than the gravitomagnetic one. However, their temporal signatures are different and would therefore allow to separate these two effects.

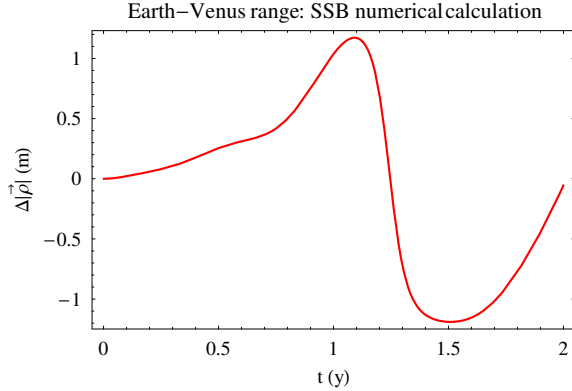


Fig. 3 Difference $\Delta|\vec{\rho}| \doteq |\vec{\rho}_P| - |\vec{\rho}_R|$ in the numerically integrated EMB-Venus ranges with ($\vec{\rho}_P$) and without ($\vec{\rho}_R$) the perturbation due to the Sun’s Lense-Thirring field over $\Delta t = 2$ yr. The same initial conditions (J2000) have been used for both the integrations. The state vectors at the reference epoch have been retrieved from the NASA JPL Horizons system. The integrations have been performed in the ICRF/J2000.0 reference frame, with the mean equinox of the reference epoch and the reference $\{xy\}$ plane rotated from the mean ecliptic of the epoch to the Sun’s equator, centered at the Solar System Barycenter (SSB).

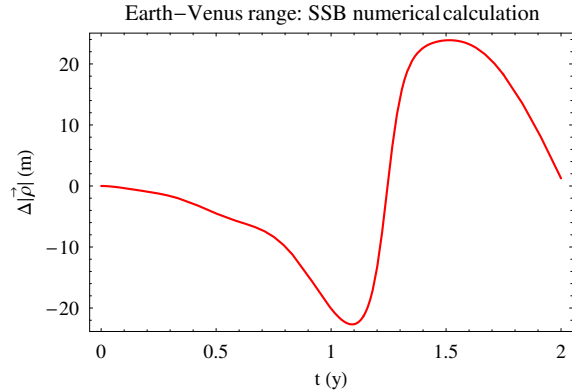


Fig. 4 Difference $\Delta|\vec{\rho}| \doteq |\vec{\rho}_P| - |\vec{\rho}_R|$ in the numerically integrated EMB-Venus ranges with ($\vec{\rho}_P$) and without ($\vec{\rho}_R$) the nominal perturbation due to the Sun’s quadrupole mass moment $J_2^\odot = 2.0 \times 10^{-7}$ over $\Delta t = 2$ yr. The same initial conditions (J2000) have been used for both the integrations. The state vectors at the reference epoch have been retrieved from the NASA JPL Horizons system. The integrations have been performed in the ICRF/J2000.0 reference frame, with the mean equinox of the reference epoch and the reference $\{xy\}$ plane rotated from the mean ecliptic of the epoch to the Sun’s equator, centered at the Solar System Barycenter (SSB).

3.3.3 Earth-Mars

For Mars we have at our disposal long time series of range residuals accurate to about 1 – 10 m-level thanks to several spacecraft (Viking, Mars Pathfinder, Mars

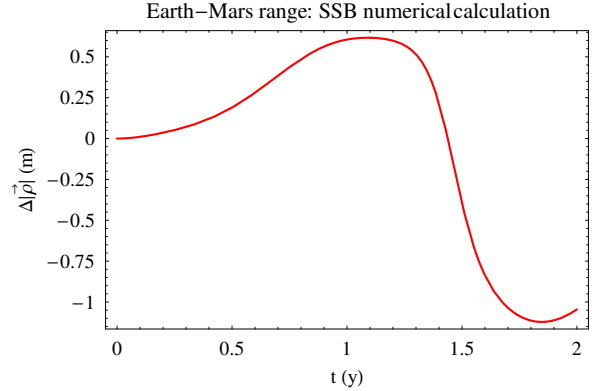


Fig. 5 Difference $\Delta|\vec{\rho}| \doteq |\vec{\rho}_P| - |\vec{\rho}_R|$ in the numerically integrated EMB-Mars ranges with ($\vec{\rho}_P$) and without ($\vec{\rho}_R$) the perturbation due to the Sun’s Lense-Thirring field over $\Delta t = 2$ yr. The same initial conditions (J2000) have been used for both integrations. The state vectors at the reference epoch have been retrieved from the NASA JPL Horizons system. The integrations have been performed in the ICRF/J2000.0 reference frame, with the mean equinox of the reference epoch and the reference $\{xy\}$ plane rotated from the mean ecliptic of the epoch to the Sun’s equator, centered at the Solar System Barycenter (SSB).

Global Surveyor, Mars Odyssey, Mars Reconnaissance Orbiter, Mars Express) which have orbited or are still orbiting the red planet. Figure B-10 of (Folkner et al. 2008) depicts the 1-way range residuals of the Viking Lander at Mars spanning from 1976 to 1982; they are approximately at the 20 m level. Figure B-11 of (Folkner et al. 2008) shows the 1-way range residuals of several post-Viking spacecraft; they generally cover a few years and are accurate to 5 – 10 m.

The Lense-Thirring range perturbation, computed in a frame aligned with the Sun’s equator, is shown in Figure 5. Its peak-to-peak amplitude is about 1.5 m, not too far from the present-day range accuracy; thus, its existence as predicted by general relativity is not in contrast with the range residuals currently available. It could be measured with a future cm-level ranging system at a 3 – 6% level.

Figure 6 illustrates the nominal signal due to the Sun’s quadrupole mass moment for $J_2^\odot = 2 \times 10^{-7}$ computed in a frame aligned with the Sun’s equator. Its peak-to-peak amplitude amounts to 25 m; thus, its effect would be well measurable at a $2 - 4 \times 10^{-3}$ level by means of a new ranging facility with an accuracy of the order of cm. Since J_2^\odot is nowadays accurate to 10^{-1} , the corresponding mismodeled signature would be as large as about 2.5 m. If not properly modeled, the Lense-Thirring effect would bias the J_2^\odot signal at a 6% level. Conversely, considering J_2^\odot as a potential source of systematic bias for the recovery of the gravito-

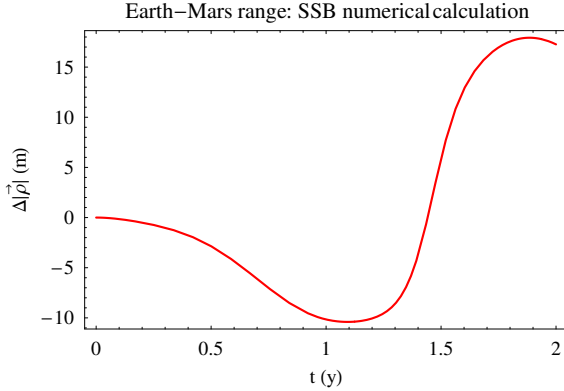


Fig. 6 Difference $\Delta|\vec{\rho}| \doteq |\vec{\rho}_P| - |\vec{\rho}_R|$ in the numerically integrated EMB-Mars ranges with ($\vec{\rho}_P$) and without ($\vec{\rho}_R$) the nominal perturbation due to the Sun's quadrupole mass moment $J_2^\odot = 2.0 \times 10^{-7}$ over $\Delta t = 2$ yr. The same initial conditions (J2000) have been used for both integrations. The state vectors at the reference epoch have been retrieved from the NASA JPL Horizons system. The integrations have been performed in the ICRF/J2000.0 reference frame, with the mean equinox of the reference epoch and the reference $\{xy\}$ plane rotated from the mean ecliptic of the epoch to the Sun's equator, centered at the Solar System Barycenter (SSB).

magnetic effect, the mismodeled signature of the Sun's quadrupolar mass moment would be 1.6 times larger than it. An improvement in its knowledge by one order of magnitude, as expected from, e.g., BepiColombo, would push its bias on the Lense-Thirring signal at 16%. However, it must be noted that their temporal evolutions are different.

4 The gravitomagnetic field of Mars: perspectives for its detection

5 General overview

Since the angular momentum of Mars can be evaluated to be

$$S_M = (1.92 \pm 0.01) \times 10^{32} \text{ kg m}^2 \text{ s}^{-1} \quad (50)$$

from the latest spacecraft-based determinations of the areophysical parameters (Konopliv et al. 2006), the corresponding gravitomagnetic length reads

$$l_g^M \doteq \frac{S_M}{M_M c} = 1.0 \text{ m}. \quad (51)$$

This has to be compared with the present-day accuracy in determining the orbit of a spacecraft like, e.g., Mars Global Surveyor (MGS) which is about 0.15 m in the radial direction (Konopliv et al. 2006) and not affected by

the gravitomagnetic force itself. Thus, it makes sense, in principle, to investigate the possibility of measuring the Lense-Thirring effect in the gravitational field of Mars as well.

In fact, Iorio (2006c, 2007g) proposed an interpretation of the time series of the RMS orbit overlap differences (Konopliv et al. 2006) of the out-of-plane part ν of the orbit of MGS over a time span ΔP of about 5 years (14 November 1999–14 January 2005 in Iorio (2007g)) in terms of the Lense-Thirring effect. It turned out that the average of such a time series over ΔP , normalized to the predicted Lense-Thirring out-of-plane mean shift over the same time span, is $\mu = 1.0018 \pm 0.0053$. The interpretation by Iorio (2006c, 2007g) has recently been questioned by Krogh (2007); a reply has been set in Iorio (2010e). Basically, various linear fits to different data sets including, among others, the full time series of the entire MGS data (4 February 1999–14 January 2005) were made as well; the predictions of general relativity turn out to be always confirmed. The analytical calculation of the competing aliasing effects due to both the gravitational and non-gravitational perturbations, which affect the in-plane orbital components of MGS, do not show up in the real data. Moreover, the non-conservative forces, whose steadily refined modeling mainly improved the in-plane orbital components of MGS, not the normal one, exhibit high-frequency, non-cumulative in time variations (Forbes et al. 2006).

In view of the never fading interest for planetological missions to the red planet, the preliminary design of a spacecraft-based dedicated mission to Mars has been investigated by Iorio (2009b). Here we will deal with such an issue in some detail. In particular, we will concentrate on the the multipolar expansion of the martian gravitational potential in order to see what are the critical issues in view of the present-day knowledge of the Martian space environment. We will not discuss here the perturbations of non-gravitational origin which depend on the shape, the instrumentation and the orbital maneuvers of such probes. They would be strongly related to possible other tasks, more consistent with planetology, which could be fruitfully assigned to such a mission in order to enhance the possibility that it may become something more than a mere, although-hopefully-interesting, speculation; in this respect the medium-long term ambitious programs of NASA to Mars may turn out to be useful also for the purpose discussed here.

5.1 The use of one nearly polar spacecraft

Let us start with a polar orbital geometry and examine the systematic error $\delta\mu$ induced by the uncertainty

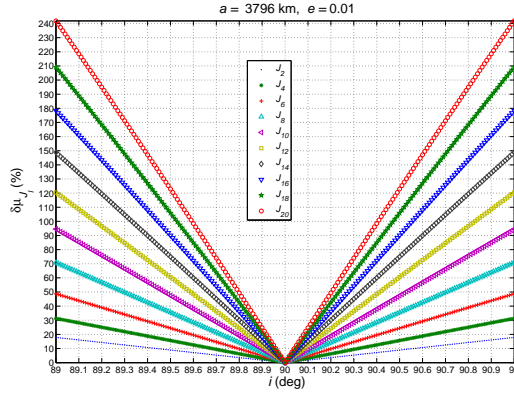


Fig. 7 Systematic percent errors $\delta\mu_{J_\ell}$ per degree ℓ due to the mismodelling in the even zonal harmonics $\delta J_\ell, \ell = 2, 4, 6, \dots$ for $a = 3796$ km, $e = 0.01$, $89 \text{ deg} \leq I \leq 91 \text{ deg}$ according to the calibrated covariance sigmas of the MGS95J global gravity solution up to $\ell = 20$. The Lense-Thirring effect amounts to 34 mas yr^{-1} corresponding to a shift in the out-of-plane direction of 0.62 m yr^{-1} .

in the even zonals δJ_ℓ on the node Ω by assuming for them the calibrated covariance sigmas of the latest Mars gravity model MGS95J (Konopliv et al. 2006). We will evaluate it as

$$\delta\mu_{J_\ell} \leq |\dot{\Omega}_{\cdot\ell}| \delta J_\ell, \ell = 2, 4, \dots \quad (52)$$

Because of the presence of $\cos I$ in all the coefficients $\dot{\Omega}_{\cdot\ell}$ of the oblateness-induced node precessions, we will concentrate on nearly polar ($I \approx 90 \text{ deg}$) orbital configurations to minimize such a corrupting effect. It turns out that altitudes of a few hundreds of km typical of the majority of the currently ongoing martian missions are definitely not suited for our scope, as shown by Figure 7. It must also be pointed out that likely more even zonals of degree higher than $\ell = 20$ would come into play for such low orbital altitudes, as in the case of the forthcoming terrestrial LARES satellite. Note that inserting a probe into an areocentric orbit is not an easy task, so that we decided to allow for a departure of up to 1 deg from the ideal polar orbital configuration to account for unavoidable orbital injection errors. Also typical mission requirements pull the inclination some degrees apart from 90 deg: for Mars Global Surveyor (MGS) $I = 92.86 \text{ deg}$. The systematic bias per degree increases for higher degrees $\ell = 2, 4, 6, \dots$ and it turns out that only a very narrow range for I , i.e. $\Delta I \approx 10^{-3} \text{ deg}$, unlikely to obtain, might push the systematic errors below the 1% level.

By keeping a near polar geometry, much larger values of the semimajor axis, comparable with that of Phobos ($a = 9380 \text{ km}$), one of the two natural satellites of Mars,

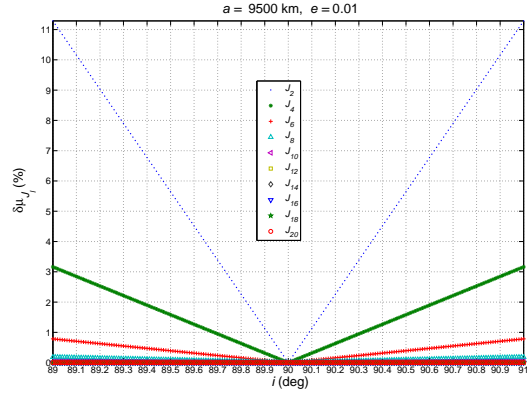


Fig. 8 Systematic percent errors $\delta\mu_{J_\ell}$ per degree ℓ due to the mismodelling in the even zonal harmonics $\delta J_\ell, \ell = 2, 4, 6, \dots$ for $a = 9500$ km, $e = 0.01$, $89 \text{ deg} \leq I \leq 91 \text{ deg}$ according to the calibrated covariance sigmas of the MGS95J gravity model up to $\ell = 20$. The Lense-Thirring effect amounts to 2 mas yr^{-1} corresponding to a shift in the out-of-plane direction of 0.10 m yr^{-1} .

yield reasonable results, as shown in Figure 8. Indeed, now the noise decreases with high degree terms and the most serious contribution is due to the first even zonal $\ell = 2$ yielding a bias up to about 11% for $\Delta I = 1 \text{ deg}$; J_4 affects the the Lense-Thirring precessions at most at the 3% level for $\Delta I = 1 \text{ deg}$. Note also that a much larger departure from 90 deg ($\Delta I \approx 0.1 \text{ deg}$) would allow a further reduction of the noise below 1%. It must be noted that for such a high-altitude orbital configuration the gravitomagnetic shift in the out-of-plane direction would amount to 0.10 m yr^{-1} ; it is certainly a small figure, but, perhaps, not too small if one considers that the average shift in the out-of-plane direction of the much lower Mars Global Surveyor is 1.6 m after about 5 yr. It poses undoubtedly challenging requirements in terms of sensitivity and overall orbit determination accuracy, but future improvements may allow to detect such a small displacement.

Finally, let us remark that, in principle, also the temporal variations of J_2 should be accounted for; however, since at present no secular trends have been detected, such changes, mainly seasonal, annual and semi-annual (Konopliv et al. 2006) would not seriously impact our measurement.

Another martian parameter which must be taken into account is the equatorial radius R along with its uncertainty. Since

$$\dot{\Omega}_{\cdot\ell} \propto R^\ell, \quad (53)$$

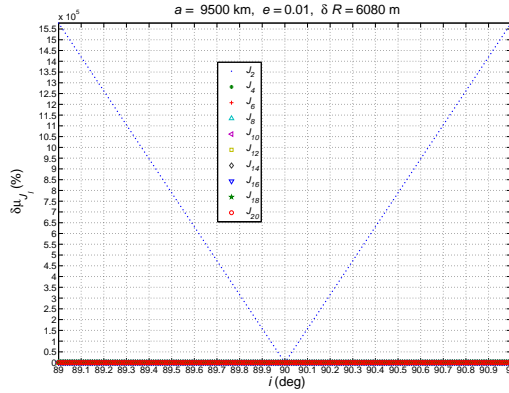


Fig. 9 Systematic percent errors $\delta\mu_{J_\ell}$ per degree ℓ due to the uncertainty in Mars' radius R , assumed to be $\delta R = 6080$ m, for $a = 9500$ km, $e = 0.01$, $89 \text{ deg} \leq i \leq 91 \text{ deg}$. The errors for $\ell = 4, 6$ are as large as 6000% and 500%, respectively.

the systematic error per degree induced by δR can be written as

$$\delta\mu_{J_\ell} \leq \ell \left(\frac{\delta R}{R} \right) \left| \dot{\Omega}_{\ell} J_\ell \right|, \quad \ell = 2, 4, 6, \dots \quad (54)$$

If we assume conservatively for it $\delta R = 6080$ m, i.e. the difference between the reference value of MGS95J (Konopliv et al. 2006) and the one in Yoder (1995), the result is depicted in Figure 9 for $a = 9500$ km. If, instead, one takes $\delta R = 0.04$ km the errors per degree are as in Figure 10 for $a = 9500$ km. Obviously, R is the most serious source of systematic error, even for high altitudes. Moreover, it might be unrealistic to expect improvements in the determination of R by future areocentric missions able to push δR below terrestrial values, i.e. $1 - 0.1$ m. Thus, R will likely remain an insurmountable obstacle if only one probe is to be used.

Concerning GM , it turns out that the impact of its mismodelling is of no concern being $\lesssim 1\%$.

In summary, in this Section we investigated a nearly polar, high-altitude Phobos-like orbit and noted that the Lense-Thirring effect amounts to a shift of 0.10 m yr^{-1} in the out-of-plane direction. Concerning the systematic errors, the most crucial source of aliasing is the radius R ($\delta\mu \approx 10000\%$ for $\delta R = 0.04$ km) and, to a lesser extent, the first even zonal harmonic J_2 of the areopotential ($\delta\mu \leq 11\%$). To reduce them the probe should be inserted into an orbit with an inclination close to 90 deg within 10^{-3} deg or less. In conjunction with such a very tight constraint, it must also be hoped that future missions to Mars will improve our knowledge of the fundamental parameters of the red planet to a sufficient extent to allow for larger departures from the ideal

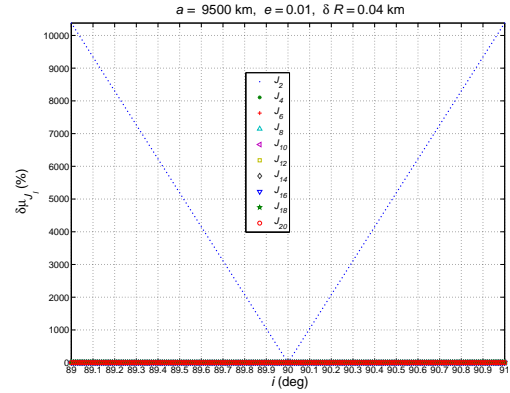


Fig. 10 Systematic percent errors $\delta\mu_{J_\ell}$ per degree ℓ due to the uncertainty in Mars' radius R , assumed to be $\delta R = 0.04$ km, for $a = 9500$ km, $e = 0.01$, $89 \text{ deg} \leq i \leq 91 \text{ deg}$. The errors for $\ell = 4, 6$ are as large as 40% and 5%, respectively.

polar geometry: after all, the gravity solution MGS95J represents an improvement of one order of magnitude with respect to the previous MGS75D model (Yuan et al. 2001). However, this may be valid for the spherical harmonic coefficients of the areopotential, not for the radius of Mars for which an uncertainty of the order of one meter would not be enough. We must conclude that the use of only one probe for measuring its nodal Lense-Thirring precession is unfeasible.

5.2 Including Phobos and Deimos

A possible solution to reduce the systematic errors would be to consider a linear combination of the nodes of the proposed probe and of the two natural satellites of Mars, i.e. Phobos ($a = 9380$ km, $I = 1.075 \text{ deg}$, $e = 0.0151$) and Deimos ($a = 23460$ km, $I = 1.793 \text{ deg}$, $e = 0.0002$), suitably designed to cancel out the impact of just δJ_2 and $\delta R/R$, according to an approach suggested for the first time in the context of the terrestrial LAGEOS-LAGEOS II test (Ciufolini 1996). A possible combination is

$$\delta\dot{\Omega}^{\text{Deimos}} + \alpha_1 \delta\dot{\Omega}^{\text{Probe}} + \alpha_2 \delta\dot{\Omega}^{\text{Phobos}}, \quad (55)$$

with $\delta\dot{\Omega}$ denoting an Observed-minus-Calculated ($O - C$) quantity accounting for unmodelled/mismodelled features of motion and extracted from the data processing with full dynamical force models. By purposely leaving the gravitomagnetic force unmodelled, it can be written as

$$\delta\dot{\Omega} = \mu X_{\text{LT}} + \dot{\Omega}_{22} \delta J_2 + \dot{\Omega}_{R2} \left(\frac{\delta R}{R} \right) + \Delta; \quad (56)$$

here $\mu = 1$ in general relativity and the coefficient $\dot{\Omega}_R$ is defined as

$$\dot{\Omega}_R = R \frac{\partial \dot{\Omega}^{(\text{obl})}}{\partial R} = \sum_{\ell=2} \ell \dot{\Omega}_\ell J_\ell, \quad (57)$$

and Δ represents all other remaining mismodelled/unmodelled effects acting on the node (e.g. $\delta J_4, \delta J_6, \dots; \delta GM$). By solving for μ one gets

$$\begin{cases} \alpha_1 = \frac{\dot{\Omega}_2^{\text{Phobos}} \dot{\Omega}_R^{\text{Deimos}} - \dot{\Omega}_2^{\text{Deimos}} \dot{\Omega}_R^{\text{Phobos}}}{\dot{\Omega}_2^{\text{Probe}} \dot{\Omega}_R^{\text{Phobos}} - \dot{\Omega}_2^{\text{Phobos}} \dot{\Omega}_R^{\text{Probe}}}, \\ \alpha_2 = \frac{\dot{\Omega}_2^{\text{Deimos}} \dot{\Omega}_R^{\text{Probe}} - \dot{\Omega}_2^{\text{Probe}} \dot{\Omega}_R^{\text{Deimos}}}{\dot{\Omega}_2^{\text{Probe}} \dot{\Omega}_R^{\text{Phobos}} - \dot{\Omega}_2^{\text{Phobos}} \dot{\Omega}_R^{\text{Probe}}}. \end{cases} \quad (58)$$

Note that α_1 , contrary to α_2 , is not defined for $I = 90$ deg because $\dot{\Omega}_\ell^{\text{Probe}}$, which is proportional to $\cos I$, vanishes for all ℓ at $I = 90$ deg. Now, the systematic bias of J_4, J_6, J_8, \dots on the combination of eq. (55) turns out to be $\delta\mu \lesssim 6\%$ for $89 \text{ deg} \leq I \leq 89.9 \text{ deg}$ where the major contribution is due to J_4 . It is an acceptable result, especially in view of the fact that the admissible range for the inclination amounts now to about 1 deg and that eq. (55) is, by construction, immune to the uncertainty in the martian radius; indeed, although it is likely that many physical properties and parameters like, e.g., the even zonals, of the red planets will be determined with increasing accuracy by the many ongoing and planned missions, it is unlikely that the radius will be known to a sufficient accuracy to change at an acceptable level the bias induced by it (see Figure 9 and Figure 10).

The combination of eq. (55) is also able to remove a large part of the effect of the mismodelling in GM

$$\delta\mu_{GM} \leq \frac{1}{2} \left(\frac{\delta GM}{GM} \right) \sum_{\ell=2}^{20} |\dot{\Omega}_\ell J_\ell|. \quad (59)$$

Indeed, the main contribution to eq. (59) is due to J_2 , which is canceled out by eq. (55) with the coefficients of eq. (58). The other terms in eq. (59), not canceled by the combination of eq. (55), yield negligible errors well below 1%.

However, it must be stressed that the node of Phobos undergoes secular precessions due to other perturbations of gravitational origin (Lainey et al. 2007) (e.g., the non-sphericity of Phobos itself, the martian tidal bulge and nutation) which have not been considered here and that would affect the combination of eq. (55). It turns out that the most relevant one is that due to the spherical harmonic coefficients c_{20} and c_{22} of Phobos itself (Borderies and Yoder 1990) whose induced secular precession amounts nominally to 200 km over 3 yr (Lainey et al. 2007). The nutation perturbation

nominally amounts to 0.3 km over 3 yr (Lainey et al. 2007). The tidally induced precession, parameterized in terms of the martian Love number k_2 would amount nominally to 0.06 km after 3 yr (Lainey et al. 2007), but being $k_2 = 0.152 \pm 0.009$ (Konopliv et al. 2006), its modelling would leave a $\approx 1 \text{ m yr}^{-1}$ mismodelled trend. The Phobos gravitomagnetic shift is 0.1 m yr^{-1} .

In terms of the detectability of the Lense-Thirring signal with the combination of eq. (55), undoubtedly a major drawback of the strategy of including Phobos and Deimos is the poor accuracy with which their orbits can be reconstructed with respect to their Lense-Thirring signal. Indeed, while their gravitomagnetic shifts are of the order of $1 - 10 \text{ cm yr}^{-1}$, the latest NASA martian ephemerides³³ for them yield an accuracy of $1 - 10 \text{ km}$ in the radial, transverse and out-of-plane orbital components (Jacobson and Rush 2006). Thus, according to the present-day level of accuracy, including the natural satellites of Mars in the combination of eq. (55) would introduce a noise which would overwhelm the relativistic trend of interest. This situation may become more favorable in the near future in view of the planned Phobos-Grunt space mission³⁴ (Marov et al. 2004) which should allow, among other things, to improve the orbit determination of Phobos as well.

5.3 Two dedicated probes

In principle, the linear combination approach could be followed by using the nodes of two other spacecraft³⁵, although sending to Mars three new probes would increase the costs and the difficulties of such a demanding mission.

It is interesting to consider a scenario involving only two probes, named P1 and P2, in a nearly polar counter-orbiting configuration, proposed for the first time by Van Patten and Everitt (1976a) in the framework of the attempts to design a suitable terrestrial mission, and later generalized by Ciufolini (1986) for other inclinations. By assuming for, say, P1 $a_1 = 9500 \text{ km}$, $I_1 = 89 \text{ deg}$, $e_1 = 0.01$, it turns out that the sum of their nodes would be an observable relatively insensitive to departures from the ideal configuration for P2, i.e. $a_2 = 9500 \text{ km}$, $I_2 = 91 \text{ deg}$, $e_2 = 0.01$, at least in regard to the mismodelling in the even zonals. For $a_2 = 9600 \text{ km}$, $90.05 \text{ deg} \leq I_2 \leq 92 \text{ deg}$, $e_2 = 0.03$ the bias due to J_2 is up to 7%, while the other even

³³See on the WEB http://ssd.jpl.nasa.gov/?sat_ephem.

³⁴See on the WEB http://www.esa.int/esaMI/ESA_Permanent_Mission_in_Russia/SEMIJFW4QWD_0.html.

³⁵For a polar geometry the Lense-Thirring precession of the pericentre ω of a spacecraft vanishes being proportional to $\cos I$.

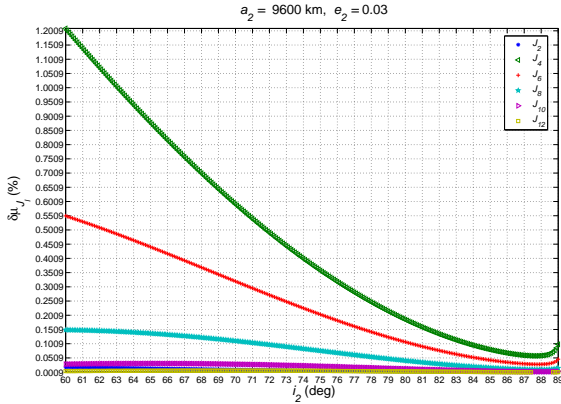


Fig. 11 Systematic errors $\delta\mu_{J_\ell}$ per degree due to the mismodelling $\delta J_2, \delta J_4, \delta J_6, \dots$ (MGS95J model) in the uncanceled even zonal harmonics in the combination of the nodes of probe P1 ($a_1 = 9500$ km, $I_1 = 89$ deg, $e_1 = 0.01$) and probe P2 ($a_2 = 9600$ km, $60 \text{ deg} \leq I_2 \leq 89$ deg, $e_2 = 0.03$) with eq. (61) which cancels out entirely the bias due to δR .

zonals would have an impact of the order of 1% or less. Unfortunately, the uncertainty in the martian radius makes such constraints much more stringent. Indeed, $\delta\mu_R \approx 10^5\%$ for $\delta R = 6080$ m and $\delta\mu_R \approx 4000\%$ for $\delta R = 0.04$ km. Also in this case, the improvement in R expected from future missions to the red planet may be not sufficient.

An approach that could be successfully followed within the framework of the linear combination strategy with two probes P1 and P2, especially in view of likely future improvements in the even zonal harmonics of the areopotential, consists in designing a combination which, by construction, entirely cancels out the bias due to the uncertainty in R

$$\delta\mu_R \leq \left| \dot{\Omega}_R^{P2} + k_1 \dot{\Omega}_R^{P1} \right| \left(\frac{\delta R}{R} \right), \quad (60)$$

being, instead, affected by $\delta J_2, \delta J_4, \delta J_6$. It is analogous to the three-nodes combination of eq. (32), with

$$k_1 = -\frac{\dot{\Omega}_R^{P2}}{\dot{\Omega}_R^{P1}}. \quad (61)$$

Indeed, as can be seen from Figure 11, $\delta\mu_{J_\ell}$ would be rather small ($\lesssim 1\%$), according to the present-day MGS95J model, provided that inclinations $I \ll 90$ deg are adopted for the second probe. It turns out that the most relevant even zonals would be J_4 and J_6 with a bias of the order of $\approx 1 - 0.5\%$. With eq. (61) an inclination range as large as ten degrees would be admissible: this is really a great advantage with respect to the other cases examined so far.

5.4 Summary

The main source of systematic bias is the mismodelling in some of the parameters entering the multipolar expansion of the Newtonian part of the areopotential, especially the Mars' equatorial radius R and, to a lesser but non-negligible extent, the even zonal harmonics $J_\ell, \ell = 2, 4, 6, \dots$. Since the resulting aliasing node precessions are proportional to $R^\ell a^{-(3/2+\ell)} \cos I$, a high-altitude ($a \approx 9500$ km), polar ($I = 90$ deg) probe would be an optimal solution, but the estimation of the unavoidable orbit injection errors showed that such an option is unfeasible because it would require too stringent constraints on the departures from the ideal case $I = 90$ deg. In principle it would be possible to suitably combine the nodes of such a probe with those of the natural satellites of Mars, Phobos and Deimos. However, the Lense-Thirring shifts of these bodies ($1 - 10 \text{ cm yr}^{-1}$) are orders of magnitude too small with respect to the present accuracy in reconstructing their orbits ($1 - 10$ km).

A viable option consists in using two probes P1 and P2 at high-altitudes ($a_1 = 9500$ km, $a_2 = 9600$ km) and different inclinations ($I_1 \approx 90$ deg, $60 \text{ deg} \leq I_2 \leq 89$ deg), and combining their nodes so as to entirely cancel out the bias due to R : the resulting bias due to $\delta J_2, \delta J_4, \delta J_6, \dots$ would be $\lesssim 1\%$, according to the present-day MGS95J gravity model, over a range of values for the inclination as large as ten degrees.

A major challenge would certainly be to reach a satisfying accuracy in reconstructing the orbits of such probes whose Lense-Thirring out-of-plane shifts would amount to about 10 cm yr^{-1} ; for example, the spacecraft should remain operative for many years, without any failure in the communication with the Earth, and it is likely that one or more landers would be required as well.

Finally, we emphasize that a different type of analysis should be done to complete the studies presented here, based on direct observable quantities like range and range-rates.

6 The gravitomagnetic field of Jupiter: perspectives in measuring the jovian angular momentum via the Lense-Thirring effect

6.1 General overview

After the original proposal by Lense and Thirring (1918) of looking at the Galilean satellites³⁶ of Jupiter as natural probes for measuring the gravitomagnetic precessions of their longitudes of perijove ϖ , Bogorodskii (1959) considered the centennial shift of the argument of perijove ω of the inner moon Amalthea ($a = 181400$ km, $e = 0.0032$) amounting to 112 arcsec, while Soffel (1989) looked at centennial node shift of Io of about 9 arcsec. No evaluations of the systematic bias posed by several competing dynamical effects of the Jovian space environment have been examined in such earlier studies. In more recent times, Iorio and Lainey (2005) revisited the Jovian system of the Galilean moons in view of the recent advancements in their orbit determination. It turned out that most of their gravitomagnetic signals would be absorbed in the estimation procedure of the satellites' initial state vectors; the remaining signatures would amount to some tens of meters, while the current best observations have an accuracy of a few tens of kilometers³⁷. Iorio and Lainey (2005) concluded that a spacecraft orbiting Jupiter would be required to reveal its gravitomagnetic field; as we will see below, such an opportunity may be offered in the near future (Iorio 2010f).

In an attempt to measure gravitomagnetism by means of the deflection of electromagnetic waves by Jupiter due to its orbital motion³⁸, a dedicated VLBI-based radio-interferometric experiment has been performed (Kopeikin & Fomalont 2006; Fomalont and Kopeikin 2008). With regard to other suggested non-gravitomagnetic tests of general relativity in the jovian gravitational field, Hiscock and Lindblom (1979) proposed to measure the much larger gravitoelectric Einstein pericenter precessions of the natural satellites of Jupiter and Saturn. There exist also plans for performing a test of the light bending due to Jupiter's monopole and quadrupole mass moments with the forthcoming astrometric mission GAIA (Crosta and Mignard 2006). Finally, also the proposal by Haas and Ross (1975) to

Table 21 Planetocentric nominal orbital parameters of Juno. a, e, I are the semi-major axis (in jovian radii $R = 71492$ km), the eccentricity and the inclination (in deg) with respect to Jupiter's equator, respectively. $\dot{\Omega}_{LT}$ and $\dot{\omega}_{LT}$ are Juno's Lense-Thirring node and perijove precessions (in mas yr⁻¹) for $S = 6.9 \times 10^{38}$ kg m² s⁻¹ (Soffel et al. 2003). P is the orbital period in days. T is the mission duration in years.

a	e	I	$\dot{\Omega}_{LT}$	$\dot{\omega}_{LT}$	P	T
20.03	0.947	90	68.5	0	11	1

measure Schiff's gyroscope precession in the gravitational field of Jupiter should be mentioned.

Another opportunity to fruitfully use the Jovian system may open after the approval of the Juno mission³⁹ by NASA (Matousek 2007) to Jupiter. Juno is a spinning, solar powered spacecraft to be placed in a highly eccentric polar orbit around Jupiter (see Table 21 for its relevant orbital parameters) specifically designed to avoid its highest radiation regions. Understanding the formation, evolution and structure of Jupiter is the primary science goal of Juno. It will carry onboard a dual frequency gravity/radio science system, a six wavelength microwave radiometer for atmospheric sounding and composition, a dual-technique magnetometer, plasma detectors, energetic particle detectors, a radio/plasma wave experiment, and an ultraviolet imager/spectrometer. The nominal mission's lifetime is 1 year. Juno is aimed, among other things, at accurately mapping the gravitational field of Jupiter (Anderson 1976) with unprecedented accuracy (Anderson et al. 2004) by exploiting the slow apsidal precession of its 11-day orbit.

Since the Lense-Thirring precession is due to the proper angular momentum \vec{S} of the orbited central body, one may also take its existence as granted and use it as a direct, dynamical measurement of Jupiter's angular momentum through the Lense-Thirring effect; this would yield further, important information concerning the interior of Jupiter. Indeed, the moment of inertia ratio C/MR^2 entering S is a measure of the concentration of mass towards the center of the planet (Irwin 2003). Such a figure, together with the measured values of the zonal⁴⁰ coefficients of the gravity field accounting for its deviations from spherical symmetry may be fitted with internal models of the variation of the density, pressure, temperature and composition with depth (Irwin 2003; Guillot 2005; Hori et al. 2008). Moreover, a dynamical, model-independent

³⁶Their semimajor axes range from 421800 km (Io) to 1882700 km (Callisto), the eccentricities being of the order of 10^{-3} . See on the WEB http://ssd.jpl.nasa.gov/?sat_elem.

³⁷See on the WEB http://ssd.jpl.nasa.gov/?sat_ephem#ref3.

³⁸In this case, the mass currents inducing a gravitomagnetic action are not those related to the Jupiter's proper rotation (intrinsic gravitomagnetism), but are due to its translational orbital motion (extrinsic gravitomagnetism).

³⁹See on the WEB <http://juno.wisc.edu/index.html>

⁴⁰They preserve the axial symmetry.

determination of S would be important also for a better knowledge of the history and formation of Jupiter (Machida et al. 2008).

6.2 Sensitivity analysis

Jupiter’s proper angular momentum amounts to (Soffel et al. 2003)

$$S \approx 6.9 \times 10^{38} \text{ kg m}^2 \text{ s}^{-1} \quad (62)$$

and the corresponding Lense-Thirring precessions of Juno’s node and perijove are listed in Table 21. It turns out that only the node experiences a GM precession corresponding to a shift $\Delta\nu$ of the cross-track component of the planetocentric position (Christodoulidis et al. 1988)

$$\Delta\nu_{\text{LT}} = a\sqrt{1 + \frac{e^2}{2}} \sin I \Delta\Omega_{\text{LT}} = 572 \text{ m } (T = 1 \text{ yr}) \quad (63)$$

over the entire duration of the mission. A total accuracy of the order of 1-10 m with respect to the km-level of the past Jupiter missions in reconstructing Juno’s orbit in a planetocentric frame does not seem an unrealistic target, although much work is clearly required in order to have a more firm answer. Note that a 1-10 m accuracy implies a 0.2 – 2% error in measuring the gravitomagnetic shift

To consider the possible detection of the Lense-Thirring effect by means of the Juno mission is also suggested by a different approach with respect to the cumulative measurement over the full mission duration previously outlined. Indeed, a gravity-science pass for Juno is defined by a continuous, coherent Doppler range-rate measurement plus and minus three hours of closest approach; in practice, most of the Lense-Thirring precession takes place just during such a six-hours pass, a near optimum condition. Another crucial factor is the orientation of the Earth with respect to Juno’s orbit: our planet will be aligned 67 deg from the probe’s orbital plane at approximately two degrees south latitude on the jovian equator. Preliminary numerical simulations of Juno’s Lense-Thirring Doppler range-rate signal show that such an orbital geometry represents a perfect compromise for measuring both Jupiter’s even zonal harmonics and the gravitomagnetic signal itself. Indeed, it turns out that the maximum Lense-Thirring Doppler signal over a single six-hour gravity pass is of the order of hundred $\mu\text{m s}^{-1}$, while the limit of accuracy for Juno’s Ka-band Doppler system is about one $\mu\text{m s}^{-1}$ over such a pass. Thus, even by taking 25 repeated passes out of a total of approximately 33, it

would be possible to reach a measurement precision below the percent level.

It should be noted that there are estimates for S in the literature in favor of smaller values than given in eq. (62) by a factor 1.5 – 1.6; for example, Machida et al. (2008) report

$$S = 4.14 \times 10^{38} \text{ kg m}^2 \text{ s}^{-1}; \quad (64)$$

the ratio of the values of eq. (62) to eq. (64) is 1.6, i.e. close to 1.5 coming from the ratio of $C/MR^2 = 2/5 = 0.4$, valid for a homogenous sphere, to $C/MR^2 = 0.264$ by Irwin (2003) who assumes a concentration of mass towards Jupiter’s center. Here we consider only the systematic uncertainty induced by the imperfect knowledge of the Newtonian part of Jupiter’s gravitational field and use the value of eq. (62) for S .

Also in this case, a major source of systematic uncertainty is due to the deviation of Jupiter’s gravitational field from spherical symmetry (Anderson 1976).

6.2.1 Analytical calculations

As seen in Section 2.1, the zonal ($m = 0$) harmonic coefficients J_ℓ of the multipolar expansion of the Newtonian part of the planet’s gravitational potential give rise to long-period, (i.e. averaged over one orbital revolution), orbital effects on the longitude of the ascending node Ω , the argument of pericentre ω and the mean anomaly \mathcal{M} of the form

$$\langle \dot{\Psi} \rangle = \sum_{\ell=2} \dot{\Psi}_{\ell} J_{\ell}, \quad \Psi = \Omega, \omega, \mathcal{M}, \quad (65)$$

where $\dot{\Psi}_{\ell}$ are coefficients depending on the planet’s GM and equatorial radius R , and on the spacecraft’s inclination I and eccentricity e through the inclination $F_{\ell mp}(I)$ and eccentricity $G_{\ell pq}(e)$ functions, respectively (Kaula 1966). Note that one of the major scientific goals of the Juno mission is a greatly improved determination of just the harmonic coefficients of the jovian gravity potential; for the present-day values of the zonals⁴¹ for $\ell = 2, 3, 4, 6$ see Table 22. According to Anderson et al. (2004), it might be possible to determine the first three even zonals with an accuracy of 10^{-9} and the other ones up to $\ell = 30$ at a 10^{-8} level. Concerning J_2 , this would be an improvement of two orders of magnitude with respect to Table 22, while the improvements in J_4 and J_6 would be of about three orders of magnitude. By using the results we are going to present below

⁴¹The Jupiter gravity field is essentially determined by the Pioneer 11 flyby at $1.6R_{\text{Jup}}$ (Anderson 1976); Voyager added little, and Galileo, which never got close to Jupiter, added nothing.

Table 22 Zonal harmonics of the Jupiter's gravity field according to the JUP230 orbit solution (Jacobson 2003). They are in unit of 10^6 .

J_2	J_3	J_4	J_6
14696.43 ± 0.21	-0.64 ± 0.90	-587.14 ± 1.68	34.25 ± 5.22

for the long-period node and pericenter precessions, it can be shown that determining the low degree zonals at the 10^{-9} level of accuracy translates into an accuracy of the order of $0.5 - 1$ mas yr $^{-1}$ in $\dot{\Omega}$ and $\dot{\omega}$, thus confirming the expectations of the previous Section.

Long-period terms fulfill the condition

$$\ell - 2p + q = 0 \quad (66)$$

which results in⁴² (Kaula 1966)

$$\begin{aligned} \dot{\Omega}_{,\ell} &= -\frac{n}{\sqrt{1-e^2} \sin I} \left(\frac{R}{a}\right)^\ell \times \\ &\times \sum_{p=0}^{\ell} \left[F'_{\ell 0 p} G_{\ell p(2p-\ell)} W_{\ell 0 p(2p-\ell)} \right], \end{aligned} \quad (67)$$

$$\begin{aligned} \dot{\omega}_{,\ell} &= -\frac{n}{\sqrt{1-e^2}} \left(\frac{R}{a}\right)^\ell \sum_{p=0}^{\ell} \left[-\cot I F'_{\ell 0 p} G_{\ell p(2p-\ell)} + \right. \\ &\left. + \frac{(1-e^2)}{e} F_{\ell 0 p} G'_{\ell p(2p-\ell)} \right] W_{\ell 0 p(2p-\ell)}, \end{aligned} \quad (68)$$

$$\begin{aligned} \dot{M}_{,\ell} &= n \left\{ 1 - \left(\frac{R}{a}\right)^\ell \sum_{p=0}^{\ell} F_{\ell 0 p} [2(\ell+1) G_{\ell p(2p-\ell)} - \right. \\ &\left. - \frac{(1-e^2)}{e} G'_{\ell p(2p-\ell)}] W_{\ell 0 p(2p-\ell)} \right\}, \end{aligned} \quad (69)$$

where $W_{\ell 0 p(2p-\ell)}$ are trigonometric functions having the pericentre as their argument. Contrary to the small eccentricity satellites like the LAGEOS ones previously examined, in this case we will be forced to keep all the terms of order $\mathcal{O}(e^k)$ with $k > 2$ in computing the eccentricity functions for given pairs of ℓ and p . Moreover, since all the non-zero eccentricity and inclination functions for a given degree ℓ are needed, we have to consider all the non-vanishing terms with $0 \leq p \leq \ell$. First, we will extend our calculations to the even zonals so far determined, i.e. $\ell = 2, 4, 6$. In this case W reads

$$W_{\ell 0 p(2p-\ell)} = \cos[(\ell - 2p)\dot{\omega}t] = \cos(q\dot{\omega}t). \quad (70)$$

It must be noted that the terms with

$$p = \frac{\ell}{2}, \quad q = 0, \quad (71)$$

i.e. $W_{\ell 0 \frac{\ell}{2} 0} = 1$, yield secular precessions, while those with

$$q = 2p - \ell \neq 0 \quad (72)$$

induce harmonic signals with circular frequencies $-q\dot{\omega}$.

For degree $\ell = 2$ only secular precessions occur and the non-vanishing inclination and eccentricity functions and their derivatives are⁴³

$$F_{201} = \frac{3}{4} s I^2 - \frac{1}{2}. \quad (73)$$

$$F'_{201} = \frac{3}{2} s I c I. \quad (74)$$

$$G_{210} = \frac{1}{(1-e^2)^{3/2}}. \quad (75)$$

$$G'_{210} = \frac{3e}{(1-e^2)^{5/2}}. \quad (76)$$

For $\ell = 4$ we find⁴⁴

$$F_{401} = -\frac{35}{32} s I^4 + \frac{15}{16} s I^2 = F_{403}, \quad (77)$$

$$F_{402} = \frac{105}{64} s I^4 - \frac{15}{8} s I^2 + \frac{3}{8}. \quad (78)$$

$$F'_{401} = \left(-\frac{35}{8} s I^3 + \frac{15}{8} s I \right) c I = F'_{403}, \quad (79)$$

$$F'_{402} = \left(\frac{105}{16} s I^3 - \frac{15}{4} s I \right) c I. \quad (80)$$

$$G_{41-2} = \frac{3}{4} \frac{e^2}{(1-e^2)^{7/2}} = G_{432}, \quad (81)$$

$$G_{420} = \frac{1 + \frac{3}{2} e^2}{(1-e^2)^{7/2}}. \quad (82)$$

⁴²Note that $2(\ell+1)$ in eq. (69) corrects a wrong 6 in (16), pag. 556 of Iorio (2010f).

⁴³Here and in the following $cI \doteq \cos I$, $sI \doteq \sin I$. Note that eq. (76) corrects a typo in (23), pag. 556 of Iorio (2010f).

⁴⁴Note that eq. (83) and eq. (84) correct typos in (30) and (31), p. 557 of Iorio (2010f).

$$G'_{41-2} = \frac{3e(1 + \frac{5}{2}e^2)}{2(1 - e^2)^{9/2}} = G'_{432}, \quad (83)$$

$$G'_{420} = \frac{10e(1 + \frac{3}{4}e^2)}{(1 - e^2)^{9/2}}, \quad (84)$$

where in addition to secular terms, also harmonic signals with the frequencies $\pm 2\dot{\omega}$ are present.

For $\ell = 6$ the inclination and eccentricity functions, along with their derivatives read⁴⁵

$$F_{601} = \frac{693}{512}sI^6 - \frac{315}{256}sI^4 = F_{605}, \quad (85)$$

$$F_{602} = -\frac{3465}{1024}sI^6 + \frac{315}{64}sI^4 - \frac{105}{64}sI^2 = F_{604}, \quad (86)$$

$$F_{603} = \frac{1155}{256}sI^6 - \frac{945}{64}sI^4 + \frac{105}{32}sI^2 - \frac{5}{16}. \quad (87)$$

$$F'_{601} = \left(\frac{2079}{256}sI^5 - \frac{315}{64}sI^3 \right) cI = F'_{605}, \quad (88)$$

$$F'_{602} = \left(-\frac{10395}{512}sI^5 + \frac{315}{16}sI^3 - \frac{105}{32}sI \right) cI = F'_{604}, \quad (89)$$

$$F'_{603} = \left(\frac{3465}{128}sI^5 - \frac{945}{16}sI^3 + \frac{105}{16}sI \right) cI. \quad (90)$$

$$G_{61-4} = \frac{5}{16} \frac{e^4}{(1 - e^2)^{11/2}} = G_{654}, \quad (91)$$

$$G_{62-2} = \frac{5}{2} \frac{e^2}{(1 - e^2)^{11/2}} \left(1 + \frac{e^2}{8} \right) = G_{642}, \quad (92)$$

$$G_{630} = \frac{1}{(1 - e^2)^{11/2}} \left(1 + 5e^2 + \frac{15}{8}e^4 \right). \quad (93)$$

$$G'_{61-4} = \frac{5}{4} \frac{e^3(1 + \frac{7}{4}e^2)}{(1 - e^2)^{13/2}} = G'_{654}, \quad (94)$$

$$G'_{62-2} = \frac{5e(1 + \frac{19}{4}e^2 + \frac{7}{16}e^4)}{(1 - e^2)^{13/2}} = G'_{642}, \quad (95)$$

$$G'_{630} = \frac{21e(1 + \frac{5}{2}e^2 + \frac{5}{8}e^4)}{(1 - e^2)^{13/2}}. \quad (96)$$

In addition to the secular rates, also harmonic signals with frequencies $\pm 4\dot{\omega}$, $\pm 2\dot{\omega}$ do occur.

Let us now focus on the action of the odd ($\ell = 3, 5, 7, \dots$) zonal ($m = 0$) harmonics. In this case

$$W_{\ell 0 p(2p-\ell)} = s[(\ell - 2p)\dot{\omega}t] = -s(q\dot{\omega}t), \quad (97)$$

so that only harmonic terms exist for $q \neq 0$.

Finally, for $\ell = 3$ we find⁴⁶

$$F_{301} = \frac{15}{16}sI^3 - \frac{3}{4}sI = -F_{302}, \quad (98)$$

$$F'_{301} = \left(\frac{45}{16}sI^2 - \frac{3}{4} \right) cI = -F'_{302}. \quad (99)$$

$$G_{31-1} = \frac{e}{(1 - e^2)^{5/2}} = G_{321}, \quad (100)$$

$$G'_{31-1} = \frac{1 + 4e^2}{(1 - e^2)^{7/2}} = G'_{321}. \quad (101)$$

Thus, we have long-period effects varying with frequencies $\pm \dot{\omega}$.

We note that the long-period even and odd zonal harmonic terms can be approximated by secular precessions with a high level of accuracy over the expected 1-yr lifetime T of the Juno mission because the period of Junos's perijove is of the order of ≈ 500 yr, i.e.

$$\cos(q\omega) = \cos(q\dot{\omega}t + q\omega_0) \approx \cos(q\omega_0), \quad 0 \leq t \leq T, \quad (102)$$

$$\sin \omega = \sin(\dot{\omega}t + \omega_0) \approx \sin \omega_0, \quad 0 \leq t \leq T. \quad (103)$$

Thus, the choice of the initial condition ω_0 will be crucial in determining the impact of the long-period terms.

Now, it would be possible, in principle, to use the node of Juno to measure the gravitomagnetic effect. Indeed, the Lense-Thirring node precession is independent of I , while all the zonal precessions of Ω vanish for $I = 90$ deg. This is not the case for the perijove and the mean anomaly, but they are not affected by the gravitomagnetic force for $I = 90$ deg. In reality, the situation will be less favorable because of the unavoidable orbit injection errors which will induce some departures δI of Juno's orbital plane from the ideal polar configuration. Thus, unwanted, corrupting node zonal secular precessions will appear; their mis-modeling due to the uncertainties δJ_ℓ may swamp the recovery of the Lense-Thirring effect if their determination by Juno will not be accurate enough. Note that there is no risk of some sort of a-priori "imprint" effect of the Lense-Thirring

⁴⁵Note that eq. (94), eq. (95) and eq. (96) correct typos in (41), (42), (43), p. 557 of Iorio (2010f).

⁴⁶Note that eq. (101) corrects a typo in (48), p. 557 of Iorio (2010f).

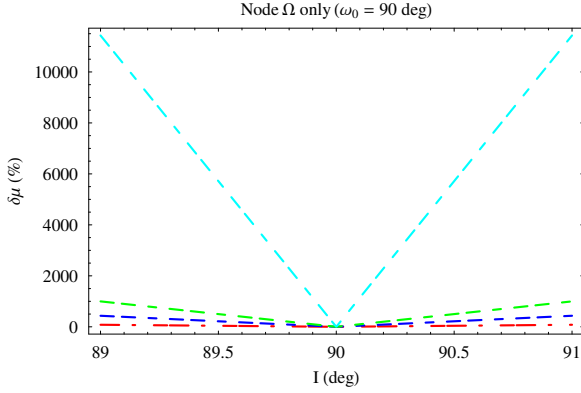


Fig. 12 Systematic percent bias on the Lense-Thirring node precession induced by the mis-modeling in the zonals J_2 (red), J_3 (blue), J_4 (green), J_6 (light blue) according to Table 22 for 89 deg $\leq I \leq 91$ deg and $\omega_0 = 90$ deg.

effect itself on the values of the zonals retrieved from the Juno’s perijove motion because the gravitomagnetic pericenter precession vanishes for polar orbits.

By assuming the values quoted in Table 22 for the uncertainties δJ_ℓ , $\ell = 2, 3, 4, 6$, let us see what is the impact of an imperfect polar orbital geometry on the nodal Lense-Thirring precessions. The results are depicted in Figure 12 for each degree ℓ separately; the initial condition $\omega_0 = 90$ deg has been used. It should be noted that, in view of the likely correlations among the determined zonals, a realistic upper bound of the total bias due to them can be computed by taking the linear sum of each mis-modeled terms. The major source of bias is the so far poorly known J_6 ; an improvement of four orders of magnitude, which sounds rather unlikely to be obtained even with Juno (Anderson et al. 2004), would be required to push its aliasing effect at a percent level of the Lense-Thirring effect. The situation for the other zonals is more favorable; J_4 should be known better than now by a factor 1000, which is, instead, a realistic goal according to Anderson et al. (2004). Thus, we conclude that a nearly-polar orbit being 1 deg off the ideal 90 deg case would likely prevent a measurement of the gravitomagnetic node precession at a decent level of accuracy.

Thanks to the high eccentricity of Juno’s orbit, also the perijove and the mean anomaly are well defined, so that they can be used in a suitable way to remove the bias of J_6 and J_2 . Let us write

$$\delta \dot{\Omega} = \dot{\Omega}_{2,2} \delta J_2 + \dot{\Omega}_{6,6} \delta J_6 + \mu \dot{\Omega}_{LT} + \Delta_\Omega, \quad (104)$$

$$\delta \dot{\omega} = \dot{\omega}_{2,2} \delta J_2 + \dot{\omega}_{6,6} \delta J_6 + \mu \dot{\omega}_{LT} + \Delta_\omega, \quad (105)$$

$$\delta \dot{\mathcal{M}} = \dot{\mathcal{M}}_{2,2} \delta J_2 + \dot{\mathcal{M}}_{6,6} \delta J_6 + \Delta_{\mathcal{M}}, \quad (106)$$

where $\delta \dot{\Psi}$ denotes some of Observed-minus-Calculated ($O-C$) quantity for the rate of the Keplerian element Ψ which accounts for every unmodeled/mis-modeled dynamical effect. It may be, for example, a correction to the modeled precessions to be phenomenologically estimated as a solve-for parameter of a global fit of Juno’s data as done by Pitjeva (2005a) with the planetary perihelia, or it could be a computed time-series of⁴⁷ “residuals” of Ψ by suitably overlapping orbital arcs. The gravitomagnetic force should be purposely not modeled in order to be fully present in $\delta \dot{\Psi}$. The parameter μ is⁴⁸ 1 in GTR and 0 in Newtonian mechanics and accounts for the Lense-Thirring effect. The Δ terms include all the other systematic errors like the precessions induced by the mis-modeled parts of the second even zonal harmonic δJ_4 and the first odd zonal harmonic δJ_3 , the mis-modeling due to the uncertainty in Jupiter’s GM , etc. By solving for μ one obtains

$$\delta \dot{\Omega} + p_1 \delta \dot{\omega} + p_2 \delta \dot{\mathcal{M}} = \dot{\Omega}_{LT} + p_1 \dot{\omega}_{LT} + \Delta, \quad (107)$$

with

$$p_1 = \frac{\dot{\mathcal{M}}_{6,6} \dot{\Omega}_{2,2} - \dot{\Omega}_{6,6} \dot{\mathcal{M}}_{2,2}}{\dot{\omega}_{6,6} \dot{\mathcal{M}}_{2,2} - \dot{\mathcal{M}}_{6,6} \dot{\omega}_{2,2}}, \quad (108)$$

$$p_2 = \frac{\dot{\Omega}_{6,6} \dot{\omega}_{2,2} - \dot{\omega}_{6,6} \dot{\Omega}_{2,2}}{\dot{\omega}_{6,6} \dot{\mathcal{M}}_{2,2} - \dot{\mathcal{M}}_{6,6} \dot{\omega}_{2,2}}. \quad (109)$$

Eq. (107) is designed, by construction, to single out the combined Lense-Thirring precessions and to cancel the combined secular⁴⁹ precessions due to J_2 and J_6 along with their mis-modeling. However, it is affected by Δ which acts as a systematic bias on the Lense-Thirring signal of interest. Δ globally includes the mis-modeled part of the combined precessions induced by J_3 and J_4 ; the sources of uncertainty reside in J_3 and J_4 themselves and in Jupiter’s GM through the mean motion n which enters the coefficients $\dot{\Omega}_{\ell,2}, \dot{\omega}_{\ell,2}, \dot{\mathcal{M}}_{\ell,2}$.

In Figure 13 the impact of the mis-modeling in J_3 and J_4 for $\omega_0 = 90$ deg is depicted. It corrects Fig. 2, p. 558 of Iorio (2010f); incidentally, Figure 13 yields smaller percent uncertainties. In Figure 14, which amends Fig. 3, p. 559 of Iorio (2010f), we use $\omega_0 = 0$ deg. In this case the situation is much more favorable because for a total departure of ± 1 deg from $I = 90$ deg, an improvement of only two orders of magnitude in J_3 , which is, today, still compatible with zero, and J_4

⁴⁷Since the Keplerian elements are not directly measurable quantities, we use here the term “residual” in an improper sense.

⁴⁸It is not one of the standard PPN parameters, but it can be expressed in terms of γ as $\mu = (1 + \gamma)/2$.

⁴⁹We include in them also the long-period harmonic terms for the reasons explained before.

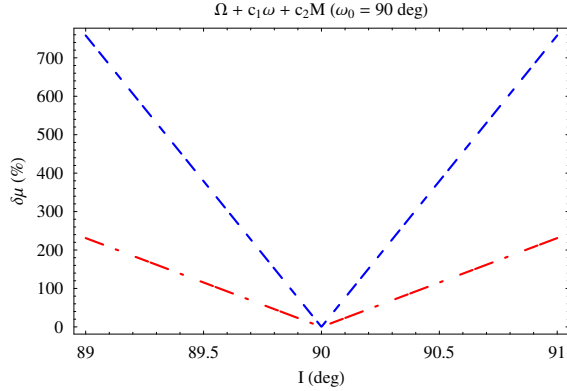


Fig. 13 Systematic percent bias on the Lense-Thirring precessions, combined according to eq. (107), induced by the mis-modeling in the uncanceled zonals J_3 (dash-dotted red line), J_4 (dotted blue line) according to Table 22 for $89 \text{ deg} \leq I \leq 91 \text{ deg}$ and $\omega_0 = 90 \text{ deg}$.

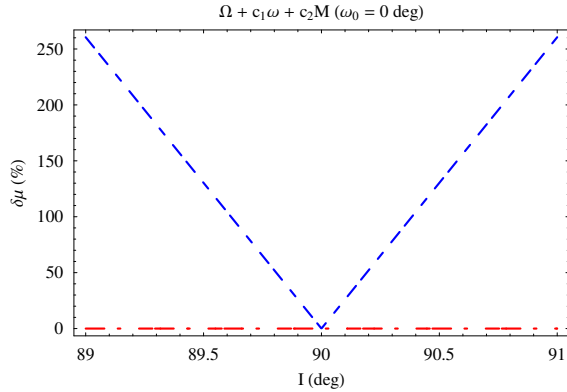


Fig. 14 Systematic percent bias on the Lense-Thirring precessions, combined according to eq. (107), induced by the mis-modeling in the uncanceled zonals J_3 (dash-dotted red line), J_4 (dotted blue line) according to Table 22 for $89 \text{ deg} \leq I \leq 91 \text{ deg}$ and $\omega_0 = 0 \text{ deg}$.

would be needed to reach the percent level; let us recall that the expected improvement in J_4 with respect to the results by Jacobson (2003) is about three orders of magnitude (Anderson et al. 2004). Note that a value of ω_0 far from 90 deg is preferable to minimize the perturbations.

Another potential source of systematic errors is Jupiter's GM whose uncertainty $\delta(GM)$ indirectly affects eq. (107) through the Keplerian mean motion n entering the uncanceled J_3 and J_4 combined precessions; δn is also present via the mean anomaly itself. However, it turns out that it is of no concern because, according to the present-day level of relative uncertainty (Jacobson 2003)

$$\frac{\delta(GM)}{GM} = 1.6 \times 10^{-8}, \quad (110)$$

its impact on the combined Lense-Thirring precessions is well below the percent level.

6.2.2 A numerical approach

Also in this case we followed an alternative approach based on preliminary numerical simulations. We investigated the impact of the uncertainties in the first two jovian even zonals on a Juno's single six-hours pass by numerically simulating the probe's Doppler range-rate signals due to δJ_2 and δJ_4 . By assuming for them values as large as 2×10^{-10} and 3×10^{-10} , respectively, it turns out that the maximum Doppler shifts are roughly $1 - 1.5 \mu\text{m s}^{-1}$. Moreover, and more importantly, the time-dependent patterns of the even zonals' Doppler signals are quite different from the Lense-Thirring one removing the risk of an insidious mimicking bias. Another encouraging fact is that such simulations indicate that an inclination of even 91 deg would not compromise the recovery of the gravitomagnetic signal of interest.

6.3 Summary

We first explored the possibility of a high accuracy measurement of the Lense-Thirring effect by performing analytical calculations and interpreting them in a rather conservative fashion. A meter-level accuracy in determining the jovicentric orbit of the Juno spacecraft should not be an unrealistic goal to be reached. Equivalently, the gravitomagnetic node precession of Juno amounts to 68.5 mas yr^{-1} , while the accuracy in measuring its node and perijove precessions should be of the order of $0.5 - 1 \text{ mas yr}^{-1}$, given the expected improvements in our knowledge of the departure of the jovian gravitational field from spherical symmetry. If Juno's orbit were perfectly polar, the long-period node precessions induced by the zonal harmonics $J_\ell, \ell = 2, 3, 4, 6, \dots$ of the non-spherical jovian gravitational potential would vanish, thus removing a major source of systematic alias on the Lense-Thirring secular precession. In reality, unavoidable orbit injection errors will displace the orbital plane of Juno from the ideal polar geometry; as a consequence, the mis-modeled part of the node zonal precessions would overwhelm the relativistic signal for just $\delta I = \pm 1 \text{ deg}$, in spite of the expected improvements in $J_\ell, \ell = 2, 4, 6$ of three orders of magnitude. A suitable linear combination of the node Ω , the perijove ω and the mean anomaly \mathcal{M} will allow to cancel out the effects of J_2 and J_6 ; the remaining uncanceled J_3 and J_4 will have an impact on the Lense-Thirring combined precessions which should be reduced down to the percent level or better by the improved low-degree zonals.

Instead of looking at the cumulative, secular effects over the entire duration of the mission, we also followed an alternative approach by looking at single Doppler range-rate measurements over time spans six hours long centered on the the probe's closest approaches to Jupiter; it turned out that, in this way, the perspectives are even more favorable. We numerically simulated the characteristic Lense-Thirring pattern for a single science pass by finding a maximum value of the order of hundreds $\mu\text{m s}^{-1}$, while the expected precision level in Juno's Doppler measurements is of the order of one $\mu\text{m s}^{-1}$. Thus, by exploiting about 25 of the planned 33 total passes of the mission it would be possible to reach a measurement accuracy below the percent level. We repeated our numerical analysis also for the Doppler range-rate signals of J_2 and J_4 by finding quite different patterns with respect to the gravitomagnetic one; moreover, for a level of mismodeling of the order of $2 - 3 \times 10^{-10}$ in such zonals the maximum value of their biasing Doppler signals is about $1 - 1.5 \mu\text{m s}^{-1}$. Our numerical analysis also shows that a departure from the nominal polar orbital geometry as large as 1 deg would not compromise the successful outcome of the measurement of interest, contrary to the conservative conclusions of our analytical analysis. Thus, this approach suggests that there is not a high correlation between the Lense-Thirring parameter and the jovian gravity field parameters, although a covariance analysis would be needed to prove it. However, such a covariance analysis is outside the scope of the present paper.

In conclusion, the potential error in the proposed Juno Lense-Thirring measurement is between 0.2 and 5 percent. Conversely, if one assumes the existence of gravitomagnetism as predicted by general relativity, the proposed measurement can also be considered as a direct, dynamical determination of the jovian proper angular momentum S by means of the Lense-Thirring effect at the percent level.

7 A note on gravitational waves: a new window into the Universe

In the Introduction we emphasized that, as gravitomagnetic effects are usually discussed in the linearized approach of GTR, they also have a strong connection with GWs within various theories of gravity (Iorio and Corda 2009, 2010; Corda et al. 2010).

In fact, interferometric GW detectors are operative at the present time (Giazotto 2008; Iorio and Corda 2010). A direct detection will be a historic confirmation of the indirect evidence of the existence of GWs

by Hulse and Taylor (1975). The realization of a GW astronomy, by giving a significant amount of new information, will be a cornerstone for a better understanding of gravitational physics too. Detectors for GWs will be important for a better knowledge of the Universe (Giazotto 2008) and also because the interferometric GW detection will be the definitive test for GTR or, alternatively, a strong endorsement for Extended Theories of Gravity (Corda 2009). In fact, if advanced projects on the detection of GWs improve their sensitivity, allowing the scientific community to perform a GW astronomy, accurate angle- and frequency-dependent response functions of interferometers for GWs arising from various theories of gravity will permit to discriminate among GTR and extended theories of gravity like Scalar Tensor Gravity, String Theory and $f(R)$ Theories. This ultimate test will work because standard GTR admits only two polarizations for GWs, while in all extended theories the number of polarization states is, at least, three; see Corda (2009) for details. On the other hand, the discovery of GW emission by the compact binary system composed of two neutron stars PSR1913+16 (Hulse and Taylor 1975) has been, for both of theoretician and experimental physicists working in this field, the fundamental thrust allowing to reach the extremely sophisticated technology needed for investigating this field of research (Iorio and Corda 2010).

GWs arise from Einsteinian GTR (Einstein 1915) and are weak perturbations of the spacetime curvature which travel at light speed (Einstein 1916, 1918). As GWs are quadrupolar waves, only asymmetric astrophysical sources can emit them (Iorio and Corda 2010). The most efficient ones are very dense and massive coalescing binary systems, like neutron stars and black holes. Instead, a single rotating pulsar, even if dense and massive, can only rely on spherical asymmetries, usually very small (Iorio and Corda 2010). Supernova explosions could have, in principle, relevant asymmetries, being potential sources of gravitational waves (Giazotto 2008; Iorio and Corda 2010). The most important cosmological source of GWs is the so called stochastic background of relic GWs which, together with the Cosmic Background Radiation (CBR), carries a huge amount of information on the early stages of the Universe evolution (Smoot and Steinhardt 1993). This reason is a rather hopeful one (Smoot and Steinhardt 1993; Allen 1997; Corda 2010). As gravitation is the weakest of the four known fundamental interactions, the small-scale perturbations of the gravitational field decoupled from the evolution of the rest of the universe at very early times. Currently, the most detailed view of the early universe comes from

the microwave background radiation, which decoupled from matter about 300.000 years after the big bang, and gives us an accurate picture of the universe at this very early time (Smoot and Steinhardt 1993; Allen 1997; Corda 2010). Some simple computations by Allen (1997) showed that if a background of relic GWs is observed, they will carry a picture of the universe as it was about 10^{-22} s after the initial singularity. This would represent a tremendous step forward in our understanding of the primordial universe. The existence of a relic stochastic background of GWs is a consequence of very general assumptions which arise from an interplay between basic principles of classical theories of gravity and of quantum field theory (Smoot and Steinhardt 1993; Allen 1997; Corda 2010). The strong variations of the gravitational field in the primordial universe amplified the zero-point quantum oscillations and produced relic GWs. This model derives from the inflationary framework of the early universe (Lyth and Liddle 2009), which is fine tuned with the WMAP data on the CBR. In fact, an exponential inflation with a spectral index of ≈ 1 agrees with inflationary theories (Spergel et al. 2003). The inflationary scenario predicts cosmological models in which the Universe undergoes a brief phase of a very rapid expansion in early times (Lyth and Liddle 2009). Such an expansion could be either a power-law or exponential in time (Lyth and Liddle 2009) and provides solutions to the horizon and flatness problems. Inflation also contains a mechanism which creates perturbations in all fields (Allen 1997; Corda 2010; Lyth and Liddle 2009). This mechanism also yields a distinctive spectrum of relic GWs (Allen 1997; Corda 2010). The GW perturbations arise from the uncertainty principle and the spectrum of relic GWs is generated from the adiabatically-amplified zero-point fluctuations (Allen 1997; Corda 2010).

Regarding the potential GW detection, recalling some historical notes is in order. In 1957 F.A.E. Pirani, a member of Hermann Bondi's research group, proposed the geodesic deviation equation as a theoretical foundation for designing a practical GW detector (Pirani 1957). In 1959, J. Weber studied a detector that, in principle, might be able to measure displacements smaller than the size of the nucleus (Weber 1959). He realized an experiment using a large suspended bar of aluminum. Such a bar had a high resonant Q at a frequency of about 1 kHz. After this, in 1960, he tried to test the general relativistic prediction of gravitational waves from strong gravity collisions (Weber 1960). Weber performed further analyses in 1969, by claiming evidence for the observation of gravitational waves from two bars separated by 1000 km (Weber 1969). Such evidence was based on coincident signals which Weber

claimed to be detected by the two bars. In order to confirm these observations, he also proposed to detect gravitational waves by using laser interferometers (Weber 1969). In fact, all the modern detectors can be considered to originate from early Weber's studies (Giazotto 2008; Iorio and Corda 2010).

Currently, five cryogenic bar detectors have been built to work at very low temperatures (< 4 K): Explorer at CERN, Nautilus at Frascati INFN National Laboratory, Auriga at Legnano National Laboratory, Allegro at Louisiana State University and Niobe in Perth (Giazotto 2008; Iorio and Corda 2010). There are also two spherical detectors, i.e. the Mario Schenberg, which operates in San Paolo (Brazil) and the Mini-GRAIL, which is trying to detect GWs at the Kamerlingh Onnes Laboratory of Leiden University; see Giazotto (2008) and Iorio and Corda (2010). Spherical detectors are quite important for the potential detection of the scalar component of GWs that is admitted by Extended Theories of Gravity (Corda 2007a). In the case of interferometric detectors, two mirrors are used like free falling masses. Such mirrors are separated by 3 km for Virgo and 4 km for LIGO. Thus, the GW tidal forces in interferometers are expected to be several order of magnitude larger than in bar detectors. Differently from bars, interferometers like LIGO have very large bandwidth (10-10000 Hz) because mirrors are suspended to pendulums having resonance in the Hz region. In this way, above such a resonance frequency, mirrors works, in a good approximation, like freely falling masses in the horizontal plane (Giazotto 2008; Iorio and Corda 2010).

Recently, starting from the analysis in Baskaran and Grishchuk (2004), some papers have shown the importance of the gravitomagnetic effects in the framework of the GW detection, too; see Iorio and Corda (2010) and Corda (2007b) and references therein. In fact, the so-called magnetic components of GWs have to be taken into account in the context of the total response functions of interferometers for GWs propagating from arbitrary directions (Baskaran and Grishchuk 2004; Corda 2007b; Iorio and Corda 2010). An extended analysis, which has been carefully reviewed in the recent work (Iorio and Corda 2010), showed that such a magnetic component becomes particularly important in the high-frequency portion of the range of ground based interferometers for GWs which arises from standard GTR. The magnetic component has been extended also to GWs arising from scalar-tensor gravity (Corda et al. 2010; Iorio and Corda 2010). Such studies showed that by considering only the low-frequency approximation of the electric contribution and thereby neglecting the magnetic contribution, a portion of about 15% of the

signal could be, in principle, lost in the case of Scalar Tensor Gravity too (Corda et al. 2010; Iorio and Corda 2010), in close analogy with the standard case of GTR (Baskaran and Grishchuk 2004; Corda 2010).

It is important to give a physical/mathematical explanation as to why the magnetic component of the gravitational field of a GW becomes important at high frequency. As interferometric GWs detection is performed in a laboratory environment on Earth, the coordinate system in which the spacetime is locally flat is typically used (Iorio and Corda 2010) and the distance between any two points is given simply by the difference in their coordinates in the sense of Newtonian physics. In this frame, called the frame of the local observer, GWs manifest themselves by exerting tidal forces on the masses (the mirror and the beam-splitter in the case of an interferometer). In the following, we work with $G = 1$, $c = 1$ and $\hbar = 1$ and we call $h_+(t_{tt} + z_{tt})$ and $h_\times(t_{tt} + z_{tt})$ the weak perturbations due to the $+$ and the \times polarizations which are expressed in terms of synchronous coordinates $t_{tt}, x_{tt}, y_{tt}, z_{tt}$ in the transverse-traceless (TT) gauge (Iorio and Corda 2010). In this way, the most general GW propagating in the z_{tt} direction can be written in terms of plane monochromatic waves (Iorio and Corda 2010; Baskaran and Grishchuk 2004)

$$\begin{aligned} h_{\mu\nu}(t_{tt} + z_{tt}) &= h_+(t_{tt} + z_{tt})e_{\mu\nu}^{(+)} + \\ &+ h_\times(t_{tt} + z_{tt})e_{\mu\nu}^{(\times)} = \\ &= h_{+0} \exp i\omega(t_{tt} + z_{tt})e_{\mu\nu}^{(+)} + \\ &+ h_{\times 0} \exp i\omega(t_{tt} + z_{tt})e_{\mu\nu}^{(\times)}, \end{aligned} \quad (111)$$

with the corresponding line element

$$\begin{aligned} ds^2 &= dt_{tt}^2 - dz_{tt}^2 - (1 + h_+)dx_{tt}^2 - (1 - h_+)dy_{tt}^2 - \\ &- 2h_\times dx_{tt}dx_{tt}. \end{aligned} \quad (112)$$

The wordlines $x_{tt}, y_{tt}, z_{tt} = \text{const.}$ are timelike geodesics representing the histories of free test masses (Iorio and Corda 2010). The coordinate transformation $x^\alpha = x^\alpha(x_{tt}^\beta)$ from the TT coordinates to the frame of the local observer is given by (Iorio and Corda 2010;

Baskaran and Grishchuk 2004)

$$\begin{aligned} t &= t_{tt} + \frac{1}{4}(x_{tt}^2 - y_{tt}^2)\dot{h}_+ - \frac{1}{2}x_{tt}y_{tt}\dot{h}_\times \\ x &= x_{tt} + \frac{1}{2}x_{tt}h_+ - \frac{1}{2}y_{tt}h_\times + \frac{1}{2}x_{tt}z_{tt}\dot{h}_+ - \\ &- \frac{1}{2}y_{tt}z_{tt}\dot{h}_\times \\ y &= y_{tt} + \frac{1}{2}y_{tt}h_+ - \frac{1}{2}x_{tt}h_\times + \frac{1}{2}y_{tt}z_{tt}\dot{h}_+ - \\ &- \frac{1}{2}x_{tt}z_{tt}\dot{h}_\times \\ z &= z_{tt} - \frac{1}{4}(x_{tt}^2 - y_{tt}^2)\dot{h}_+ + \frac{1}{2}x_{tt}y_{tt}\dot{h}_\times, \end{aligned} \quad (113)$$

and

$$\begin{aligned} \dot{h}_+ &\equiv \frac{\partial h_+}{\partial t}, \\ \dot{h}_\times &\equiv \frac{\partial h_\times}{\partial t}. \end{aligned} \quad (114)$$

The coefficients of this transformation (components of the metric and its first time derivative) are taken along the central worldline of the local observer (Iorio and Corda 2010; Baskaran and Grishchuk 2004). It is well known that the linear and quadratic terms, as powers of x_{tt}^α , are unambiguously determined by the conditions of the frame of the local observer, while the cubic and higher-order corrections are not determined by these conditions (Iorio and Corda 2010; Baskaran and Grishchuk 2004). Thus, at high-frequencies, the expansion in terms of higher-order corrections breaks down (Iorio and Corda 2010; Baskaran and Grishchuk 2004). Considering a free mass riding on a timelike geodesic ($x = l_1, y = l_2, z = l_3$) (Iorio and Corda 2010; Baskaran and Grishchuk 2004), eq. (113) defines the motion of this mass with respect to the introduced frame of the local observer. In concrete terms one gets

$$\begin{aligned} x(t) &= l_1 + \frac{1}{2}[l_1h_+(t) - l_2h_\times(t)] + \frac{1}{2}l_1l_3\dot{h}_+(t) + \\ &+ \frac{1}{2}l_2l_3\dot{h}_\times(t) \\ y(t) &= l_2 - \frac{1}{2}[l_2h_+(t) + l_1h_\times(t)] - \frac{1}{2}l_2l_3\dot{h}_+(t) + \\ &+ \frac{1}{2}l_1l_3\dot{h}_\times(t) \\ z(t) &= l_3 - \frac{1}{4}(l_1^2 - l_2^2)\dot{h}_+(t) + 2l_1l_2\dot{h}_\times(t). \end{aligned} \quad (115)$$

In the absence of GWs the position of the mass is (l_1, l_2, l_3) and the effect of the GW is to induce oscillations of the mass. Thus, in general, from eq. (115) all three components of motion are present (Iorio and

Corda 2010; Baskaran and Grishchuk 2004). Neglecting the terms with \dot{h}_+ and \dot{h}_\times in eq. (115), the “traditional” equations for the mass motion are obtained (Iorio and Corda 2010; Baskaran and Grishchuk 2004)

$$\begin{aligned} x(t) &= l_1 + \frac{1}{2}[l_1 h_+(t) - l_2 h_\times(t)] \\ y(t) &= l_2 - \frac{1}{2}[l_2 h_+(t) + l_1 h_\times(t)] \\ z(t) &= l_3. \end{aligned} \quad (116)$$

Clearly, this is the analogon of the electric component of motion in electrodynamics (Iorio and Corda 2010; Baskaran and Grishchuk 2004), while the equations

$$\begin{aligned} x(t) &= l_1 + \frac{1}{2}l_1 l_3 \dot{h}_+(t) + \frac{1}{2}l_2 l_3 \dot{h}_\times(t) \\ y(t) &= l_2 - \frac{1}{2}l_2 l_3 \dot{h}_+(t) + \frac{1}{2}l_1 l_3 \dot{h}_\times(t) \\ z(t) &= l_3 - \frac{1}{4}[l_1^2 - l_2^2]\dot{h}_+(t) + 2l_1 l_2 \dot{h}_\times(t), \end{aligned} \quad (117)$$

are the analogues of the magnetic component of motion. One could think that the presence of these “magnetic” components is a “frame artefact” due to the transformation of eq. (113), but in Section 4 of Baskaran and Grishchuk (2004) eq. (115) has been directly obtained from the geodesic deviation equation too, thus the magnetic components have a real physical significance. The fundamental point of Iorio and Corda (2010); Baskaran and Grishchuk (2004) is that the “magnetic” components become important when the frequency of the wave increases but only in the low-frequency regime. This can be understood directly from eq. (115). In fact, by using eq. (111) and eq. (113), it turns out that eq. (115) becomes

$$\begin{aligned} x(t) &= l_1 + \frac{1}{2}[l_1 h_+(t) - l_2 h_\times(t)] + \\ &\quad + \frac{1}{2}l_1 l_3 \omega h_+(t - \frac{\pi}{2}) + \frac{1}{2}l_2 l_3 \omega h_\times(t - \frac{\pi}{2}) \\ y(t) &= l_2 - \frac{1}{2}[l_2 h_+(t) + l_1 h_\times(t)] - \\ &\quad - \frac{1}{2}l_2 l_3 \omega h_+(t - \frac{\pi}{2}) + \frac{1}{2}l_1 l_3 \omega h_\times(t - \frac{\pi}{2}) \\ z(t) &= l_3 - \frac{1}{4}[l_1^2 - l_2^2]\omega h_+(t - \frac{\pi}{2}) + \\ &\quad + 2l_1 l_2 \omega h_\times(t - \frac{\pi}{2}). \end{aligned} \quad (118)$$

Thus, the terms with \dot{h}_+ and \dot{h}_\times in eq. (115) can be neglected only when the wavelength goes to infinity, while, at high-frequencies, the expansion in terms of $\omega l_i l_j$ corrections, with $i, j = 1, 2, 3$, breaks down (Iorio and Corda 2010; Baskaran and Grishchuk 2004). The attentive reader could be surprised that gravitomagnetic

effects in the field of a GW have been ignored in the past. Actually, the key point is that realizing the first direct detection has been always the most important goal for scientists in this research field. To obtain such a first detection, the low frequency approximation is considered sufficient, i.e. only the “electric” component is needed for ground based interferometers (Baskaran and Grishchuk 2004). On the other hand, if the scientific community aims to realize a concrete GW astronomy, the above discussion shows that gravitomagnetic effects in the field of a GW have to be taken in due account. Finally, we recall that GM effects are important in the process of producing GWs too. Indeed, Capozziello et al. (2010) studied corrections to the relativistic orbits by considering high order approximations induced by GM effects for very massive binary systems (e.g. a very massive black hole on which a stellar object is spiralling in). Such corrections have been explained by taking into account “magnetic” components in the weak field limit of the gravitational field. New nutation effects of order c^{-3} have been found. These effects work beside the standard periastron corrections and affect the GW emission and the gravitational waveforms due by the orbital motion of the two massive bodies (Capozziello et al. 2010). The GM corrections emerge as soon as matter-current densities and vector gravitational potentials cannot be discarded into dynamics (Capozziello et al. 2010). GWs emitted through massive binary systems have been studied in the quadrupole approximation (Capozziello et al. 2010).

8 Conclusions

Measuring gravitomagnetism, and, in particular, the Lense-Thirring effect is a challenging and difficult enterprise. In this review we have shown how the detection of such a general relativistic signal is closely related to a number of other competing dynamical features of motion, so that a genuine interdisciplinary attitude is required. Looking for the prediction by Lense and Thirring may help in shedding light on different aspects of the solar system scenarios in which it is attempted to be measured. Conversely, a better knowledge of the forces acting on dynamical systems may be of great help in reliably and accurately measuring the gravitomagnetic field itself.

The current tests with the LAGEOS satellites in the gravitational field of the Earth, which represent the first implemented attempts to measure the Lense-Thirring effect, should be repeated by directly modeling the gravitomagnetic force and explicitly solving for it in the data processing. Moreover, they should

be complemented by a re-analysis of the data sets of the currently ongoing spacecraft-based missions dedicated to accurately measuring the global gravitational field of the Earth like GRACE taking into account general relativity itself; new global solutions in which one or more parameters accounting for the Lense-Thirring effect are solved-for should be produced. For the moment, a conservative evaluation of the systematic bias in the LAGEOS-LAGEOS II tests due to the imperfect knowledge of the classical part of the Earth's gravitational field points toward a 20 – 30% level; more optimistic evaluations yield a 10 – 15% uncertainty. It is unclear if the future LARES mission will be able to measure the Lense-Thirring precessions at the repeatedly claimed $\approx 1\%$ accuracy. Indeed, its orbital configuration, different from that originally proposed, may enhance some competing dynamical effects of gravitational and non-gravitational origin at a level whose uncertainty is difficult to be realistically evaluated.

The present-day level of accuracy in the orbit determination of the inner planets of the solar system has basically reached the magnitude of the Lense-Thirring precessions. The most important systematic error due to mis-modeled dynamical effects is associated with the first even zonal harmonic of the non-spherical gravitational field of the Sun, which particularly affects Mercury. Anyway, an accurate measurement of the Sun's oblateness is one of the goals of future spacecraft-based missions. The analysis of more accurate ranging data to present and future spacecraft like, e.g., BepiColombo and, especially, future interplanetary laser ranging devices should drastically improve the situation allowing for a reasonably accurate measurement of the solar gravitomagnetic field.

After the preliminary attempts with the Mars Global Surveyor probe which have paved the way, also Mars may become suitable for reliably measuring the Lense-Thirring orbital precessions in the near future. To this aim, the forthcoming Phobos-Grunt mission, scheduled for launch in late 2011 or early 2012, will improve our knowledge of some key physical properties of Mars and of the orbit of its satellite Phobos.

The Juno mission to Jupiter, scheduled for launch in 2011, may yield the opportunity for an accurate measurement of the Jovian angular momentum through the Lense-Thirring effect itself.

Finally, we emphasized the relevant connection between gravitomagnetic effects and GWs. In fact, the scientific community expects the first direct detection of GWs within the next years. The importance of gravitomagnetic effects in the framework of GWs increases in the high-frequency portion of the range of ground based interferometers for both of GWs which arise from stan-

dard GTR as well as those coming from scalar-tensor gravity. If one neglects the magnetic contribution considering only the low-frequency approximation of the electric contribution, a portion of about 15% of the signal could be lost by interferometric detectors. Thus, a carefully analysis of the “magnetic”-type contribution of GWs is needed in order to establish a GW astronomy within the next years.

Acknowledgments

L.I. thanks L.F.O. Costa for useful suggestions and critical remarks. The authors gratefully thank an anonymous referee for her/his valuable comments who contributed to improve the manuscript.

References

- Abshire, J.B., Sun, X., Neumann, G., McGarry, J., Zagwodzki, T., Jester, P., Riris, H., Zuber, M.T., Smith, D.E.: In: Conference on Lasers and Electro-Optics (CLEO-06), Long Beach, California, May 2006: Laser Pulses from Earth Detected at Mars
- Allen, B.: In: Marck, J.-A., Lasota, J.-P. (eds.) *Relativistic Gravitation and Gravitational Radiation: The stochastic gravity-wave background: sources and detection*. 373, Cambridge: Cambridge University Press, (1997)
- Anderson, J.D.: In: Gehrels, T., Matthews, M.S. (eds.) *Jupiter: Studies of the Interior, Atmosphere, Magnetosphere, and Satellites: The gravity field of Jupiter*. 113, Tucson: University of Arizona Press, (1976)
- Anderson, J.D., Lau, E.L., Schubert, G., Palguta, J.L.: Gravity Inversion Considerations for Radio Doppler Data from the JUNO Jupiter Polar Orbiter American Astronomical Society, DPS meeting #36, #14.09, (2004) <http://aas.org/archives/BAAS/v36n4/dps2004/158.htm>. Cited 20 Mar 2010
- Andrés, J.I.: *Enhanced Modelling of LAGEOS Non-Gravitational Perturbations*. PhD thesis, Sieca Repro Turbineweg, Delft, (2007)
- Appourchaux, T., Burston, R., Chen, Y., Cruise, M., Dittus, H., Foulon, B., Gill, P., Gizon, L., Klein, H., Klioner, S.A., Kopeikin, S.M., Krüger, H., Lämmerzahl, C., Lobo, A., Luo, X., Margolis, H., Ni, W.-T., Pulido Patón, A., Peng, Q., Peters, A., Rasel, E., Rüdiger, A., Samain, É., Selig, H., Shaul, D., Sumner, T., Thei, S., Touboul, P., Turyshev, S.G., Wang, H., Wang, L., Wen, L., Wicht, A., Wu, J., Zhang, X., Zhao, C.: *Astrodynamical Space Test of Relativity Using Optical Devices I (ASTROD I)* A class-M fundamental physics mission proposal for Cosmic Vision 20152025. *Experimental Astronomy* **23**, 491 (2009)
- Arvanitaki, A., Dubovsky, S.: Exploring the String Axiverse with Precision Black Hole Physics. *Phys. Rev. D* **81**, 123530 (2010)
- Ashby, N., Allison, T.: Canonical planetary equations for velocity-dependent forces, and the Lense-Thirring precession. *Celest. Mech. Dyn. Astron.* **57**, 537 (1993)
- Ashby, N., Bender, P., Wahr, J.M.: Future gravitational physics tests from ranging to the BepiColombo Mercury planetary orbiter. *Phys. Rev. D* **75**, 022001 (2007)
- Balogh, A., Grard, R., Solomon, S.C., Schulz, R., Langevin, Y., Kasaba, Y., Fujimoto, M.: Missions to Mercury. *Space Sci. Rev.* **132**, 611 (2007)
- Barker, B.M., O'Connell, R.F.: Derivation of the Equations of Motion of a Gyroscope from the Quantum Theory of Gravitation. *Phys. Rev. D* **2**, 1428 (1970)
- Barker, B.M., O'Connell, R.F.: Relativity Gyroscope Experiment at Arbitrary Orbit Inclinations. *Phys. Rev. D* **6**, 956 (1972)
- Barker, B.M., O'Connell, R.F.: Effect of the rotation of the central body on the orbit of a satellite. *Phys. Rev. D* **10**, 1340 (1974)
- Baskaran, D., Grishchuk, L.P.: Components of the gravitational force in the field of a gravitational wave. *Class. Quant. Grav.* **21**, 4041 (2004)
- Beck, J.G., Giles, P.: Helioseismic Determination of the Solar Rotation Axis. *Astrophys. J. Lett.* **621**, L153 (2005)
- Bedford, D., Krumm, P.: On relativistic gravitation. *Am. J. Phys.* **53**, 889 (1985)
- Bini, D., Cherubini, C., Chiccone, C., Mashhoon, B.: Gravitational induction. *Class. Quantum Grav.* **25**, 225014 (2008)
- Biswas, A., Mani, K.R.S.: Relativistic perihelion precession of orbits of Venus and the Earth. *Central European Journal of Physics*. **6**, 754 (2008)
- Bogorodskii, A.F.: Relativistic Effects in the Motion of an Artificial Earth Satellite. *Soviet Astronomy* **3**, 857 (1959)
- Borderies, N., Yoder, C.F.: Phobos' gravity field and its influence on its orbit and physical librations. *Astron. Astrophys.* **233**, 235 (1990)
- Braginsky, V.B., Polnarev, A.G.: Relativistic spin quadrupole gravitational effect. *J. Exp. Theor. Phys. Lett.* **31**, 415 (1980)
- Braginsky, V.B., Caves, C.M., Thorne, K.S.: Laboratory experiments to test relativistic gravity. *Phys. Rev. D* **15**, 2047 (1977)
- Braginsky, V.B., Polnarev, A.G., Thorne, K.S.: Foucault Pendulum at the South Pole: Proposal for an Experiment to Detect the Earth's General Relativistic Gravitomagnetic Field. *Phys. Rev. Lett.* **53**, 863 (1984)
- Camacho, A., Ahluwalia, D.W.: Quantum Zeno Effect and the Detection of Gravitomagnetism. *Int. J. Mod. Phys. D* **10**, 9 (2001)
- Capozziello, S., De Laurentis, M., Garufi, F., Milano, L.: Relativistic orbits with gravitomagnetic corrections. *Physica Scripta*. **79**, 025901 (2009)
- Capozziello, S., De Laurentis, M., Forte, L., Garufi, F., Milano, L.: Gravitomagnetic corrections on gravitational waves. *Physica Scripta*. **81**, 035008 (2010)
- Cavendish, H.: Experiments to Determine the Density of the Earth. By Henry Cavendish, Esq. *F. R. S. and A. S. Phil. Trans. Roy. Soc. London* **88**, 469 (1798)
- Cerdonio, M., Prodi, G.A., Vitale, S.: Dragging of inertial frames by the rotating Earth: proposal and feasibility for a ground-based detection. *Gen. Relativ. Gravit.* **20**, 83 (1988)
- Chandler, J.F., Pearlman, M.R., Reasenberg, R.D., Degnan, J.J.: In: R. Noomen, R., Davila, J.M., Garate, J., Noll, C., Pearlman, M. (eds.) *Proc. 14-th International Workshop on Laser Ranging*, San Fernando, Spain, June 7-11 2004: *Solar-System Dynamics and Tests of General Relativity with Planetary Laser Ranging* http://cddis.nasa.gov/lw14/docs/papers/_sci7b_jcm.pdf.
- Chashchina, O., Iorio, L., Silagadze, Z.: Elementary Derivation of the LenseThirring Precession. *Acta Phys. Pol. B* **40**, 2363 (2009)
- Chauvenet, W.: *A Manual of Spherical and Practical Astronomy*. Vol.2: *Theory and Use of Astronomical Instruments*. Method of Least Squares. 1st edition. Lippincott, Philadelphia, (1863); Unabridged and unaltered republication of the fifth revised and corrected edition 1891. Dover, New York, (1960)
- Christodoulidis, D.C., Smith, D.E., Williams, R.G., Klosko, S.M.: Observed Tidal Braking in the Earth/Moon/Sun System. *J. Geophys. Res.* **93**, 6216 (1988)
- Ciufolini, I., Measurement of the Lense-Thirring drag on high-altitude, laser-ranged artificial satellites. *Phys. Rev. Lett.* **56**, 278 (1986)

- Ciufolini, I., A Comprehensive Introduction to the LAGEOS Gravitomagnetic Experiment: from the Importance of the Gravitomagnetic Field in Physics to Preliminary Error Analysis and Error Budget. *Int. J. Mod. Phys. A* **4**, 3083 (1989)
- Ciufolini, I., Gravitomagnetism and status of the LAGEOS III experiment. *Class. Quantum Grav.* **11**, A73 (1994)
- Ciufolini, I., On a new method to measure the gravitomagnetic field using two orbiting satellites. *N. Cim. A* **109**, 1709 (1996)
- Ciufolini, I., LARES/WEBER-SAT, frame-dragging and fundamental physics. gr-qc/0412001 (2004, unpublished)
- Ciufolini, I., On the orbit of the LARES satellite. gr-qc/0609081 (2006, unpublished)
- Ciufolini, I., Dragging of inertial frames. *Nature* **449**, 41 (2007)
- Ciufolini, I., Frame-dragging, gravitomagnetism and Lunar Laser Ranging. *New Astron.* **15**, 332 (2010)
- Ciufolini, I., Pavlis, E.C., A confirmation of the general relativistic prediction of the Lense-Thirring effect. *Nature* **431**, 958 (2004)
- Ciufolini, I., Pavlis, E.C., On the measurement of the Lense-Thirring effect using the nodes of the LAGEOS satellites, in reply to "On the reliability of the so far performed tests for measuring the Lense-Thirring effect with the LAGEOS satellites" by Iorio, L.,. *New Astron.* **10**, 636 (2005)
- Ciufolini, I., Lucchesi, D.M., Vespe, F., Mandiello, A.: Measurement of Dragging of Inertial Frames and Gravitomagnetic Field Using Laser-Ranged Satellites. *N. Cim. A* **109**, 575 (1996)
- Ciufolini, I., Lucchesi, D.M., Vespe, F., Chieppa, F.: Measurement of gravitomagnetism. *Europhys. Lett.* **39**, 359 (1997a)
- Ciufolini, I., Chieppa, F., Lucchesi, D.M., Vespe, F., Test of Lense-Thirring orbital shift due to spin. *Class. Quantum Grav.* **14**, 2701 (1997b)
- Ciufolini, I., Pavlis, E.C., Chieppa, F., Fernandes-Vieira, E., Pérez-Mercader, J.: Test of General Relativity and Measurement of the Lense-Thirring Effect with Two Earth Satellites. *Science* **279**, 2100 (1998a)
- Ciufolini, I., et al.: *LARES Phase A*. Rome: University La Sapienza, (1998b)
- Ciufolini, I., Pavlis, E.C., Peron, R., Determination of frame-dragging using Earth gravity models from CHAMP and GRACE. *New Astron.* **11**, 527 (2006)
- Ciufolini, I., Paolozzi, A., Pavlis, E.C., Ries, J.C., Koenig, R., Matzner, R.A., Sindoni, G., Neumayer, H.: Towards a One Percent Measurement of Frame Dragging by Spin with Satellite Laser Ranging to LAGEOS, LAGEOS 2 and LARES and GRACE Gravity Models. *Space Sci. Rev.* **148**, 71 (2009)
- Clark, S.J., Tucker, R.W.: Gauge symmetry and gravitoelectromagnetism. *Class. Quantum Gravity* **17**, 4125 (2000)
- Cohen, S.C., Smith, D.E. (eds.): LAGEOS (Laser Geodynamic Satellite) special issue. *J. Geophys. Res.* **90**, 9215 (1985)
- Cohen, J.M., Mashhoon, B.: Standard Clocks, Interferometry, and Gravitomagnetism. *Phys. Lett. A* **181**, 353 (1993)
- Combrinck, L.: In: Schillak, S. (ed.) *Proc. 16th Int. Laser Ranging Workshop*, (Poznań (PL) 13-17 October 2008) Evaluation of PPN parameter Gamma as a test of General Relativity using SLR data (2008) http://cddis.gsfc.nasa.gov/lw16/docs/papers/sci_6_Combrinck_p.pdf Cited 20 Mar 2010
- Conklin, J.W., The Gravity Probe B Collaboration: The Gravity Probe B experiment and early results. *Journal of Physics: Conference Series* **140**, 012001 (2008)
- Corda, C.: The Virgo-MiniGRAIL cross correlation for the detection of scalar gravitational waves. *Mod. Phys. Lett. A* **22**, 1727 (2007a)
- Corda, C.: The Importance of the "magnetic" Components of Gravitational Waves in the Response Functions of Interferometers. *Int. J. Mod. Phys. D* **16**, 1497 (2007b)
- Corda, C.: Interferometric detection of gravitational waves: the definitive test for General Relativity. *Int. J. Mod. Phys. D* **18**, 2275 (2009)
- Corda, C.: A review of the stochastic background of gravitational waves in $f(R)$ gravity with WMAP constraints. *The Open Astronomy Journal*. ArXiv:0901.1193 (2010, in press)
- Corda, C., Ali, S.A., Cafaro, C.: Interferometer Response to Scalar Gravitational Waves. *Int. J. Mod. Phys. D*. ArXiv:0902.0093 (2010, in press)
- Costa, L.F.O., Herdeiro, C.A.R.: Gravitoelectromagnetic analogy based on tidal tensors. *Phys. Rev. D* **78**, 024021 (2008)
- Costa, L.F.O., Herdeiro, C.A.R.: In: Klioner, S.A., Seidelmann, P.K., Soffel, M.H. (eds.) *Relativity in Fundamental Astronomy: Dynamics, Reference Frames, and Data Analysis*, Proceedings IAU Symposium No. 261: EPM ephemerides and relativity. 31, Cambridge: Cambridge University Press, (2010)
- Crosta, M.T., Mignard, F.: Microarcsecond light bending by Jupiter. *Class. Quantum Grav.* **23**, 4853 (2006)
- Cugusi, L., Proverbio, E.: Relativistic effects on the Motion of the Earth's Satellites. *J. Geod.* **51**, 249 (1977)
- Cugusi, L., Proverbio, E.: Relativistic Effects on the Motion of Earth's Artificial Satellites. *Astron. Astrophys.* **69**, 321 (1978)
- Degnan, J.J.: Satellite laser ranging: current status and future prospects. *IEEE Trans. Geosci. Remote Sensing*. **GE-23**, 398 (1985)
- Degnan, J.J.: In: *Proc. 15-th International Workshop on Laser Ranging*, Canberra, Australia, October 15-20 2006: Simulating Interplanetary Transponder and Laser Communications Experiments Via Dual Station Ranging To SLR Satellites [http://cddis.gsfc.nasa.gov/lw15/docs/papers/Simulating Interplanetary Transponder and Laser Communications Experiments via Dual Station Ranging to SLR Satellites.pdf](http://cddis.gsfc.nasa.gov/lw15/docs/papers/Simulating%20Interplanetary%20Transponder%20and%20Laser%20Communications%20Experiments%20via%20Dual%20Station%20Ranging%20to%20SLR%20Satellites.pdf) Cited 20 Mar 2010
- Degnan, J.J.: In: Dittus, H., Lämmerzahl, C., Turyshev, S.G. (eds.) *Lasers, Clocks and Drag-Free Control Exploration of Relativistic Gravity in Space: Laser Transponders for High-Accuracy Interplanetary Laser Ranging and Time Transfer*. 231, Berlin: Springer, (2008)
- de Boer, H.: In: Taylor, B.N., Phillips, W.D. (eds.) *Precision Measurement and Fundamental Constants*. Natl. Bur. Stand. US. Spec. Publ. 617: Experiments relating to the Newtonian gravitational constant. 561, Washington: Natl. Bur. Stand. US, (1984)

- de Sitter, W.: Einstein's theory of gravitation and its astronomical consequences. *Mon. Not. R. Astron. Soc.* **76**, 699 (1916)
- Dickey, J.O., Bender, P.L., Faller, J.E., Newhall, X.X., Ricklefs, R.L., Ries, J.G., Shelus, P.J., Veillet, C., Whipple, A.L., Wiant, J.R., Williams, J.G., Yoder, C.F.: Lunar Laser Ranging: A Continuing Legacy of the Apollo Program. *Science* **265**, 482 (1994)
- Dymnikova, I.G.: Motion of particles and photons in the gravitational field of a rotating body (In memory of Vladimir Afanas'evich Ruban). *Sov. Phys. Usp.* **29**, 215 (1986)
- Eddington, A.S.: *The Mathematical Theory of Relativity*. Cambridge: Cambridge University Press, (1922)
- Einstein, A.: Zum gegenwärtigen stande des Gravitationsproblem. *Phys. Z.* **14**, 1249 (1913)
- Einstein, A.: Zur allgemeinen Relativitätstheorie. *Sitzungsberichte der Königlich Preußischen Akademie der Wissenschaften* **XLIV**, 778 (1915)
- Einstein, A.: Näherungsweise Integration der Feldgleichungen der Gravitation. *Sitzungsberichte der Königlich Preußischen Akademie der Wissenschaften*, 688 (1916)
- Einstein, A.: Über Gravitationswellen. *Sitzungsberichte der Königlich Preußischen Akademie der Wissenschaften* **8**, 154 (1918)
- Everitt, C.W.F.: In: Bertotti, B. (ed.) *Proc. Int. School Phys. "Enrico Fermi" Course LVI: The Gyroscope Experiment I. General Description and Analysis of Gyroscope Performance*. 331, New York: New Academic Press, (1974)
- Everitt, C.W.F., et al.: In: Lämmerzahl, C., Everitt, C.W.F., Hehl, F.W. (eds.) *Gyros, Clocks, Interferometers...: Testing Relativistic Gravity in Space: Gravity Probe B: Countdown to Launch*. 52, Berlin: Springer, (2001)
- Everitt, C.W.F., et al.: Gravity Probe B Data Analysis. *Space Sci. Rev.* **148**, 53 (2009)
- Fairbank, W.M., Schiff, L.I.: *Proposed Experimental Test of General Relativity*. Proposal to NASA. Stanford: Stanford University, (1961)
- Fienga, A., Manche, H., Laskar, J., Gastineau, M.: INPOP06: a new numerical planetary ephemeris. *Astron. Astrophys.* **477**, 315 (2008)
- Fienga, A., Laskar, J., Morley, T., Manche, H., Kuchynka, P., Le Poncin-Lafitte, C., Budnik, F., Gastineau, M., Somenzi, L.: INPOP08, a 4-D planetary ephemeris: from asteroid and time-scale computations to ESA Mars Express and Venus Express contributions. *Astron. Astrophys.* **507**, 1675 (2009)
- Fienga, A., Laskar, J., Kuchynka, P., Le Poncin-Lafitte, C., Manche, H., Gastineau, M.: In: Klioner, S.A., Seidelmann, P.K., Soffel, M.H. (eds.) *Relativity in Fundamental Astronomy: Dynamics, Reference Frames, and Data Analysis*, Proceedings IAU Symposium No. 261: Gravity tests with INPOP planetary ephemerides. 159, Cambridge: Cambridge University Press, (2010)
- Folkner, W.M., Williams, J.G.: Boggs, D.H.: *The Planetary and Lunar Ephemeris DE 421*. Memorandum IOM 343R-08-003. California Institute of Technology: Jet Propulsion Laboratory, (2008)
- Fomalont, E.B., Kopeikin, S.M.: In: Jin, W.J., Platais, I., Perryman, M.A.C. (eds.) *A Giant Step: from Milli- to Micro-arcsecond Astrometry Proceedings IAU Symposium No. 248*, 2007: Radio interferometric tests of general relativity. 383, Cambridge: Cambridge University Press, (2008)
- Forbes, J.M., Bruinsma, S., Lemoine, F.G., Bowman, B.R., Konopliv, A.S.: Variability of the Satellite Drag Environments of Earth, Mars and Venus due to Rotation of the Sun, American Geophysical Union, Fall Meeting 2006, abstract #SA22A-04 (2006)
- Förste, Ch., Flechtner, F., Schmidt, R., König, R., Meyer, U., Stubenvoll, R., Rothacher, M., Barthelmes, F., Neumayer, H., Biancale, R., Bruinsma, S., Lemoine, J.-M., Loyer, S.: A mean global gravity field model from the combination of satellite mission and altimetry/gravimetry surface data - EIGEN-GL04C. *Geophys. Res. Abstracts* **8**, 03462 (2006)
- Förste, Ch., Flechtner, F., Schmidt, R., Stubenvoll, R., Rothacher, M., Kusche, J., Neumayer, H., Biancale, R., Lemoine, J.-M., Barthelmes, F., Bruinsma, S., König, R., Meyer, U.: EIGEN-GL05C - A new global combined high-resolution GRACE-based gravity field model of the GFZ-GRGS cooperation. *Geophys. Res. Abstracts* **10**, 03426 (2008)
- Giazotto, A.: Status of gravitational wave detection. *Journ. of Phys. Conf. Ser.* **120**, 032002 (2008)
- Ginzburg, V.L.: The use of artificial earth satellites for verifying the general theory of relativity. *Uspekhi Fizicheskikh Nauk (Advances in Physical Science)* **63**, 119 (1957)
- Ginzburg, V.L.: Artificial Satellites and the Theory of Relativity. *Scientific American* **200**, 149 (1959)
- Ginzburg, V.L.: In: *Recent Developments in General Relativity: Experimental Verifications of the General Theory of Relativity*. 57, London: Pergamon press, (1962)
- Gronwald, F., Gruber, E., Lichtenegger, H.I.M., Puntigam, R.A.: Gravity Probe C(lock) - Probing the gravitomagnetic field of the Earth by means of a clock experiment. *ESA SP-420*, 29 (1997)
- Guillot, T.: THE INTERIORS OF GIANT PLANETS: Models and Outstanding Questions. *Ann. Rev. Earth Planet. Sci.* **33**, 493 (2005)
- Haas, M.R., Ross, D.K.: Measurement of the angular momentum of Jupiter and the Sun by use of the Lense-Thirring effect. *Astrophys. Space Sci.* **32**, 3 (1975)
- Heaviside, O.: *Electromagnetic Theory*, Volume I. London: The Electrician Printing and Publishing Co., (1894)
- Hiscock, W.A., Lindblom, L.: Post-Newtonian effects on satellite orbits near Jupiter and Saturn. *Astrophys. J.* **231**, 224 (1979)
- Holzmüller, G.: Ueber die Anwendung der Jacobi-Hamilton'schen Methode auf den Fall der Anziehung nach dem elektrodynamischen Gesetze von Weber. *Zeitschrift für Mathematik und Physik* **15**, 69 (1870)
- Hori, Y., Sano, T., Ikoma, M., Ida, S.: In: Sun, Y.-S., Ferraz-Mello, S., Zhou, J.-L. (eds.) *EXOPLANETS: Detection, Formation and Dynamics Proceedings IAU Symposium No. 249: On uncertainty of Jupiter's core mass due to observational errors*, Cambridge: Cambridge University Press, 163 (2008)

- Hulse, R.A., Taylor, J.H.: Discovery of a pulsar in a binary system. *Astrophys. J. Lett.* **195**, L51 (1975)
- Inversi, P., Vespe, F.: Direct and indirect solar radiation effects acting on LAGEOS satellite: Some refinements. *Adv. Space Res.* **14**, 73 (1994)
- Iorio, L.: An alternative derivation of the Lense-Thirring drag on the orbit of a test body. *Nuovo Cim. B* **116**, 777 (2001)
- Iorio, L.: Satellite non-gravitational orbital perturbations and the detection of the gravitomagnetic clock effect. *Class. Quantum Grav.* **18**, 4303 (2001b)
- Iorio, L.: Satellite gravitational orbital perturbations and the gravitomagnetic clock effect. *Int. J. Mod. Phys. D* **11**, 599 (2001c)
- Iorio, L.: LETTER TO THE EDITOR: A critical approach to the concept of a polar, low-altitude LARES satellite. *Class. Quantum Grav.* **19**, L175 (2002)
- Iorio, L.: LETTER TO THE EDITOR: On the possibility of measuring the Earth's gravitomagnetic force in a new laboratory experiment. *Class. Quantum Grav.* **20**, L5 (2003a)
- Iorio, L.: A new proposal for measuring the Lense-Thirring effect with a pair of supplementary satellites in the gravitational field of the Earth. *Phys. Lett. A* **308**, 81 (2003b)
- Iorio, L.: The impact of the static part of the Earth's gravity field on some tests of General Relativity with Satellite Laser Ranging. *Celest. Mech. Dyn. Astron.* **86**, 277 (2003c)
- Iorio, L.: On the reliability of the so-far performed tests for measuring the Lense-Thirring effect with the LAGEOS satellites. *New Astron.* **10**, 603 (2005a)
- Iorio, L.: The impact of the new Earth gravity models on the measurement of the Lense-Thirring effect with a new satellite. *New Astron.* **10**, 616 (2005b)
- Iorio, L.: On the possibility of testing the Dvali Gabadadze Porrati brane-world scenario with orbital motions in the Solar System. *J. Cosmol. Astropart. Phys.* **7**, 8 (2005c)
- Iorio, L.: Is it possible to measure the Lense-Thirring effect on the orbits of the planets in the gravitational field of the Sun? *Astron. Astrophys.* **431**, 385 (2005d)
- Iorio, L.: On the impossibility of measuring the general relativistic part of the terrestrial acceleration of gravity with superconducting gravimeters. *J. Geophys. Res.* **167**, 567 (2006a)
- Iorio, L.: A critical analysis of a recent test of the Lense-Thirring effect with the LAGEOS satellites. *J. Geod.* **80**, 128 (2006b)
- Iorio, L.: COMMENTS, REPLIES AND NOTES: A note on the evidence of the gravitomagnetic field of Mars. *Class. Quantum Grav.* **23**, 5451 (2006c)
- Iorio, L. (ed.), *The Measurement of Gravitomagnetism: A Challenging Enterprise*. Hauppauge: NOVA, (2007a)
- Iorio, L.: A comment on the paper "On the orbit of the LARES satellite", by Ciufolini, I., *Planet. Space Sci.* **55**, 1198 (2007b)
- Iorio, L.: LARES/WEBER-SAT and the equivalence principle. *Europhys. Lett.* **80**, 40007 (2007c)
- Iorio, L.: An assessment of the measurement of the Lense-Thirring effect in the Earth gravity field, in reply to: "On the measurement of the Lense-Thirring effect using the nodes of the LAGEOS satellites, in reply to "On the reliability of the so far performed tests for measuring the Lense-Thirring effect with the LAGEOS satellites" by Iorio, L.: ", by Ciufolini, I., and E. Pavlis. *Planet. Space Sci.* **55**, 503 (2007d)
- Iorio, L.: First preliminary tests of the general relativistic gravitomagnetic field of the Sun and new constraints on a Yukawa-like fifth force from planetary data. *Planet. Space Sci.* **55**, 1290 (2007e)
- Iorio, L.: Dynamical determination of the mass of the Kuiper Belt from motions of the inner planets of the Solar system. *Mon. Not. R. Astron. Soc.* **375**, 1311 (2007f)
- Iorio, L.: In: Iorio, L. (ed.) *The Measurement of Gravitomagnetism: A Challenging Enterprise: Is it Possible to Measure the Lense-Thirring Effect in the Gravitational Fields of the Sun and of Mars?*, Hauppauge: NOVA, 177, (2007g)
- Iorio, L.: Advances in the measurement of the Lense-Thirring effect with planetary motions in the field of the Sun. *Scholarly Research Exchange* **2008**, 105235 (2008)
- Iorio, L.: Will it be Possible to Measure Intrinsic Gravitomagnetism with Lunar Laser Ranging?. *Int. J. Mod. Phys. D* **18**, 1319 (2009a)
- Iorio, L.: Mars and frame-dragging: study for a dedicated mission. *Gen. Relativ. Gravit.* **41**, 1273 (2009b)
- Iorio, L.: An Assessment of the Systematic Uncertainty in Present and Future Tests of the Lense-Thirring Effect with Satellite Laser Ranging. *Space Science Reviews* **148**, 363 (2009c)
- Iorio, L.: A conservative approach to the evaluation of the uncertainty in the LAGEOS-LAGEOS II Lense-Thirring test. *Centr. Eur. J. Phys.* **8**, 25 (2010a)
- Iorio, L.: On possible a-priori "imprinting" of General Relativity itself on the performed Lense-Thirring tests with LAGEOS satellites. *Communication and Network* **2**, 26 (2010b)
- Iorio, L.: On the Impact of the Atmospheric Drag on the LARES Mission. *Acta Physica Polonica B* **4**, 753 (2010c)
- Iorio, L.: Effects of standard and modified gravity on interplanetary ranges. <http://arxiv.org/abs/1002.4585> (2010d)
- Iorio, L.: On the Lense-Thirring test with the Mars Global Surveyor in the gravitational field of Mars. *Centr. Eur. J. Phys.* **8**, 509 (2010e)
- Iorio, L.: Juno, the angular momentum of Jupiter and the Lense-Thirring effect. *New Astron.* **15**, 554 (2010f)
- Iorio, L., Morea, A.: The impact of the new Earth gravity models on the measurement of the Lense-Thirring effect. *Gen. Relativ. Gravit.* **36**, 1321 (2004)
- Iorio, L., Lichtenegger, H.I.M.: On the possibility of measuring the gravitomagnetic clock effect in an Earth space-based experiment. *Class. Quantum Grav.* **22**, 119 (2005)
- Iorio, L., Lainey, V.: The Lense-Thirring effect in the Jovian system of the Galilean satellites and its measurability. *Int. J. Mod. Phys. D* **14**, 2039 (2005)
- Iorio, L., Lucchesi, D.M., Ciufolini, I.: The LARES mission revisited: an alternative scenario. *Class. Quantum Grav.* **19**, 4311 (2002a)
- Iorio, L., Lichtenegger, H.I.M., Mashhoon, B.: An alternative derivation of the gravitomagnetic clock effect. *Class. Quantum Grav.* **19**, 39 (2002b)

- Iorio, L., Corda, C.: Gravitomagnetic effect in gravitational waves. *AIP Conf. Proc.* **1168**, 1072 (2009)
- Iorio, L., Corda, C.: Gravitomagnetism and gravitational waves. *Open Astronomy Journal*. ArXiv:1001.3951 (2010, in press)
- Irwin, P.: *Giant Planets of Our Solar System*. Berlin: Springer, (2003)
- Jacobson, R.A.: JUP230 orbit solution. (2003)
- Jacobson, R.A., Rush, B.: Ephemerides of the Martian Satellites - MAR063, JPL IOM 343R-06-004 (2006)
- Jäggi, A., Beutler, G., Mervart, L.: GRACE Gravity Field Determination using the Celestial Mechanics Approach - First Results, presented at the IAG Symposium on "Gravity, Geoid, and Earth Observation 2008", (Chania, GR, 23-27 June 2008)
- Jäggi, A., Beutler, G., Meyer, U., Prange, L., Dach, R., Mervart, L.: AIUB-GRACE02S - Status of GRACE Gravity Field Recovery using the Celestial Mechanics Approach, presented at the IAG Scientific Assembly 2009, (Buenos Aires, Argentina, August 31 - September 4 2009)
- Kaula, W.M.: *Theory of Satellite Geodesy*. Waltham: Blaisdell, (1966)
- Keiser, G.M., Kolodziejczak, J., Silbergleit, A.S.: Misalignment and Resonance Torques and Their Treatment in the GP-B Data Analysis. *Space Sci. Rev.* **148**, 383 (2009)
- Khan, A.R., O'Connell, R.F.: Gravitational analogue of magnetic force. *Nature* **261**, 480 (1976)
- Klein, M.J., Kox, A.J., Schulmann, R. (eds.): *The Collected Papers of Albert Einstein*. Vol. 4. *The Swiss Years: Writings, 1912-1914*, 344, Princeton: Princeton University Press, (1995)
- Kolbenstvedt, H.: Gravomagnetism in special relativity. *Am. J. Phys.* **56**, 523 (1988)
- Konopliv, A.S., Yoder, C.F., Standish, E.M., Yuan, D.-N., Sjogren, W.L.: A global solution for the Mars static and seasonal gravity, Mars orientation, Phobos and Deimos masses, and Mars ephemeris. *Icarus* **182**, 23 (2006)
- Kopeikin, S.M., Fomalont, E.B.: Aberration and the Fundamental Speed of Gravity in the Jovian Deflection Experiment. *Found. Phys.* **36**, 1244 (2006)
- Kopeikin, S.M.: Comment on "Gravitomagnetic Influence on Gyroscopes and on the Lunar Orbit". *Phys. Rev. Lett.* **98**, 229001 (2007)
- Kramer, M., Stairs, I.H., Manchester, R.N., McLaughlin, M.A., Lyne, A.G., Ferdman, R.D., Burgay, M., Lorimer, D.R., Possenti, A., D'Amico, N., Sarkissian, J.M., Hobbs, G.B., Reynolds, J.E., Freire, P.C.C., Camilo, F.: Tests of General Relativity from Timing the Double Pulsar. *Science* **314**, 97 (2006)
- Krasinsky, G.A., Pitjeva, E.V., Vasilyev, M.V., Yagudina, E.I.: Hidden Mass in the Asteroid Belt. *Icarus* **158**, 98 (2002)
- Krogh, K.: COMMENTS, REPLIES AND NOTES: Comment on 'Evidence of the gravitomagnetic field of Mars'. *Class. Quantum Grav.* **24**, 5709 (2007)
- Lainey, V., Dehant, V., Pätzold, M.: First numerical ephemerides of the Martian moons. *Astron. Astrophys.* **465**, 1075 (2007)
- Landau, L.D., Lifshitz, E.M.: *The Classical Theory of Fields*. Fourth edition. New York: Pergamon press, (1975)
- Lämmerzahl, C., Neugebauer, G.: In: Lämmerzahl, C., Everitt, C.W.F., Hehl, F.W. (eds.) *Gyros, Clocks, Interferometers...: Testing Relativistic Gravity in Space: The Lense-Thirring Effect: From the Basic Notions to the Observed Effects*, 31, Berlin: Springer, (2001a)
- Lemoine, F.G., Kenyon, S.C., Factor, J.K., Trimmer, R.G., Pavlis, N.K., Chinn, D.S., Cox, C.M., Klosko, S.M., Luthcke, S.B., Torrence, M.H., Wang, Y.M., Williamson, R.G., Pavlis, E.C., Rapp, R.H., Olson, T.R.: The Development of the Joint NASA GSFC and the National Imagery Mapping Agency (NIMA) Geopotential Model EGM96. NASA/TP-1998-206861 (1998)
- Lense, J., Thirring, H.: Über den Einfluss der Eigenrotation der Zentralkörper auf die Bewegung der Planeten und Monde nach der Einsteinschen Gravitationstheorie. *Phys. Z.* **19**, 156 (1918)
- Lerch, F.J., Nerem, R.S., Putney, B.H., Felsentreger, T.L., Sanchez, B.V., Marshall, J.A., Klosko, S.M., Patel, G.B., Williamson, R.G., Chinn, D.S.: A geopotential model from satellite tracking, altimeter, and surface gravity data: GEM-T3. *J. Geophys. Res.* **99**, 2815 (1994)
- Lichtenegger, H.I.M., Gronwald, F., Mashhoon, B.: On detecting the gravitomagnetic field of the Earth by means of orbiting clocks. *Adv. Space Res.* **25**, 1255 (2000)
- Lichtenegger, H.I.M., Iorio, L., Mashhoon, B.: The gravitomagnetic clock effect and its possible observation. *Ann. der Phys.* **15**, 868 (2006)
- Lichtenegger, H.I.M., Iorio, L.: In: Iorio, L. (ed.) *The Measurement of Gravitomagnetism: A Challenging Enterprise: Post-Newtonian orbital perturbations*, Hauppauge: NOVA, 87, (2007)
- Ljubičić, A., Logan, B.A.: A proposed test of the general validity of Mach's principle. *Phys. Lett. A* **172**, 3 (1992)
- Lucchesi, D.M.: Reassessment of the error modelling of non-gravitational perturbations on LAGEOS II and their impact in the Lense-Thirring determination. Part I. *Planet. Space Sci.* **49**, 447 (2001)
- Lucchesi, D.M.: Reassessment of the error modelling of non-gravitational perturbations on LAGEOS II and their impact in the Lense-Thirring determination. Part II. *Planet. Space Sci.* **50**, 1067 (2002)
- Lucchesi, D.M.: The asymmetric reflectivity effect on the LAGEOS satellites and the germanium retroreflectors. *Geophys. Res. Lett.* **30**, 1957 (2003)
- Lucchesi, D.M.: LAGEOS Satellites Germanium Cube-Corner-Retroreflectors and the Asymmetric Reflectivity Effect. *Celest. Mech. Dyn. Astron.* **88**, 269 (2004)
- Lucchesi, D.M.: The impact of the even zonal harmonics secular variations on the Lense-Thirring effect measurement with the two Lageos satellites. *Int. J. Mod. Phys. D* **14**, 1989 (2005)
- Lucchesi, D.M.: The Lense Thirring effect measurement and LAGEOS satellites orbit analysis with the new gravity field model from the CHAMP mission. *Adv. Sp. Res.* **39**, 324 (2007a)
- Lucchesi, D.M.: The LAGEOS satellites orbital residuals determination and the way to extract gravitational and non-gravitational unmodeled perturbing effects. *Adv. Sp. Res.* **39**, 1559 (2007b)
- Lucchesi, D.M., Paolozzi, A.: A cost effective approach for LARES satellite. XVI Congresso Nazionale AIDAA (Palermo, IT, 24-28 September 2001)

- Lucchesi, D.M., Ciufolini, I., Andrés, J.I., Pavlis, E.C., Peron, R., Noomen, R., Currie, D.G.: LAGEOS II perigee rate and eccentricity vector excitations residuals and the Yarkovsky-Schach effect. *Planet. Space Sci.* **52**, 699 (2004)
- Lucchesi, D.M., Balmino, G.: The LAGEOS satellites orbital residuals determination and the Lense Thirring effect measurement. *Planet. Space Sci.* **54**, 581 (2006)
- Lyth, D.H., Liddle, A.R.: *Primordial Density Perturbation*. Cambridge: Cambridge University Press, (2009)
- Machida, M.N., Kokubo, E., Inutsuka, S., Matsumoto, T.: Angular Momentum Accretion onto a Gas Giant Planet. *Astroph. J.* **685**, 1220 (2008)
- Marov, M.Ya., Avduevsky, V.S., Akim, E.L., Eneev, T.M., Kremnev, R.S., Kulikov, S.D., Pichkhadze, K.M., Popov, G.A., Rogovsky, G.N.: Phobos-Grunt: Russian sample return mission. *Adv. Space Res.* **33**, 2276 (2004)
- Mashhoon, B.: In: Iorio, L. (ed.) *The Measurement of Gravitomagnetism: A Challenging Enterprise: Gravitoelectromagnetism: A Brief Review*, 29, Hauppauge: NOVA, (2007)
- Mashhoon, B., Theiss, D.S.: Relativistic Tidal Forces and the Possibility of Measuring Them. *Phys. Rev. Lett.* **49**, 1542 (1982)
- Mashhoon, B., Paik, H.J., Will, C.M.: Detection of the gravitomagnetic field using an orbiting superconducting gravity gradiometer. Theoretical principles. *Phys. Rev. D* **39**, 2825 (1989)
- Mashhoon, B., Gronwald, F., Theiss, D.S.: On measuring gravitomagnetism via spaceborne clocks: a gravitomagnetic clock effect. *Ann. der Phys.* **8**, 135 (1999)
- Mashhoon, B., Gronwald, F., Lichtenegger, H.I.M.: In: Lämmerzahl, C., Everitt, C.W.F., Hehl, F.W. (eds.) *Gyros, Clocks, Interferometers...: Testing Relativistic Gravity in Space: Gravitomagnetism and the Clock Effect*, 83, Berlin: Springer, (2001a)
- Mashhoon, B., Iorio, L., Lichtenegger, H.I.M.: On the gravitomagnetic clock effect. *Phys. Lett. A* **292**, 49 (2001b)
- Mathisson, M.: Neue Mechanik materieller systemes. *Acta Physica Polonica* **6**, 163 (1937)
- Matousek, S.: The Juno New Frontiers mission. *Acta Astronautica* **61**, 932 (2007)
- Mayer-Gürr, T., Eicker, A., Ilk, K.-H.: ITG-GRACE02s: a GRACE gravity field derived from short arcs of the satellite's orbit 1st Int. Symp. of the International Gravity Field Service "GRAVITY FIELD OF THE EARTH" (Istanbul, TR, 28 August–1 September 2006)
- Mayer-Gürr, T.: ITG-Grace03s: The latest GRACE gravity field solution computed in Bonn Joint Int. GSTM and DFG SPP Symp. (Potsdam, D, 15–17 October 2007) <http://www.igg.uni-bonn.de/apmg/index.php?id=itg-grace03>. Cited 20 Mar 2010
- Mayer-Gürr, T., Kurtenbach, E., Eicker, A.: THE SATELLITE-ONLY GRAVITY FIELD MODEL ITG-Grace2010s. <http://www.igg.uni-bonn.de/apmg/index.php?id=itg-grace2010>. Cited 20 Mar 2010
- McCarthy, D.D., Petit, G.: *IERS Conventions* (2003), 106, Frankfurt am Main: Verlag des Bundesamtes für Kartographie und Geodäsie, (2004)
- Merkowitz, S.M., Dabney, P.W., Livas, J.C., McGarry, J.F., Neumann, G.A., Zagwodzki, T.W.: *Laser Ranging for Gravitational, Lunar and Planetary Science*. *Int. J. Mod. Phys. D* **16**, 2151 (2007)
- Milani, A., Nobili, A.M., Farinella, P.: *Non-gravitational perturbations and satellite geodesy*. Bristol: Adam Hilger, (1987)
- Milani, A., Vokrouhlický, D., Villani, D., Bonanno, C., Rossi, A.: Testing general relativity with the Bepi-Colombo radio science experiment. *Phys. Rev. D* **66**, 082001 (2002)
- Milani, A., Tommei, G., Vokrouhlický, D., Latorre, E., Cicalò, S.: In: Klioner, S.A., Seidelmann, P.K., Soffel, M.H. (eds.) *Proceedings of the International Astronomical Union, IAU Symposium, Volume 261: Relativistic models for the BepiColombo radioscience experiment, Relativity in Fundamental Astronomy: Dynamics, Reference Frames, and Data Analysis*. 356, Cambridge: Cambridge University Press, (2008)
- Misner, C.W., Thorne, K.S., Wheeler, J.A.: *Gravitation*. San Francisco: Freeman, (1973)
- Mohr, P.J., Taylor, B.N.: CODATA Recommended Values for the Fundamental Physical Constants: 1998. *J. Phys. Chem. Ref. Data* **28**, 1713 (1999)
- Muhlfelder, B., Adams, M., Clarke, B., Keiser, G.M., Kolodziejczak, J., Li, J., Lockhart, J.M., Worden, P.: GP-B Systematic Error Determination. *Space Sci. Rev.* **148**, 429 (2009)
- Murphy, T.W., Nordtvedt, K., Turyshev, S.G.: Gravitomagnetic Influence on Gyroscopes and on the Lunar Orbit. *Phys. Rev. Lett.* **98**, 071102 (2007a)
- Murphy, T.W., Nordtvedt, K., Turyshev, S.G.: Murphy, Nordtvedt, and Turyshev Reply. *Phys. Rev. Lett.* **98**, 229002 (2007b)
- Murphy, T.W., Adelberger, E.G., Battat, J.B.R., Carey, L.N., Hoyle, C.D., Leblanc, P., Michelsen, E.L., Nordtvedt Jr., K., Orin, A.E., Strasburg, J.D., Stubbs, C.W., Swanson, H.E., Williams, E.: The Apache Point Observatory Lunar Laser-ranging Operation: Instrument Description and First Detections. *Publ. Astron. Soc. Pacif.* **120**, 20 (2008)
- Neumann, G., Cavanaugh, J., Coyle, B., McGarry, J., Smith, D., Sun, X., Zagwodzki, T., Zuber, M.: In: *Proc. 15-th International Workshop on Laser Ranging, Canberra, Australia, October 15-20, 2006: Laser Ranging at Interplanetary Distances* http://cdsis.gsfc.nasa.gov/lw-15/docs/papers/Laser_Ranging_at_Interplanetary_Distances.pdf. Cited 20 Mar 2010
- Newhall, X.X., Standish, E.M., Williams, J.G.: DE 102 - A numerically integrated ephemeris of the moon and planets spanning forty-four centuries. *Astron. Astrophys.* **125**, 150 (1983)
- Ni, W.-T.: Theoretic Frameworks for Testing Relativistic Gravity IV. *Astrophys. J.* **176**, 769 (1972)
- Ni, W.-T.: ASTROD and ASTROD I-Overview and Progress. *Int. J. Mod. Phys. D* **17**, 921 (2008)
- Nordtved Jr, K.: Equivalence Principle for Massive Bodies II: Theory. *Phys. Rev.* **169**, 1017 (1968)
- Nordtved Jr, K.: Equivalence Principle for Massive Bodies Including Rotational Energy and Radiation Pressure. *Phys. Rev.* **180**, 1293 (1969)

- Nordtvedt Jr., K.: Existence of the gravitomagnetic interaction. *Int. J. Theor. Phys.* **27**, 1395 (1988)
- Nordtvedt Jr., K.: *Slr Contributions To Fundamental Physics. Surv. Geophys.* **22**, 597 (2001)
- Nordtvedt Jr., K.: In: Ruffini, R.J., Sigismondi, C. (eds.) *Nonlinear Gravitodynamics. The Lense-Thirring Effect: Some Considerations on the Varieties of Frame Dragging*, 35, Singapore: World Scientific, Singapore, (2003)
- North, J.D.: *The Measure of the Universe*. New York: Dover, (1989)
- Ohanian, H.C., Ruffini, R.J.: *Gravitation and Spacetime*. 2nd Edition. New York: W.W. Norton & Company, (1994)
- Paik, H.-J.: Tests of general relativity in earth orbit using a superconducting gravity gradiometer. *Adv. Sp. Res.* **9**, 41 (1989)
- Paik, H.-J.: Detection of the gravitomagnetic field using an orbiting superconducting gravity gradiometer: principle and experimental considerations. *Gen. Relativ. Gravit.* **40**, 907 (2008)
- Papapetrou, A.: Spinning Test-Particles in General Relativity. I. Proceedings of the Royal Society of London. Series A, Mathematical and Physical Sciences **209**, 248 (1951)
- Pavlis, E.C.: In: Cianci, R., Collina, R., Francaviglia, M., Fré, P. (eds.) *Recent Developments in General Relativity: Proc. 14th SIGRAV Conf. on General Relativity and Gravitational Physics (Genova, IT, 18–22 September 2000)*: Geodetic contributions to gravitational experiments in space, 217, Milan: Springer, (2002)
- Peirce, B.: Criterion for the rejection of doubtful observations. *Astron. J.* **2**, 161 (1852); Errata. *Astron. J.* **2**, 176 (1852)
- Pfister, H.: On the history of the so-called Lense-Thirring effect. *Gen. Relativ. Gravit.* **39**, 1735 (2007)
- Pijpers, F.P.: Helioseismic determination of the solar gravitational quadrupole moment. *Mon. Not. R. Astron. Soc.* **297**, L76 (1998)
- Pijpers, F.P.: Asteroseismic determination of stellar angular momentum. *Astron. Astrophys.* **402**, 683 (2003)
- Pirani, F.A.E.: On the physical significance of the Riemann tensor. *Acta Physica Polonica* **15**, 389 (1956)
- Pirani, F.A.E.: Invariant Formulation of Gravitational Radiation Theory. *Phys. Rev.* **105**, 1089 (1957)
- Pireaux, S., Rozelot, J.-P.: Solar quadrupole moment and purely relativistic gravitation contributions to Mercury's perihelion advance. *Astrophys. Space Sci.* **284**, 1159 (2003)
- Pitjeva, E.V.: Relativistic Effects and Solar Oblateness from Radar Observations of Planets and Spacecraft. *Astron. Lett.* **31**, 340 (2005a)
- Pitjeva, E.V.: High-Precision Ephemerides of Planets EPM and Determination of Some Astronomical Constants. *Sol. Syst. Res.* **39**, 176 (2005b)
- Pitjeva, E.V.: In: Jin, W.J., Platais, I., Perryman, M.A.C. (eds.) *A Giant Step: from Milli- to Micro-arcsecond Astrometry: Use of optical and radio astrometric observations of planets, satellites and spacecraft for ephemeris astronomy*, 20, Cambridge: Cambridge University Press, (2008)
- Pitjeva, E.V.: In: Klioner, S.A., Seidelmann, P.K., Soffel, M.H. (eds.) *Relativity in Fundamental Astronomy: Dynamics, Reference Frames, and Data Analysis, Proceedings IAU Symposium No. 261: EPM ephemerides and relativity*. 170, Cambridge: Cambridge University Press, (2010)
- Polnarev, A.G.: In: Kovalevsky, J., Brumberg, V.H. (eds.) *Relativity in Celestial Mechanics and Astrometry. High Precision Dynamical Theories and Observational Verifications Proceedings IAU Symposium No. 114: Proposals for an Experiment to Detect the Earth's Gravitomagnetic Field*. 401, Dordrecht: D. Reidel Publishing Company, (1986)
- Pugh, G.E.: WSEG Research Memorandum No. 11 (1959)
- Reigber, Ch., Schmidt, R., Flechtner, F., König, R., Meyer, U., Neumayer, K.-H., Schwintzer, P., Zhu, S.Y.: An Earth gravity field model complete to degree and order 150 from GRACE: EIGEN-GRACE02S. *J. Geodyn.* **39**, 1 (2005)
- Ries, J.C., Eanes, R.J., Watkins, M.M., Tapley, B.D.: Joint NASA/ASI Study on Measuring the Lense-Thirring Precession Using a Second LAGEOS Satellite CSR-89-3, Austin: Center for Space Research, (1989)
- Ries, J.C., Eanes, R.J., Tapley, B.D.: In: Ruffini, R.J., Sigismondi, C. (eds.) *Nonlinear Gravitodynamics. The Lense-Thirring Effect: Lense-Thirring Precession Determination from Laser Ranging to Artificial Satellites*, 201, Singapore: World Scientific, (2003a)
- Ries, J.C., Eanes, R.J., Tapley, B.D., Peterson, G.E.: In: Noomen, R., Klosko, S., Noll, C., Pearlman, M. (eds.) *Proc. 13th Int. Laser Ranging Workshop, NASA CP (2003-212248): Prospects for an Improved Lense-Thirring Test with SLR and the GRACE Gravity Mission, Greenbelt: NASA Goddard*, (2003b). http://cddis.gsfc.nasa.gov/lw13/docs/papers/sci_ries_lm.pdf. Cited 20 Mar 2010
- Ries, J.C., Eanes, R.J., Watkins, M.M.: In: Schillak, S. (ed.) *Proc. 16th Int. Laser Ranging Workshop, (Poznań (PL) 13-17 October 2008): Confirming the Frame-Dragging Effect with Satellite Laser Ranging*, (2008) http://cddis.gsfc.nasa.gov/lw16/docs/papers/sci_3_Ries_p.pdf. Cited 20 Mar 2010
- Ries, J.C.: Relativity in Satellite Laser Ranging. *Bull. Am. Astron. Soc.* **41**, 889 (2009)
- Rindler, W.: *Relativity. Special, General and Cosmological*. Oxford: Oxford University Press, (2001)
- Ross, S.M.: Peirce's Criterion for the Elimination of Suspect Experimental Data. *J. Engineering Technology* (Fall 2003)
- Roy, A.E.: *Orbital Motion*. Fourth Edition. Bristol: Institute of Physics, (2005)
- Rubincam, D.P.: On the secular decrease in the semimajor axis of Lageos's orbit. *Celest. Mech. Dyn. Astron.* **26**, 361 (1982)
- Ruggiero, M.L., Tartaglia, A.: Gravitomagnetic effects. *N. Cim. B* **117**, 743 (2002)
- Schäfer, G.: Gravitomagnetic Effects. *Gen. Relativ. Gravit.* **36**, 2223 (2004)
- Schäfer, G.: Gravitomagnetism in Physics and Astrophysics. *Space Sci. rev.* **148**, 37 (2009)
- Schiff, L.I.: Possible New Experimental Test of General Relativity Theory. *Phys. Rev. Lett.* **4**, 215 (1960a)

- Schiff, L.I.: On experimental tests of the general theory of relativity. *Am. J. Phys.* **28**, 340 (1960b)
- Schiff, L.I.: Motion of gyroscope according to Einsteins theory of gravitation. *Proc. Nat. Acad. Sci.* **46**, 871 (1960c)
- Schulmann, R. Kox, A.J., Janssen, M., Illy, J. (eds.): *The Collected Papers of Albert Einstein*. Vol. 8. The Berlin Years: Correspondence, 1914-1918. Princeton: Princeton University Press, (1998), Documents 361, 369, 401, 405
- Silbergleit, A.S., Conklin, J., DeBra, D., Dolphin, M., Keiser, G.M., Kozaczuk, J., Santiago, D., Salomon, M., Worden P.: Polhode Motion, Trapped Flux, and the GP-B Science Data Analysis. *Space Sci. Rev.* **148**, 397 (2009)
- Smith, D.E., Zuber, M.T., Sun, X., Neumann, G.A., Cavanaugh, J.F., McGarry, J.F., Zagwodzki, T.W.: Two-Way Laser Link over Interplanetary Distance. *Science* **311**, 53 (2006)
- Smoot, G.F., Steinhardt, P.J., Gravity's rainbow. *Gen. Relativ. Gravit.* **25**, 1095 (1993)
- Soffel, M.H.: *Relativity in Astrometry, Celestial Mechanics and Geodesy*. Berlin: Springer, (1989)
- Soffel, M.H., Klioner, S.A., Petit, G. Wolf, P., Kopeikin, S.M., Bretagnon, P., Brumberg, V.A., Capitaine, N., et al.: The IAU 2000 Resolutions for Astrometry, Celestial Mechanics, and Metrology in the Relativistic Framework: Explanatory Supplement. *Astron. J.* **126**, 2687 (2003)
- Soffel, M.H., Klioner, S.A., Müller, J., Biskupek, L.: Gravitomagnetism and lunar laser ranging. *Phys. Rev. D* **78**, 024033 (2008)
- Spergel, D.N., Verde, D.N., Peiris, H.V., Komatsu, E., Nolte, M.R., et al.: First Year Wilkinson Microwave Anisotropy Probe (WMAP) Observations: Determination of Cosmological Parameters. *Astrophys. J. Suppl.* **148**, 175 (2003)
- Standish, E.M.: JPL Planetary and Lunar Ephemerides, DE414 Interoffice Memo IOM 343R-06-002, (2006)
- Stedman, G.E., Schreiber, K.U., Bilger, H.R.: On the detectability of the Lense Thirring field from rotating laboratory masses using ring laser gyroscope interferometers. *Class. Quantum Grav.* **20**, 2527 (2003)
- Stella, L., Possenti, A.: Lense-Thirring Precession in the Astrophysical Context. *Space Sci. Rev.* **148**, 105 (2009)
- Tapley, B.D., Ries, J.C., Bettadpur, S., Chambers, D., Cheng, M.K., Condi, F., Gunter, B., Kang, Z., Nagel, P., Pastor, R., Pekker, T., Poole, S., Wang, F.: GGM02- An improved Earth gravity field model from GRACE. *J. Geod.* **79**, 467 (2005)
- Tapley, B.D., Ries, J.C., Bettadpur, S., Chambers, D., Cheng, M.K., Condi, F., Poole, S.: American Geophysical Union, Fall Meeting 2007, abstract #G42A-03
- Tartaglia, A.: Geometric Treatment of the Gravitomagnetic Clock Effect. *Gen. Relativ. Gravit.* **32**, 1745 (2000a)
- Tartaglia, A.: Detection of the gravitomagnetic clock effect. *Class. Quantum Grav.* **17**, 783 (2000b)
- Tartaglia, A., Ruggiero, M.L.: Angular Momentum Effects in Michelson-Morley Type Experiments. *Gen. Relativ. Gravit.* **34**, 1371 (2002)
- Tartaglia, A., Ruggiero, M.L.: Gravito-Electromagnetism versus electromagnetism. *Eur. J. Phys.* **25**, 203 (2004)
- Taylor, J.: *Error Analysis*, 2nd edition. 166, Sausalito: University Sci. Books, (1997)
- Theiss, D.S.: A General Relativistic Effect of a Rotating Spherical Mass and the Possibility of Measuring it in a Space Experiment *Phys. Lett. A* **109**, 19 (1985)
- Thirring, H.: Über die formale Analogie zwischen den elektromagnetischen Grundgleichungen und den Einsteinschen Gravitationsgleichungen erster Näherung. *Phys. Z.* **19**, 204 (1918a)
- Thirring, H.: Über die Wirkung rotierender ferner Massen in der Einsteinschen Gravitationstheorie. *Phys. Z.* **19**, 33 (1918b)
- Thirring, H.: Berichtigung zu meiner Arbeit: "Über die Wirkung rotierender ferner Massen in der Einsteinschen Gravitationstheorie". *Phys. Z.* **22**, 29 (1921)
- Thorne, K.S., MacDonald, D.A., Price, R.H. (eds.): *Black Holes: The Membrane Paradigm*, Yale: Yale University Press, (1986)
- Thorne, K.S.: In: Fairbank, J.D., Deaver, B.S., Everitt, C.W.F., Michelson, P.F. (eds.) *Near Zero: New Frontiers of Physics: Gravitomagnetism, Jets in Quasars, and the Stanford Gyroscope Experiment*, 573, New York: W. H. Freeman and Company, (1988)
- Tisserand, F.F.: Sur le mouvement des planètes au tour du Soleil, d'après la loi électrodynamique de Weber. *Comptes Rendus de l' Académie des Sciences (Paris)*. **75**, 760 (1872)
- Tisserand, F.F.: Sur le mouvement des planètes, en supposant l'attraction représentée par l'une des lois électrodynamiques de Gauss ou de Weber. *Comptes Rendus de l' Académie des Sciences (Paris)*. **100**, 313 (1890)
- Turyshev, S.G., Williams, J.G.: Space-Based Tests of Gravity with Laser Ranging. *Int. J. Mod. Phys. D* **16**, 2165 (2007)
- Turyshev, S.G., Shao, M., Nordtvedt, K., Dittus, H., Lämmerzahl, C., Theil, S., Salomon, C., Reynaud, S., Damour, T., Johann, U., Bouyer, P., Touboul, P., Foulon, B., Bertolami, O., Páramos, J.: Advancing fundamental physics with the Laser Astrometric Test of Relativity. The LATOR mission. *Experimental Astronomy* **27**, 27 (2009)
- Van Patten, R.A., Everitt, C.W.F.: Possible Experiment with Two Counter-Orbiting Drag-Free Satellites to Obtain a New Test of Einsteins's General Theory of Relativity and Improved Measurements in Geodesy. *Phys. Rev. Lett.* **36**, 629 (1976a)
- Van Patten, R.A., Everitt, C.W.F.: A possible experiment with two counter-rotating drag-free satellites to obtain a new test of Einsteins general theory of relativity and improved measurements in geodesy. *Celest. Mech. Dyn. Astron.* **13**, 429 (1976b)
- Vespe, F.: The Perturbations Of Earth Penumbra on LA-GEOS II Perigee and the Measurement of Lense-Thirring Gravitomagnetic Effect. *Adv. Space Res.* **23**, 699 (1999)
- Vladimirov, Yu., Mitskiévic, N., Horsky, J.: *Space Time Gravitation*. 91, Moscow: Mir, (1987)
- Vrbik, J.: Zonal-Harmonics Perturbations *Celest. Mech. Dyn. Astron.* **91**, 217 (2005)
- Weber, J.: *Gravitational Waves*. First Award at the 1959 Gravity Research Foundation Competition. Available from www.gravityresearchfoundation.org (1959)
- Weber, J.: Detection and Generation of Gravitational Waves. *Phys. Rev.* **117**, 306 (1960)

- Weber, J.: Evidence for Discovery of Gravitational Radiation. *Phys. Rev. Lett.* **22**, 1320 (1969)
- Weber, W.: Elektrodynamische Massbestimmungen über ein allgemeines Grundgesetz der elektrischen Wirkung. *Abhandlungen der Königlichen Sächsischen Gesellschaft der Wissenschaften.* 211 (1846)
- Wermuth, M., Svehla, D., Földvary, L., Gerlach, Ch., Gruber, T., Frommknecht, B., Peters, T., Rothacher, M., Rummel, R., Steigenberger, P.: A gravity field model from two years of CHAMP kinematic orbits using the energy balance approach. Presentation at EGU 1st General Assembly, 25-30 April 2004, Nice, France
- Whittaker, E.: *A History of the Theories of Aether and Electricity, Volume I: The Classical Theories.* New York: Harper and Brothers, (1960)
- Will, C.M.: Theoretical Frameworks for Testing Relativistic Gravity II: Parameterized Post-Newtonian Hydrodynamics and the Nordtvedt Effect. *Astrophys. J.* **163**, 611 (1971)
- Will, C.M., Nordtvedt Jr., K.: Conservation Laws and Preferred Frames in Relativistic Gravity I. *Astrophys. J.* **177**, 757 (1972)
- Will, C.M.: *Theory and experiment in gravitational physics.* Revised edition. Cambridge: Cambridge University Press, (1993)
- Will, C.M.: The Confrontation between General Relativity and Experiment. *Living Rev. Relativity* **9**, 3 (2006). Cited 29 Jul 2010 <http://www.livingreviews.org/lrr-2006-3>
- Williams, R.K.: Extracting X rays, γ rays, and relativistic $e-e+$ pairs from supermassive Kerr black holes using the Penrose mechanism. *Phys. Rev. D* **51**, 5387 (1995)
- Williams, R.K.: Collimated escaping vortical polar $e-e+$ jets intrinsically produced by rotating black holes and Penrose processes. *Astrophys. J.* **611**, 952 (2004)
- Yilmaz, H.: Proposed Test of the Nature of Gravitational Interaction. *Bulletin of the American Physical Society* **4**, 65 (1959)
- Yoder, C.F.: In: Ahrens, T.J. (ed.) *Global earth physics a handbook of physical constants: Astrometric and Geodetic Properties of Earth and the Solar System.* Table 6 AGU reference shelf Series, vol. no. 1 (1995)
- You, R.J.: The gravitational Larmor precession of the Earth's artificial satellite orbital motion. *Bollettino di Geodesia e Scienze Affini* **57**, 453 (1998)
- Yuan, D.-N., Sjogren, W.L., Konopliv, A.S., Kucinskas, A.B.: Gravity field of Mars: A 75th Degree and Order Model. *J. Geophys. Res.* **106**, 23377 (2001)
- Zel'dovich, Ya. B.: Analog of the Zeeman effect in the gravitational field of a rotating star. *J. Exp. Theor. Phys. Lett.* **1**, 95 (1965)
- Zel'dovich, Ya. B., Novikov, I.D.: *Stars and Relativity.* Chicago: The University of Chicago Press, (1971)
- Zerbini, S.: In: Mueller, I.I., Zerbini, S. (eds) *The Interdisciplinary Role of Space Geodesy Proceedings of an International Workshop held at "Ettore Majorana" Center for Scientific Culture, International School of Geodesy- Director, Enzo Boschi-Erice, Sicily, Italy, July 23-29, 1988: Appendix 5 The LAGEOS II project*, 269 Berlin: Springer (1989)
- Zuber, M.T., Smith, D.E.: In: *Proc. 16-th International Workshop on Laser Ranging, Poznań, Poland, October 12-17 2008: One-Way Ranging to the Planets* http://cddis.gsfc.nasa.gov/lw16/docs/presentations/llr_9_Zuber.pdf. Cited 20 Mar 2010